学 位 申 請 論 文

三宅 亮

主論文1

Molecular Dynamics Simulations on Phase Transitions of Plagioclase Feldspar

by

Akira Miyake

December, 1997

Doctoral Thesis,

Department of Geology and Mineralogy,

Faculty of Science, Kyoto University.

Abstract

The parameters of molecular dynamics (MD) simulations in the NaO-CaO-MgO-Al_2O_3-SiO_2 system were newly evaluated and applied successfully to reproduction of 21 crystals in the MD simulations. In the present study, the phase transitions and thermodynamic behavior of pure anorthtie, pure albite and plagioclase feldspar solid solution were studied using the MD simulation.

Pure anorthite: The $P\bar{1}$-$I\bar{1}$ phase transition of MD-simulated fully ordered anorthite was first order and during this phase transition Ca motion and the behavior of the framework were strongly coupled. On the other hand, the transition of MD-simulated partly disordered anorthite with Al-O-Al violating the Al-avoidance rule was non-first order similar to that of real anorthite. Ca 'split' positions reported in real anorthite were not observed in MD-simulated fully ordered anorthite. Ca atoms in MD-simulated partly disordered anorthite occupied multiple sites, implying the existence of Ca 'split' positions in real anorthite.

Pure albite: MD simulations of pure albite with various degrees of the Al/Si ordering showed that the symmetry reduction from C2/m to $C\bar{1}$ was dominated by 2nd order transition due to both the displacement of atoms and the Al/Si ordering, and that there was no thermal crossover between high- and low-albite. Na atoms in the MD-simulated fully ordered albite kept positions in the $C\bar{1}$ structure and those in the MD-simulated partly disordered albite

were distributed at multiple sites breaking the $C\bar{1}$ symmetry.

Plagioclase feldspar solid solution: In the low temperature ranges where the MD-simulated fully ordered plagioclase was a stable phase, the phase separation between pure albite and pure anorthite may occur. The phase separation was supported by the result that the excess enthalpy of mixing of MD-simulated plagioclase with a lamellae structure consisting of pure albite and pure anorthite was smaller than that of MD-simulated fully ordered plagioclase with the same bulk composition. The present MD simulation on plagioclase showed that peristerite gap could not be explained thermodynamically in the system ignoring the existence of 'e'-plagioclase even when the composition dependency of the Al/Si ordering was changed..

Contents

1. Introduction

Plagioclase feldspar is one of the most important rock-forming minerals. The compositions of most natural plagioclase lie in albite ($NaAlSi_3O_8$) anorthite ($CaAl_2Si_2O_8$). The fundamental structure of plagioclase feldspar consists of an aluminosilicate tetrahedral framework within which Ca and Na cations occupy large interstitial sites. There have been known four commensurate structures (space groups of C2/m, $C\bar{1}$, $I\bar{1}$ and $P\bar{1}$) and one incommensurate structure ('e' plagioclase) for plagioclase feldspars. Though plagioclase feldspar has a wide range of solid solution at high temperature, the phase relations have not been precisely established, except for several tentative ones (e.g., Smith, 1974; Carpenter, 1994). In the intermediate composition range, three miscibility gaps have been recognized; peristerite gap, Bøggild gap and Huttenlocher gap. Because of the existence of five structural states and three miscibility gaps, plagioclase feldspar has various phenomena such as the phase transitions and the phase separations and they are intricately entangled.

In the present study, the phase transitions of pure anorthite, pure albite and plagioclase solid solution and the origin of peristerite miscibility gap were studied, because of their importance in understanding the behavior of plagioclase feldspar in nature.

Pure anorthite: The phase transition from the $P\bar{1}$ phase to the $I\bar{1}$ phase occurs at around 515K in anorthite. This phase transition has been subsequently studied by various experimental methods (e.g., high temperature x-ray and neutron diffraction methods, electron microscopy, and the others). Various hypotheses of the mechanism of this phase transition

and a high temperature structure, e.g., space average model, Ca-jumping model, and soft-mode model, have been proposed till now (several of them will be briefly reviewed in chapter of pure anorthite). It is currently thought that this phase transition is tricritical transition and essentially displacive transition.

Pure albite: Pure albite has been thought to have two phase transitions; one is between monalbite and high-albite and the other between high- and low-albite. These phase transitions have been subsequently studied by various experimental methods (for a historical review, see Smith, 1974; Ribbe, 1983; Smith and Brown, 1988). However, until the mid 1980's, two processes have been related with these phase transitions independently: the displacive process of atomic positions and the Al/Si ordering process in tetrahedral sites. Recently, Salje (1985) and Salje et al. (1985) first studied the effect of coupling the displacive process and the Al/Si ordering process to phase transitions. Based on the Landau theory, they presented that both processes are involved in the structural phase transition between monalbite and high-albite near 1250K and that the thermal crossover between high- and low-albite is smooth function of temperature.

Peristerite miscibility gap: Plagioclase feldspar has the peristerite miscibility gap in the albite rich compositional range (for a historical review, Goldsmith, 1982; Smith and Brown, 1988). The maximum extent of the peristerite two phase field is generally taken to be from ~An_1 to ~An_{25}. Three kinds of models for the origin of the peristerite miscibility gap have been proposed: a solvus, a binary loop associated with a first order transition of albite, and a conditional spinodal with a non-first order transition. The currently accepted hypothesis is

that the driving force for exsolution is due primarily to the free energy of ordering in albite, and that the existence of the miscibility gap is conditional upon the Al/Si ordering taking place.

However, there are still many basic problems unsolved such as the mechanism of the phase transition and the phase separation. One of the difficulties in the study of plagioclase comes from the extreme sluggishness, even on a geological time scale, of such a complete reconstruction of the Al, Si framework and the diffusion of Al and Si, and Na and Ca at temperatures below 700°C. Therefore, the degree of the Al/Si ordering can not be controlled in experiments using natural and synthetic specimens. This is the reason why no detailed phase diagram of plagioclase feldspar has been constructed and many models have been published on the phase transitions and the phase separation.

On the other hand, the molecular-dynamics (MD) simulation using appropriate interatomic potentials between atoms has been widely used for investigating the physical properties of materials and in particular the structures of crystal, liquid and gas. MD simulation gives the positions and the velocities of atoms as a function of time. Therefore, these information of each atom or each element can be extracted from MD simulation and the phase transition can be described at the atomistic level. Further, initial atomic positions can be chosen at will and MD simulations can be calculated even under the conditions difficult in laboratory experiments. That is, initial atomic positions with any Al/Si order and any chemical compositions of plagioclase can be chosen on MD simulation and then MD simulations from the structures with the initial positions can be carried out.

Many MD simulations have been carried out, e.g., MgO (Matsui, 1989), SiO_2 (Tsuneyuki et al., 1990), crystals in the MgO-SiO_2 system (Belonoshko and Dubrovinsky, 1996a), $MgSiO_3$ polymorphs (Matsui, 1988; Matsui and Price, 1992; Wentzcovithc et al., 1993), liquids and glasses in the system $NaAlSiO_4$-SiO_2 (Stein and Spera, 1995), stishovite melting (Belonoshko and Dubrovinsky, 1995), and NaCl and MgO melting (Belonoshko and Dubrovinsky, 1996b). Recently, Akamatsu et al. (1994) applied MD simulation to solid solutions (Na, K)Cl and (Mg, Ca)O with the NaCl type structure, and then they applied to solid solutions (Na, K)Cl with the CsCl type structure (Akamatsu et al., 1995) and to solid solutions (Ca, Sr)TiO_3 and (Mg, Ca)SiO_3 with the perovskite type structure (Akamatsu et al., 1996). However, MD simulation using the existent parameter set do not reproduce plagioclase feldspar. In the present study, therefore, parameters were newly evaluated to reproduce many crystals, in particular plagioclase feldspar, at first. Using this parameter set, we carry out the MD simulations of I) pure anorthite, II) pure albite, and III) plagioclase feldspar solid solution in particular Ab-rich plagioclase as described below:

I) *pure anorthite*: The correlation between Ca motions and lattice distortion of framework during the $P\bar{1}$-$I\bar{1}$ phase transition and the behavior of Ca atoms in the high temperature phase were studied by using MD simulation. MD simulations of a fully ordered anorthite and an anorthite with a certain irregularity of atomic arrangements were also carried out to investigate the influence of the Al/Si disorder and the antiphase domain (APD) on the phase transition and the Ca position.

II) *pure albite*: The thermodynamic properties of albite; in particular the phase transition of both C2/m-C$\bar{1}$ and high albite - low albite, and the behavior of Na atom at low temperature were studied by using MD simulation. MD simulations of a fully ordered albite and disordered albite were also carried out to investigate the correlation between the lattice distortion and the Al/Si disorder during C2/m-C$\bar{1}$ and high - low albite phase transition and the influence of the Al/Si disorder on the behavior of Na atoms.

III) *plagioclase feldspar solid solution*: The thermodynamic property of plagioclase feldspar solid solution, in particular Ab-rich plagioclase, was studied using MD simulations. MD-simulations of fully ordered plagioclase feldspar and disordered plagioclase with various Al/Si order were also carried out to investigate the phase relation of Ab-rich plagioclase and the existence of the phase separation between pure albite and pure anorthite at low temperature.

2. Molecular Dynamics (MD) Method

2.1 MD simulation

In the present study, we employed an interatomic potential model, where the interatomic potential function (Φ_{ij}) between two atoms (i, j) consists of the Coulombic, the short range repulsion, the van der Waals attraction, and the Morse potential terms as given by

$$\Phi_{ij}(r_{ij}) = z_i z_j e^2/r_{ij} + f_0(b_i+b_j)\exp(a_i+a_j-r_{ij}/b_i+b_j) - c_i c_j/r_{ij}^6 + D_{ij}\{\exp[-2\beta_{ij}(r_{ij}-r_{ij}^*)] - 2\exp[-\beta_{ij}(r_{ij}-r_{ij}^*)]\} \quad , \qquad (1)$$

where r_{ij} is an interatomic distance, f_0 (=6.9511x10^{-11}N) a constant, e the electronic charge, z, a, b and c parameters for each atomic species, and D_{ij}, β_{ij} and r^*_{ij} parameters for cation-anion pairs. These parameters in the NaO-CaO-MgO-Al_2O_3-SiO_2 (NCMAS) system were newly evaluated by trial and error procedures so as to reproduce the crystal structures (the cell parameters, the densities, and the space groups) of anorthite, albite, and forsterite at 300K within the errors of 3% from experimental determined values (anorthite: Wainwright and Starkey, 1971; albite: Winter et al., 1977; forsterite: Fujino et al., 1981), and to show the same temperature dependencies as the experimental determined dependencies of the cell parameters of anorthite and albite from 300K to 500K (anorthite: Redfern and Salje, 1987; albite: Winter et al., 1977). The electrostatic valences of ions, z, were constrained to be $z(Na)=1/2z(Ca)=1/2z(Mg)=1/3z(Al)=1/4z(Si)=-1/2z(O)$ in order to apply the potential to

crystals with any composition in the NCMAS system and these valences were then empirically chosen to be 48% of the full charges. The Morse term was applied to Si-O, Al-O, Mg-O, and Ca-O pairs. The parameters used in the present study are shown in Table 2-1.

Cell parameters of the observed and MD-simulated crystal of the 21 crystals at 300K and 1atm are compared in Table 2-2; periclase (MgO), lime (CaO), corundum (Al_2O_3), spinel ($MgAl_2O_4$), quartz (SiO_2), enstatite ($MgSiO_3$), clinoenstatite ($MgSiO_3$), diopside ($CaMgSi_2O_6$), wollastonite ($CaSiO_3$), jadeite ($NaAlSi_2O_6$), omphacite ($NaCaMgAlSi_2O_6$), forsterite (Mg_2SiO_4), Ca-olivine (Ca_2SiO_4), monticellite ($CaMgSiO_4$), Al_2SiO_5 polymorphs (andalusite, sillimanite, kyanite), pyrope ($Mg_3Al_2Si_3O_{12}$), grossular ($Ca_3Al_2Si_3O_{12}$), albite ($NaAlSi_3O_8$), and anorthite ($CaAl_2Si_2O_8$). And crystal symmetries of MD-simulated crystals determined by using the program to calculate structure factors (Miyake et al., 1997) are also given in Table 2-2. As seen in the table, the cell parameters of the 21 crystals and the symmetry of 20 crystals except for only quartz are quite successfully reproduced in the present MD simulation.

MD simulations were carried out by using an MD program, MXDTRICL (Kawamura, 1997). The Ewald method was applied for the summations of Coulombic interactions. Integration of motions of ions was carried out using the Verlet's algorithm (Δf=2.0fs). Temperature and pressure were controlled by scaling particle velocities and simulation cell lengths, respectively. In the present study, the MD simulations on three kinds of feldspars were carried out; pure anorthite, pure albite and plagioclase feldspar solid solution. Details of each MD simulation will be described in each section.

Table 2-1. Potential parameters used in the present study.

Ion	z (e)	a (Å)	b (Å)	c ($KJ^{½}Å^{3}mol^{½}$)	Ion pair	D (KJ/mol)	β ($Å^{-1}$)	r* (Å)
O	-0.96	1.7700	0.138	51.23				
Si	1.92	0.5983	0.025	0.00	Si-O	63.0	2.0	1.47
Al	1.44	0.6758	0.030	0.00	Al-O	50.4	2.0	1.58
Mg	0.96	0.9400	0.040	20.49	Mg-O	42.0	2.0	1.75
Ca	0.96	1.1425	0.042	30.74	Ca-O	21.0	2.0	2.20
Na	0.48	1.0450	0.050	20.49	others	0.00	0.0	0.00

Table 2-2. Cell parameters of 21 observed and MD-simulated crystals at 300K, 1atm. The values of (%) mean |Obs-MD|×100/MD.

		a (Å)	b (Å)	c (Å)	α (°)	β (°)	γ (°)	Space Group
Periclase	Obs[*1]	4.211	4.211	4.211	90	90	90	Fm3m
MgO	MD	4.170	4.169	4.1790	90.000	90.008	89.996	Fm3m
	(%)	0.98	1.01	0.77	0.00	0.01	0.00	○
Lime	Obs[*2]	4.812	4.812	4.812	90	90	90	Fm3m
CaO	MD	4.660	4.661	4.660	90.030	90.000	89.991	Fm3m
	(%)	3.26	3.24	3.26	0.03	0.00	0.01	○
Corundum	Obs[*3]	4.758	4.758	12.991	90	90	120	$R\bar{3}c$
Al_2O_3	MD	4.754	4.754	13.200	89.999	90.004	119.997	$R\bar{3}c$
	(%)	0.08	0.08	1.58	0.00	0.00	0.00	○
Spinel	Obs[*4]	8.083	8.083	8.083	90	90	90	Fd3m
$MgAl_2O_4$	MD	8.146	8.146	8.148	90.004	90.000	89.996	Fd3m
	(%)	0.77	0.77	0.80	0.00	0.00	0.00	○
Quartz	Obs[*5]	4.913	4.913	5.405	90	90	120	$P3_221$
SiO_2	MD	5.142	5.143	5.677	89.998	89.998	119.987	$P6_422$
	(%)	4.45	4.47	4.79	0.00	0.00	0.01	×
Enstatite	Obs[*6]	18.225	8.813	5.180	90	90	90	Pbca
$MgSiO_3$	MD	18.554	8.702	5.208	90.003	89.998	90.009	Pbca
	(%)	1.77	1.28	0.54	0.00	0.00	0.01	○
Clinoenstatite	Obs[*7]	9.626	8.825	5.188	90	108.33	90	$P2_1/c$
$MgSiO_3$	MD	9.746	8.695	5.200	89.997	107.813	90.007	$P2_1/c$
	(%)	1.23	1.50	0.23	0.00	0.48	0.01	○
Diopside	Obs[*8]	9.746	8.899	5.251	90	105.63	90	C2/c
$CaMgSi_2O_6$	MD	9.856	8.814	5.292	89.994	105.838	90.006	C2/c
	(%)	1.12	0.96	0.77	0.01	0.20	0.01	○

Wollastonite	Obs[*9]	7.94	7.32	7.07	90.033	95.367	103.433	P$\bar{1}$
$CaSiO_3$	MD	7.700	7.335	7.102	90.080	93.216	103.861	P$\bar{1}$
	(%)	3.12	0.20	0.45	0.05	2.31	0.41	○
Jadeite	Obs[*10]	9.418	8.562	5.219	90	107.58	90	C2/c
$NaAlSi_2O_6$	MD	9.588	8.661	5.367	90.005	108.140	90.000	C2/c
	(%)	1.77	1.14	2.76	0.01	0.52	0.00	○
Omphacite	Obs[*11]	9.585	8.776	5.260	90	106.85	90	P2/n
$NaCaMgAlSiO_6$	MD	9.697	8.794	5.355	89.996	108.047	90.020	P2/n
	(%)	1.15	0.20	1.77	0.00	1.11	0.02	○
Forsterite	Obs[*12]	4.753	10.190	5.978	90	90	90	Pbnm
Mg_2SiO_4	MD	4.817	10.067	5.972	90.007	89.999	90.002	Pbnm
	(%)	1.33	1.22	0.10	0.01	0.00	0.00	○
Ca-Olivine	Obs[*13]	5.078	11.225	6.760	90	90	90	Pbnm
Ca_2SiO_4	MD	5.123	11.000	6.609	90.003	90.006	90.007	Pbnm
	(%)	0.88	2.05	2.28	0.00	0.01	0.01	○
Monticellite	Obs[*14]	4.825	11.111	6.383	90	90	90	Pbnm
$CaMgSiO_4$	MD	4.846	10.920	6.329	90.002	90.005	90.001	Pbnm
	(%)	0.43	1.75	0.85	0.00	0.01	0.00	○
Andalusite	Obs[*15]	7.798	7.903	5.557	90	90	90	Pnnm
Al_2SiO_5	MD	7.951	8.121	5.516	89.996	90.004	89.999	Pnnm
	(%)	1.92	2.68	0.74	0.00	0.00	0.00	○
Sillimanite	Obs[*16]	7.488	7.681	5.777	90	90	90	Pbnm
Al_2SiO_5	MD	7.567	7.627	5.837	90.000	89.992	90.005	Pbnm
	(%)	1.04	0.71	1.03	0.00	0.01	0.01	○
Kyanite	Obs[*17]	7.126	7.852	5.572	89.99	101.11	106.03	P$\bar{1}$
Al_2SiO_5	MD	7.229	7.913	5.607	89.708	101.031	105.960	P$\bar{1}$
	(%)	1.42	0.77	0.62	0.31	0.08	0.07	○
Pyrope	Obs[*18]	11.456	11.456	11.456	90	90	90	Ia3d
$Mg_3Al_2Si_3O_{12}$	MD	11.567	11.546	11.546	90.000	90.002	90.010	Ia3d
	(%)	0.96	0.78	0.78	0.00	0.00	0.01	○

Grossular	Obs[*19]	11.846	11.846	11.846	90	90	90	Ia3d
$Ca_3Al_2Si_3O_{12}$	MD	11.869	11.869	11.869	90.000	90.002	89.999	Ia3d
	(%)	0.19	0.19	0.19	0.00	0.00	0.00	O
Albite	Obs[*20]	8.152	12.784	7.165	94.28	116.67	87.74	$C\bar{1}$
$NaAlSi_3O_8$	MD	8.055	13.089	7.323	95.509	117.554	88.194	$C\bar{1}$
	(%)	1.20	2.33	2.16	1.29	0.75	0.51	O
Anorthite	Obs[*21]	8.173	12.869	14.165	93.113	115.913	91.261	$P\bar{1}$
$CaAl_2Si_2O_8$	MD	8.056	13.032	14.281	94.635	116.265	90.653	$P\bar{1}$
	(%)	1.45	1.25	0.81	1.61	0.30	0.67	O

*1 Hazen (1976), *2 Wychoff (1963), *3 Newnham and deHaan (1962), *4 Fischer (1967), *5 Wright and Lehmann (1981), *6 Ohashi (1984), *7 Morimoto (1960), *8 Clark et al. (1969), *9 Peacor and Prewitt (1963), *10 Prewitt and Burnham (1966), *11 Matsumoto et al. (1975), *12 Fujino et al. (1981), *13 Czaya (1971), *14 Lager and Meagher (1978), *15, *16, and *17, Winter and Ghose (1979), *18 Hazen and Finger (1978), *19 Meagher (1975), *20 Winter et al. (1977), and *21 Wainwright and Starkey (1971).

2.2 The influence of cell size on the MD simulation

Especially, the size of MD cell affects strongly to the reproducibility, when MD simulations of albite, anorthite and plagioclase feldspar solid solution with various states of Al/Si and Na/Ca ordering are carried out. The reproducibility of MD simulations become more accurate with the larger size of MD cell. However, MD simulation which has too large MD cell can not be carried out because of the limitation of the computer and in the case of small size the reproducibility of MD simulation become wrong. Therefore, we first examined how large a cell size of MD simulations is required for such MD simulation of crystals with ordering. So simulations of fully disordered albite with five different cell size (1, 4, 12, 24 and 48 crystallographic unit cells of albite) and with ten different Al/Si arrangement were carried out. Fig. 2-1 shows the variations of the cell parameters and the internal energy (U) with cell sizes for MD calculation. These values scatter for small cell size (<10 crystallographic unit cells) and then become almost constant with increasing the cell size. We conclude, therefore, that a cell size of more than 15 is necessary to obtain constant values for the physical properties of an MD-simulated crystal.

In the present study, 24 crystallographic unit cells for albite (1248 atoms; $a_{MD}=3a_{ab}$, $b_{MD}=2a_{ab}$, $c_{MD}=4a_{ab}$), 12 unit cells for anorthite (1248 atoms; $a_{MD}=3a_{an}$, $b_{MD}=2a_{an}$, $c_{MD}=2a_{an}$), and 1248 atoms for plagioclase ($a_{MD}=3a_{ab}$, $b_{MD}=2a_{ab}$, $c_{MD}=4a_{ab}$) were used for all MD simulations except for a few simulations.

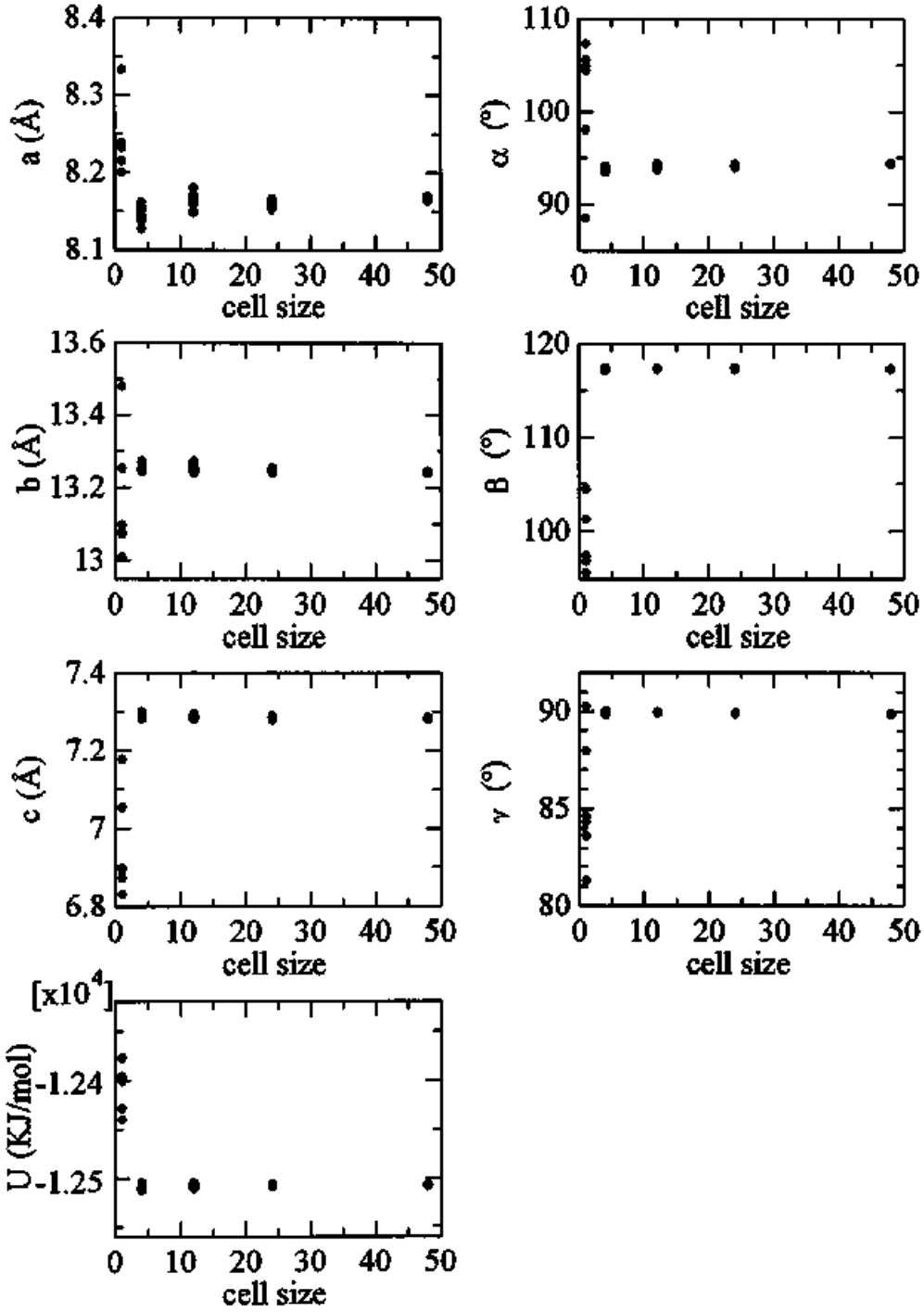

Fig. 2-1. Variations of the cell parameters of MD simulated fully disordered albite with the size of MD cells.

3. Pure Anorthite

3.1 Introduction

The fundamental structure of anorthite, $CaAl_2Si_2O_8$, consists of an aluminosilicate tetrahedral framework within which calcium cations occupy large interstitial sites (Kempster et al., 1962). Brown et al. (1963) first discovered a reversible phase transition of anorthite from the $P\bar{1}$ structure at room temperature to the $I\bar{1}$ structure at high temperature by showing that the *c* type reflections (h+k=even, l=odd, as defined by Bown and Gay, 1958) decreased continuously with increasing temperature and disappeared above the transition temperature (Tc). This phase transition has been subsequently studied by the high temperature x-ray and neutron diffraction methods (Foit and Peacor, 1973; Frey et al., 1977; Adlhart et al., 1980; Ghose et al. 1993), ^{27}Al nuclear magnetic resonance (NMR) (Staehli and Brinkmann, 1974), ^{29}Si MAS NMR (Philips and Kirkpatrick, 1995), electron microscopy (Czank et al., 1973b; Van Tendeloo et al., 1989), the order parameter treatment in terms of Landau theory (Salje, 1987; Redfern and Salje, 1987; Hatch and Ghose, 1989) and hard mode infrared spectroscopy (Redfern and Salje, 1992). The various hypotheses of the mechanism of this phase transition and a high temperature structure have been proposed till now. Several basic models of them will be briefly reviewed below.

Space Average Model: Czank et al. (1972) and Czank et al. (1973a) showed that in the $I\bar{1}$ phase the framework atoms are body centered, but Ca atoms are in split positions in the primitive unit cell, based on an x-ray diffraction method and an electron microscopic

observation. They suggested that the observed body-centered structure is due to the space averaging of atomic positions in the primitive structure. Further, Foit and Peacor (1973) reported the similar conclusions based on the structure refinement of an anorthite at 683 and 1103K.

The Ca-Jumping Model: Staehli and Brinkmann (1974) indicated that eight inequivalent sites at the Al sites symmetry in the primitive structure are reduced to four sites above the transition temperature. They suggested that the framework becomes body centered at Tc and that the Ca atoms most likely "jump" between the split positions. Smith (1974) offered that Ca atoms of I-anorthite jump rapidly between two positions in a deep double well potential related to those in P-anorthite.

Soft-Mode model: Adlhart et al. (1980) showed that a complete and reversible continuous phase transition $P\bar{1} \rightarrow I\bar{1}$ for all structural elements occurs at a defined transition temperature base on an x-ray and elastic neutron measurements up to 703K, and proposed the 'soft-mode' model with a condensing zone-boundary phonon, where the amplitudes become larger and, finally, condense out when coming from high temperatures. They concluded that the Ca atoms mainly drive this phase transition. However, they did not explain the split calcium positions in the $I\bar{1}$ structure above transition temperature.

Salje (1987) proposed an order parameter treatment, coupling between Al/Si order arising from the high temperature $C\bar{1}$-$I\bar{1}$ symmetry reduction and spontaneous strain as

determined from the lattice distortion at the phase transition, of this phase transition in terms of the Landau theory. Redfern and Salje (1987) and Redfern et al. (1988) presented experimental evidence for the tricritical behavior of the $P\bar{1}$-$I\bar{1}$ phase transition in pure anorthite and for the second order in Ca-rich plagioclase based on the observation of the temperature evolution of the spontaneous strain. Further, Redfern and Salje (1992) implied that based on the hard mode infrared spectroscopy this phase transition can be described essentially as an displacive transition and that previous order-disorder models such as *space average model* and *Ca-jumping model* of the $I\bar{1}$ structure are not supported.

Ghose et al. (1988), Van Tendeloo et al. (1989), and Hatch and Ghose (1989) proposed the dynamical model for the phase transition, which is initially driven by a soft-mode mechanism, followed by an order-disorder mechanism near Tc. Van Tendeloo et al. (1989) interpreted the high temperature body-centered phase as a statistical dynamical average of very small *c* type antiphase domains of primitive anorthite. Ghose et al. (1988) suggested that this transition is actually first order (nearly second order) comparable to the alpha-beta quartz transition.

The detailed nature of the $P\bar{1}$-$I\bar{1}$ phase transition in pure anorthite remains enigmatic and is in a chaotic state as yet. One of this cause is considered that there is no making perfect anorthite without Al/Si disorder and antiphase domain in a laboratory and it is impossible to experiment for the phase transition of perfect anorthite. It is necessary to obtain the information of the shorter time and the smaller space change of each atom than that obtained

by x-ray and neutron diffraction method and electron microscopy to clear this phase transition.

On the other hand, the MD simulation using appropriate interatomic potentials between atoms has been widely used for investigating the physical properties of materials and in particular the structures of crystal, liquid and gas. MD simulation gives the positions and the velocities of atoms as a function time. Therefore, these information of each atom or each element from MD simulation can be extracted and the phase transition can be described at atomistic level. Further, any Al/Si ordering can be chosen at an initial stage of MD simulation.

In the present study, the MD simulations of anorthite were carried out to clarify the correlation between Ca motions and lattice distortion of framework through $P\bar{1}$-$I\bar{1}$ phase transition and the calcium positions in high temperature phase. Further, natural samples which were used in many studies may not be fully ordered anorthite but may show partial Al/Si disorder violating *Al-avoidance rule*. To investigate the influence of the Al/Si disorder and the antiphase domain (APD) on the phase transition and the Ca position, we carried out MD simulations of not only a perfect anorthite but an anorthite which has a certain disorderness.

3.2 Procedure and Result

To study the mechanism of the $P\bar{1}$-$I\bar{1}$ phase transition and the behavior of Ca atoms, the MD-simulation of the fully ordered anorthite was carried out. In addition, three more structures of anorthite; structures with partly disordered arrangement of Al/Si and with antiphase domain (APD) and a structure with fully disordered Al/Si arrangement were also simulated by the MD method in order to investigate the influence of the Al/Si disorder and antiphase domains on the phase transition and the Ca 'split' positions. In the present study, pressure was maintained at 1 atm throughout every run of the MD simulation. The unit cell used in the present MD simulation (MD cell) was parallelepiped and the number of atoms in the system was 1248 (containing 12 crystallographic unit cells of anorthite; $a_{MD}=3a_{an}$, $b_{MD}=2a_{an}$, $c_{MD}=2c_{an}$). Table 3-1 shows MD simulations of anorthite carried out in the present study.

3.2.1 Fully ordered anorthite (foAn)

heating experiments

The MD-simulation on anorthite with fully ordered arrangement of Al/Si and Ca positions (foAn) was started by taking atomic positions of $P\bar{1}$-anorthite determined experimentally by Wainwright and Starkey (1971). The structure was annealed for 20ps

(10000 steps) at 300K so as to obtain an equilibrium atomic configuration. This MD-simulated foAn was also used as an initial structure for further MD calculations at all other temperatures. A temperature range of 300-1500K was investigated. After raising the temperature of the system to a required level using the initial structure of foAn, the foAn was 'annealed' for at least 20ps (10000 steps), to obtain an equilibrium atomic configuration. After attaining equilibration, a production run of 20ps (10000 steps) was performed, and various properties and atomic positions were, then, evaluated.

Cell parameters obtained from the MD-simulated structure of foAn at 300K show good agreement with those of real $P\bar{1}$ anorthite determined by the X-ray diffraction method (Wainwright and Starkey, 1971) (Table. 2-2 or Table. 3-2). Temperature dependencies of the cell parameters and the volume of the MD-simulated foAn are compared with those of real anorthite measured by the powder X-ray method (Redfern and Salje, 1987) (Fig. 3-1a, b). The lengths of a, b, and c-axes of the MD-simulated foAn increase gradually with temperature up to 1000K. The α angle decreases gradually with temperature up to 500K and above this temperature becomes to be almost constant, while the fluctuation of the experimental data on real anorthite is observed at the range from 400K to 700K. The β^* and γ angles of the MD-simulated foAn increase gradually with temperature up to about 500K, jump discontinuously to the larger value around 500K and then decrease gradually with temperature above 500K. These tendencies are similar to those of real anorthite measured by the X-ray method except the jump of β^* and γ angles around 500K. The unit cell volume obtained by the MD simulation increases gradually with temperature up to 1000K, but jumps to the larger value around 500K. The transition temperatures (Tc) from $P\bar{1}$- to $I\bar{1}$-anorthite of

real anorthite and the MD-simulated foAn are then estimated based on the abrupt change of the cell parameters as 515K and 500K, respectively. The difference between Tc's of a real anorthite and the MD-simulated foAn is only 15K.

Space groups of low and high temperature phases of real anorthite are $P\bar{1}$ and $I\bar{1}$, respectively. The conditions for possible reflections for *hkl* reflections are none for $P\bar{1}$ and $h+k+l=2n$ for $I\bar{1}$. Structure factors of an MD-simulated foAn show that every $|\langle F_{MD}(hkl)\rangle|$ has a non-negligible value below 500K or Tc. But above Tc, every $|\langle F_{MD}(hkl)\rangle|$ with $h+k+l=2n$ is negligible small, indicating the I-lattice. Symmetry of the structure factors in reciprocal space indicates that the space groups of low and high temperature forms of an MD-simulated foAn are $P\bar{1}$ and $I\bar{1}$, respectively.

The temperature dependency of $I_{obs}(hkl)$ has been measured by the X-ray and neutron scattering methods (Frey et al., 1977, Adlhart et al., 1980). $I_{MD}^{foAn}(025)$ of the MD-simulated crystal is compared with $I_{obs}(025)$ measured experimentally by Adlhart et al. (1980) (Fig. 3-2), because 025 reflection was used to show the linear correlation between the spontaneous strain and the intensity of this reflection by Redfern and Salje (1987). With increasing temperature, $I_{MD}^{foAn}(025)$ and $I_{obs}(025)$ decrease gradually up to Tc=500K for the MD-simulated crystal and Tc=515K for real anorthite (estimated from the abrupt change of the cell parameters), respectively. Above these temperatures, both $I_{MD}^{foAn}(025)$ and $I_{obs}(025)$ are almost zero. The intensities of the MD-simulated crystal change discontinuously at Tc, while those of real anorthite do not show such a discontinuity around Tc.

cooling experiments

In addition to heating experiments, the MD simulations of the reverse experiments with the fully ordered anorthite were carried out. The MD-simulated anorthite calculated at 500K in the foAn was used as a starting MD-simulated anorthite in the reverse simulations. This starting MD-simulated anorthite was quenched to 300 or 450K and annealed at each temperature for 20ps (10000 steps) so as to obtain an equilibrium atomic configuration. After attaining equilibration, a production run of 20ps (10000 steps) was performed, and various properties and atomic positions were, then, evaluated.

Temperature dependencies of the cell parameters of the MD-simulated anorthite in the reverse simulations are shown in Fig. 3-1b. As compared with the MD-simulated foAn, these cell parameters have the similar values as extrapolated the values of high temperature structure to low temperature. And, the fact that $|\langle F_{MD}(hkl)\rangle|$ with $h+k+l=2n$ is negligible small indicates that the structure cooled down in the reverse simulation still remains as the $I\bar{1}$ structure.

Two kinds of additional experiments were carried out as below, to investigate the reason why the MD-simulated anorthite in the reverse simulations still has the $I\bar{1}$ structure at the temperature where $P\bar{1}$ is a stable phase;

I) The average positions in the $I\bar{1}$ structure at 300K were used as the initial positions of O, Si, and Al atoms constructing the framework, and the average positions in the $P\bar{1}$

structure at 300K were used as that of Ca atoms. This simulation was termed as the ficp-simulation. Starting from these atomic positions, an MD-simulated anorthite was annealed for 40ps (20000 steps) at 300 K.

II) The average positions in the $P\bar{1}$ structure at 300K were used as the initial positions of O, Si, and Al atoms, and the average positions in the $I\bar{1}$ structure at 300K were used as that of Ca atoms. This simulation was termed as the fpci-simulation. Starting from these atomic positions, an MD-simulated anorthite was annealed for 40ps (20000 steps) at 300 K.

The cell parameters obtained by both kinds of simulations are plotted in the Fig. 3-1b. The parameters in the fpci-simulation have the similar values as extrapolated the values of high temperature structure ($I\bar{1}$). On the other hand, the parameters in the ficp-simulation have the values of low temperature structure ($P\bar{1}$).

The calculation of structure factors shows that the space groups of the MD-simulated anorthite in the ficp- and fpci-simulations are $P\bar{1}$ and $I\bar{1}$, respectively. The structure factors from only Ca atoms and the others constructing the framework of both simulations are compared with that of MD-simulated foAn (Table. 3-3). The structure factors of ficp-simulation have similar values to those of MD-simulated foAn. On the other hand, those of fpci-simulation are negligible. These results indicate that both the Ca position and the framework in ficp-simulation have $P\bar{1}$ symmetry and that both in fpci-simulation have $I\bar{1}$ symmetry.

The average values of the standard deviations of Ca atomic positions at 300K in the

reverse-, ficp- and fpci-simulations (Table 3-4) are almost the same. However, the standard deviations of the time-averaged coordinates of Ca atoms at 300K in each simulation (Table 3-5a~c) are larger in the reverse- and fpci-simulations than in the ficp-simulation. These facts indicate that although Ca atoms in every simulation have similar amplitude of vibration, Ca atoms occupy multiple-sites in the reverse- and fpci-simulations, but only the $P\bar{1}$ sites in the ficp-simulation.

3.2.2 Partly Al/Si disordered anorthite (pdAn)

The structure with partly disordered arrangement of Al/Si for the MD-simulation (pdAn) was constructed by exchanging Al and Si atoms in tetrahedral sites from that of fully ordered anorthite. Although there are the various methods to make the disordered arrangement of Al/Si, in the present study a simple method that Al and Si are exchanged in only one crystallographic unit in a MD cell containing twelve crystallographic unit cells was adopted. The resulting structure includes Al-O-Al linkages. Starting from the structure, an MD-simulated pdAn was annealed for 20ps (10000 steps) at 300K so as to obtain an equilibrium atomic configuration. This MD-simulated pdAn was also used as an initial structure for MD-simulation at a desired temperature in the range of 300-1000K. After raising the temperature of the system to the required level using starting MD-simulated pdAn, the resulting MD-simulated pdAn was 'annealed' for at least 20ps (10000 steps), to obtain an equilibrium atomic configuration. After attaining equilibration, a production run of 20ps (10000 steps) was performed, and various properties and atomic positions were, then, evaluated.

Temperature dependencies of the cell parameters and the volume of MD-simulated pdAn are shown in Fig. 3-1c. The lengths of a, b, and c-axes increase gradually with temperature up to 1000K. The α angle decreases gradually with temperature up to 500K and above 500K becomes to be almost constant. The β^* and γ angles increase gradually with temperature up to about 550K and then decrease gradually with temperature above 550K. The volume increases gradually with temperature up to 1000K, showing a kink around 550K. Jumps of the cell parameters are not clearly observed in the present case of pdAn, different

from the case of foAn. No clear jumps are also observed in the case of real anorthite (Redfern and Salje, 1987). The transition temperature from $P\bar{1}$- to $I\bar{1}$-anorthite of the MD-simulated pdAn is estimated from the positions of kinks of temperature dependence curves, to be 550K. The temperature is smaller than Tc of real anorthite by only 30K.

Structure factors show that every $|\langle F_{MD}(hkl)\rangle|$ has a non-negligible value below Tc (550K). But above Tc, $|\langle F_{MD}(hkl)\rangle|$ with $h+k+l=2n$ is negligible small, indicating the I-lattice. The behavior of the structure factors indicates that the low temperature phase of an MD-simulated crystal is $P\bar{1}$ and the high temperature phase $I\bar{1}$.

The temperature dependency of $I_{MD}^{pdAn}(025)$ is shown in Fig. 3-2. Differing from the tendency of $I_{MD}^{foAn}(025)$ of foAn, $I_{MD}^{pdAn}(025)$ does not show a jump clearly around Tc.

3.2.3 Anorthite with antiphase domain (AnAPD)

The initial structure with antiphase domains (APD) in a MD cell may be constructed by different two methods; quenching from a high temperature form and artificial induction by changing atomic arrangement. For the quenching method, foAn was, at the first stage, annealed for 20ps (10000 steps) at 1000K so as to obtain an equilibrium atomic configuration. After equilibration, a run of 10000 steps was further performed at 1000K, and it was confirmed that the space group of this MD-simulated anorthite was $I\bar{1}$. This MD-simulated anorthite was subsequently quenched to 300K and simulated for 160ps (80000 steps) at 300K to obtain an antiphase domain (APD) structure in a MD cell. However, structure factors of this MD-simulated anorthite show that the space group still remains as $I\bar{1}$. This may be caused by too small number of atoms in the system and by too short annealing time at 300K for the structure to transform.

The second method, therefore, to induce APD in a MD cell is employed. Half of atoms in a MD cell was shifted from (x, y, z) in foAn to (x+½, y+½, z+½). Starting from the resultant structure, a MD crystal of AnAPD was annealed for 20ps (10000 steps) at 300K. However, this structure was not maintained and the equilibrium atomic configuration was not obtained. This is probably because the number of atoms in the system is too small and the strain energy in antiphase domain boundary is too large.

Therefore, the influence of APD on the phase transition and the Ca 'split' position do not are reported in the present study.

3.2.4 Fully disordered anorthite (fdAn)

The initial structure with fully disordered anorthite was constructed, starting from foAn, by distributing Al and Si atoms randomly into sixteen non-equivalent tetrahedral sites (T-sites). In the resultant structure, the ratio of Al and Si atoms in each site is 1, and there are some oxygen atoms forming Al-O-Al linkages. Starting from the initial structure, an MD-simulated fdAn was annealed for 20ps (10000 steps) at 300 K so as to obtain an equilibrium atomic configuration. This MD-simulated fdAn was also used as a starting MD-simulated crystal in the fully disordered anorthite. A temperature range of 300-1500, and 1800K was investigated. After raising the temperature of the system to the required level using starting MD-simulated fdAn, the resulting MD-simulated fdAn was 'annealed' for at least 20ps (10000 steps), to obtain an equilibrium atomic configuration. After attaining equilibration, a production run of 20ps (10000 steps) was performed, and various properties and atomic positions were, then, evaluated.

It has been thought that the space group of fully disordered anorthite at very high temperature is $C\bar{1}$ (e.g., Carpenter, 1992). The extinction condition for *hkl* reflections for $C\bar{1}$ is $h+k=2n$, $l=2n$. Structure factors of an MD-simulated fdAn show that above 1500K $|\langle F_{MD}(hkl)\rangle|$ without $h+k=2n$, $l=2n$ is negligible small, indicating the C-lattice. The behavior of the structure factors indicates that the high temperature phase of MD-simulated fdAn is C $\bar{1}$.

Table 3-1a. MD simulations of fully ordered anorthite carried out to in the present study are tabulated as follow;

MD simulation	fully ordered An (heating experiments)	fully ordered An (cooling experiments)	fully ordered An (cooling experiments)	fully ordered An (cooling experiments)
Abbreviation	foAn	reverse	ficp	fpci
Initial position	Wainwright and Starkey (1971)	foAn at 500K	framework = I$\bar{1}$ Ca position = P$\bar{1}$	framework = P$\bar{1}$ Ca position = I$\bar{1}$
Al-avoidance rule	O	O	O	O
Pauling rule	O	O	O	O
Temperature	300 - 1000K	300, 450K	300K	300K
Purpose	· P$\bar{1}$-I$\bar{1}$ transition Ca 'split' position	· reverse simulation of P$\bar{1}$-I$\bar{1}$ transition	· reverse simulation of P$\bar{1}$-I$\bar{1}$ transition	· reverse simulation of P$\bar{1}$-I$\bar{1}$ transition

Table 3-1b. MD simulations of anorthite carried out to in the present study are tabulated as follow;

Abbreviation	partly disordered An	An with APD	fully disordered An
Initial position	pdAn	AnAPD	fdAn
Al-avoidance rule	exchange Al/Si in 1/12 of MD cell	—	ratio of Al/Si in each T-site = 1
Pauling rule	×	○	×
Temperature	○	○	○
Purpose	300 - 1000K	—	300 - 1000K
Page	· $P\bar{1}$-$I\bar{1}$ transition Ca 'split' position	· $P\bar{1}$-$I\bar{1}$ transition · Ca 'split' position	· $C\bar{1}$ transition

Table 3-2. Cell parameters of natural anorthite obtained by an X-ray method (Wainwaright and Starekey, 1971) and those by the MD-simulated foAn at 300K, 1atm.

	a (Å)	b (Å)	c (Å)	α (°)	β (°)	γ (°)	ρ (g/cm^3)
X-ray	8.173	12.869	14.165	93.113	115.913	91.261	2.76
simulation	8.056	13.032	14.281	94.635	116.265	90.653	2.762

Table 3-3. Amplitudes of the structure factors of 025 reflection from only Ca atoms and the other atoms composing the frame in the MD-simulated foAn, ficp- and fpci-simulations.

	$\lvert\langle F_{Ca}(025)\rangle\rvert$	$\lvert\langle F_{oth}(025)\rangle\rvert$
foAn	42.60	40.69
ficp	42.64	40.84
fpci	0.01	0.40

Table 3-4. Average values of standard deviations of Ca atomic positions at 300K in the reverse-, ficp-, and fpci-simulations.

	x	y	z
Ca (reverse)	4.345×10^{-03}	5.987×10^{-03}	4.358×10^{-03}
Ca (ficp)	3.990×10^{-03}	5.026×10^{-03}	3.687×10^{-03}
Ca (fpci)	4.300×10^{-03}	6.092×10^{-03}	4.381×10^{-03}

Table 3-5. Standard deviations of the time-averaged coordinates of Ca atoms at 300K in a) the reverse-simulation (in the upper part), b) the ficp-simulation (in the middle part), and c) the fpci-simulation (in the lower part).

a) the reverse-simulation

	x	y	z
Ca1	4.942×10^{-04}	3.565×10^{-04}	1.405×10^{-04}
Ca2	6.015×10^{-04}	1.369×10^{-03}	9.473×10^{-04}
Ca3	5.689×10^{-04}	4.724×10^{-04}	1.625×10^{-04}
Ca4	5.507×10^{-04}	1.197×10^{-03}	7.574×10^{-04}

b) the ficp-simulation

	x	y	z
Ca1	2.247×10^{-04}	7.268×10^{-04}	2.017×10^{-04}
Ca2	2.645×10^{-04}	3.194×10^{-04}	1.637×10^{-04}
Ca3	4.257×10^{-04}	3.307×10^{-04}	1.777×10^{-04}
Ca4	3.069×10^{-04}	6.394×10^{-04}	2.472×10^{-04}

c) the fpci-simulation

	x	y	z
Ca1	8.126×10^{-04}	6.914×10^{-04}	2.383×10^{-04}
Ca2	6.869×10^{-04}	1.222×10^{-03}	8.475×10^{-04}
Ca3	7.511×10^{-04}	5.616×10^{-04}	1.559×10^{-04}
Ca4	7.419×10^{-04}	1.507×10^{-03}	9.450×10^{-04}

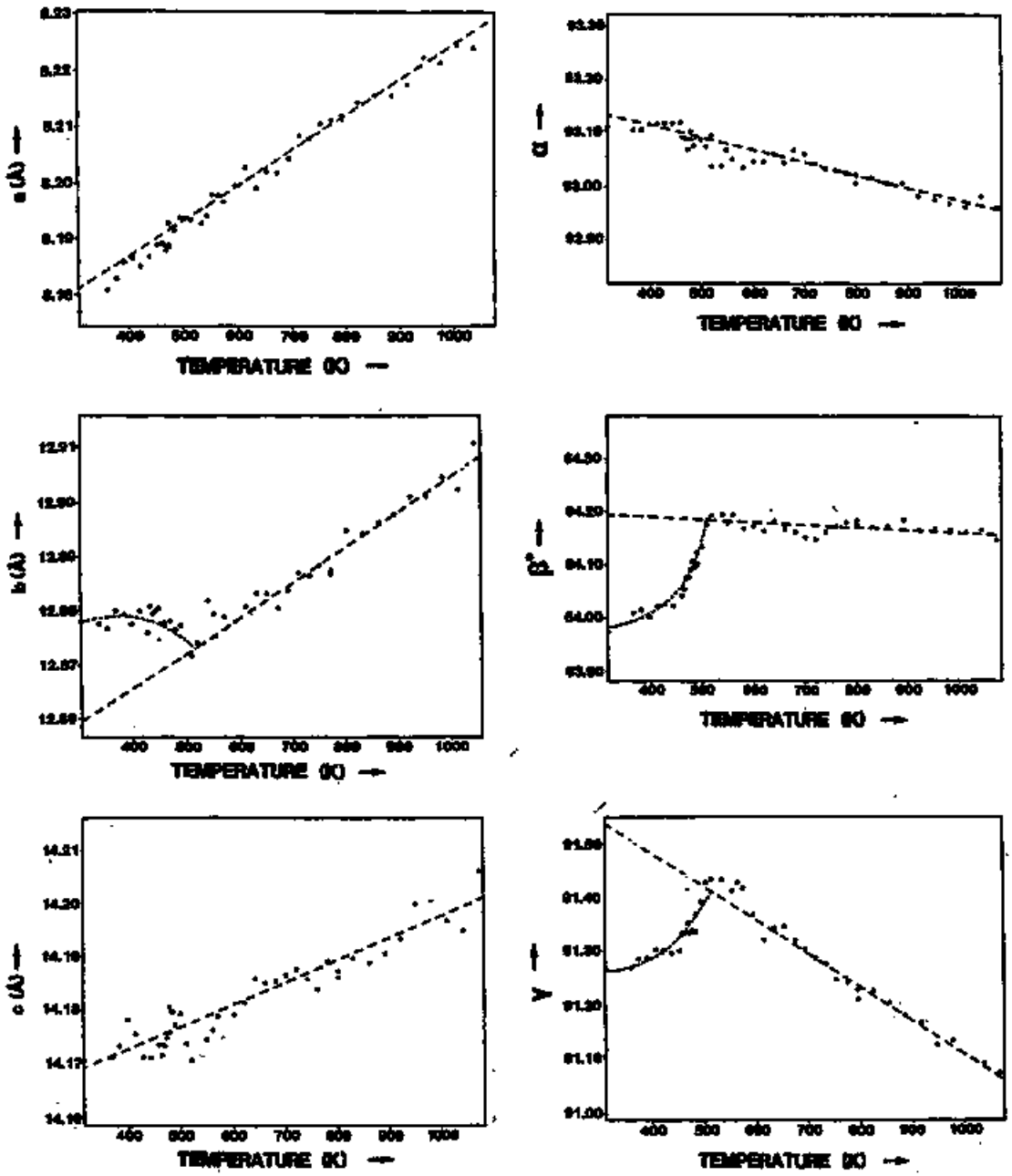

Fig. 3-1a. Temperature dependencies of the cell parameters of natural anorthite (Redfern and Salje, 1987)).

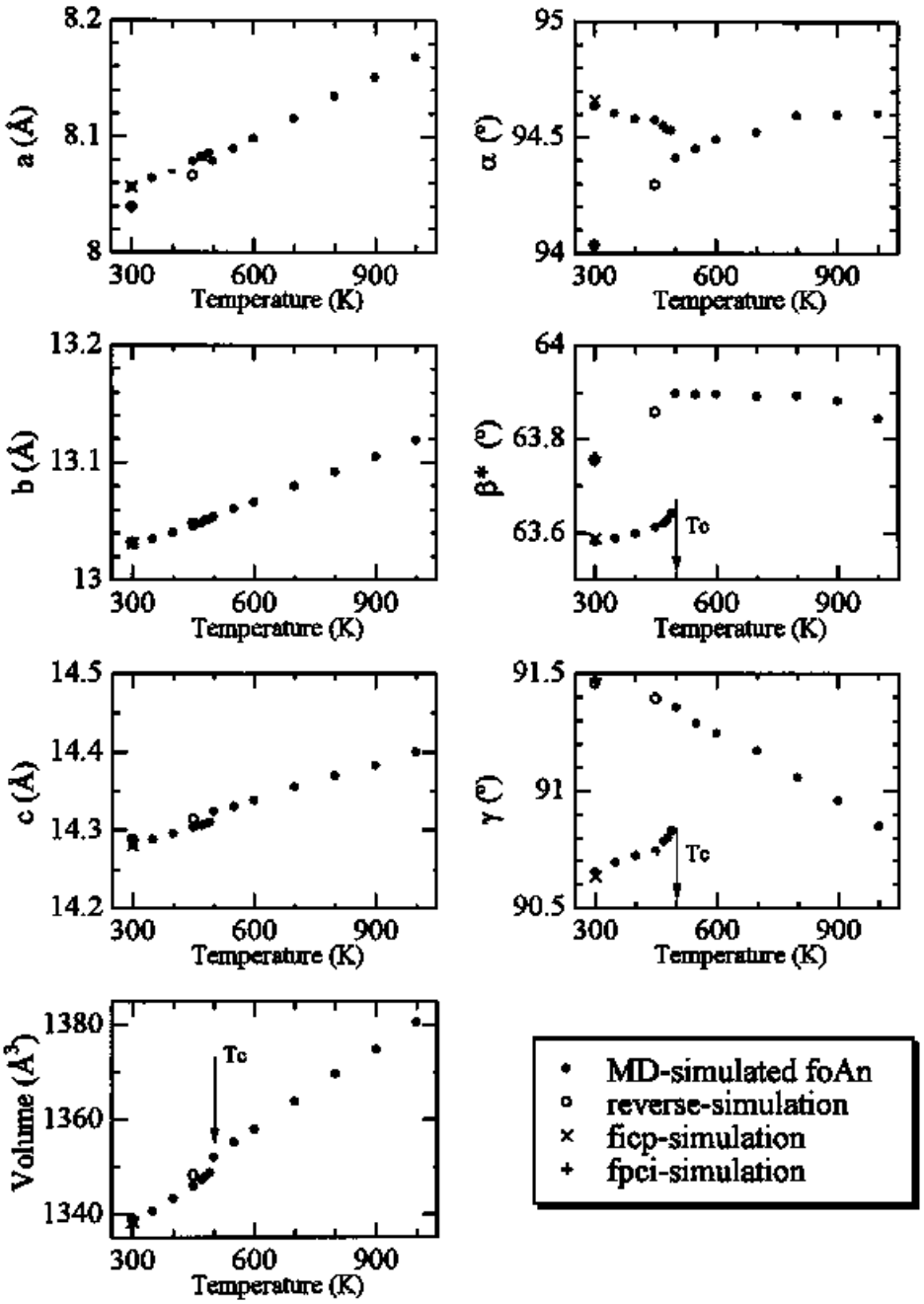

Fig. 3-1b. Temperature dependencies of the cell parameters and the volume of MD-simulated foAn, reverse simulation, ficp-simulation, and fpci-simulation. Transition temperature (Tc) is indicated by arrows.

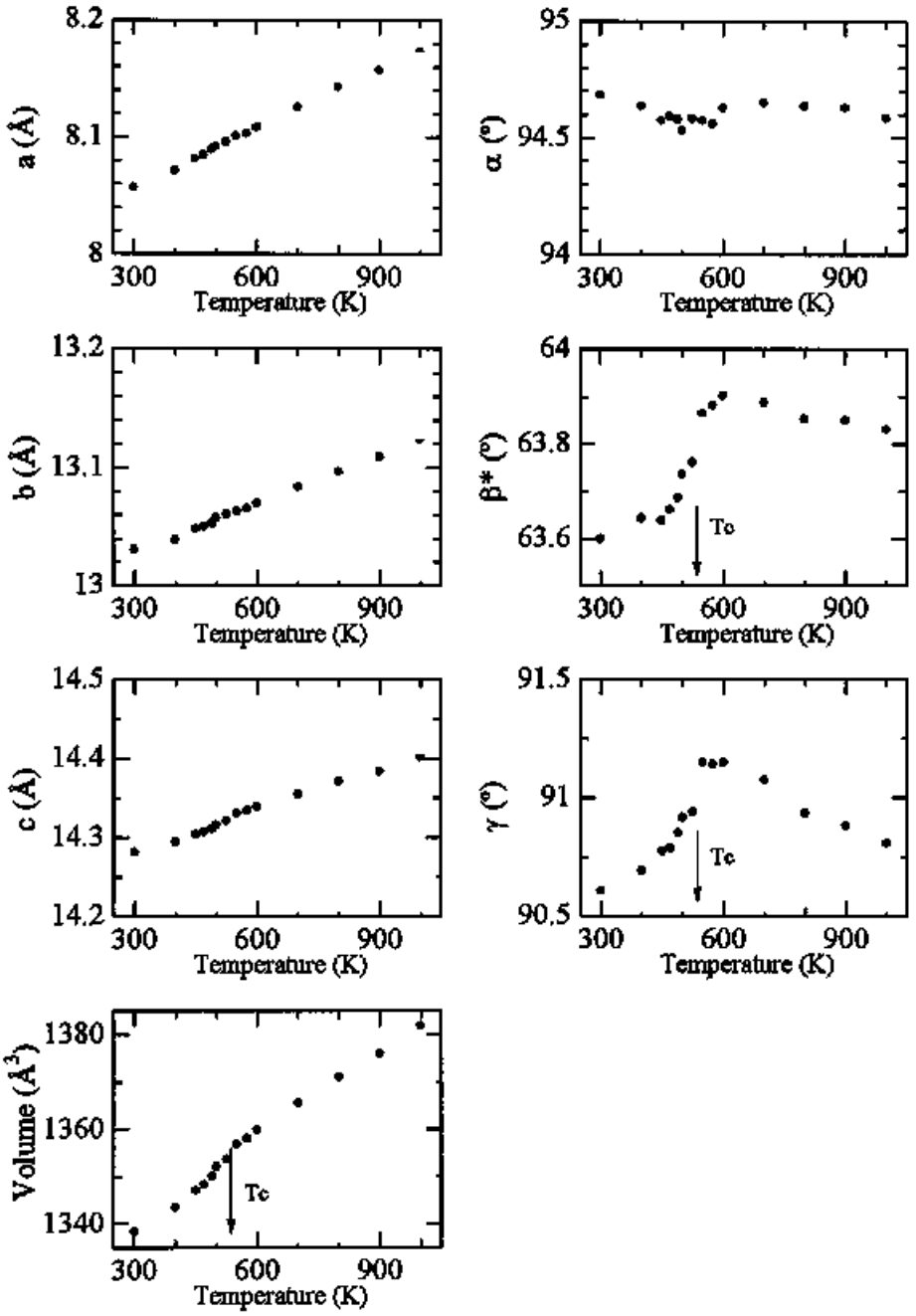

Fig. 3-1c. Temperature dependencies of the cell parameters and the volume of MD-simulated pdAn. Tc; transition temperature.

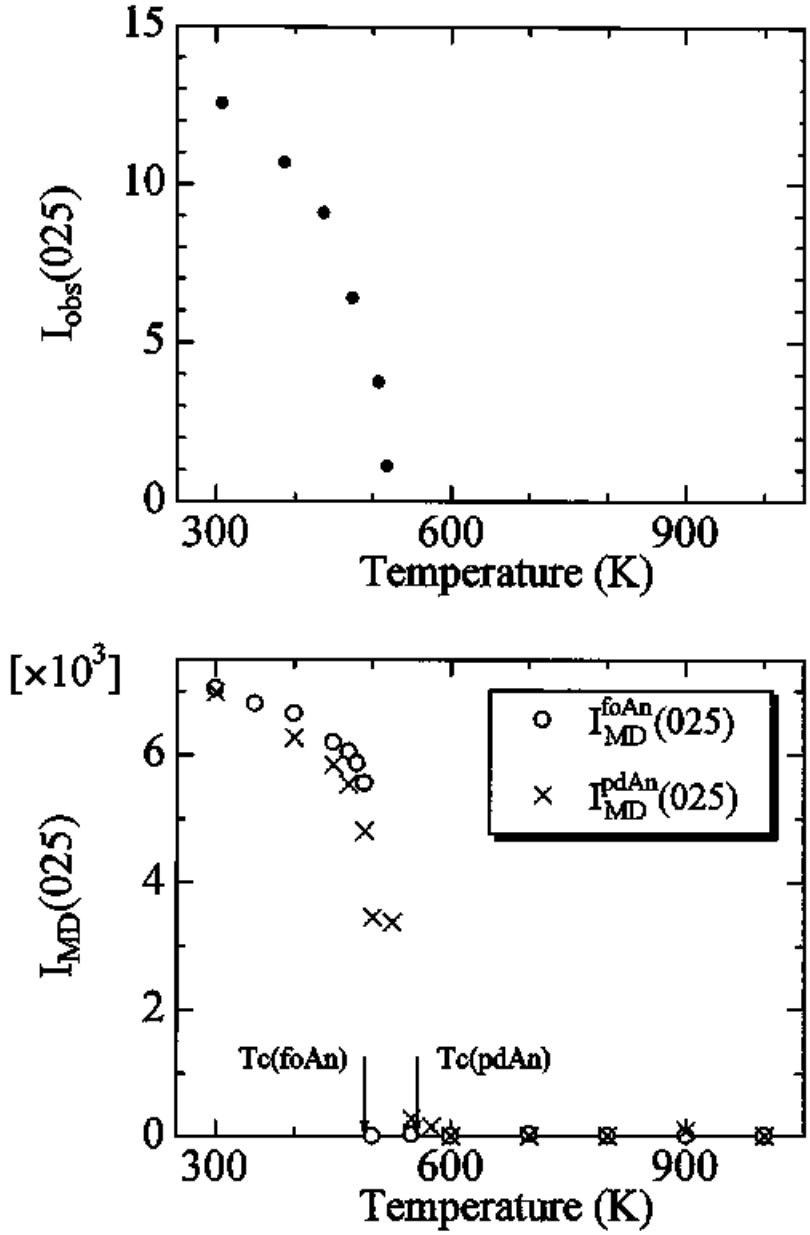

Fig. 3-2. Temperature dependencies of intensities of real anorthite, $I_{obs}(025)$ observed by an X-ray diffraction method (Adlhart et al., 1980) (in the upper part), and those of two kinds of MD-simulated anorthite, $I_{MD}^{foAn}(025)$ and $I_{MD}^{pdAn}(025)$ (in the lower part). Tc; transition temperature.

3.3 Discussion

For the $P\bar{1}$-$I\bar{1}$ phase transition in anorthite, the most essential problem is the correlation between Ca motions and the puckering of the framework. Based on these two behaviors, the order of the phase transition (3.3.1), the microscopic mechanism of the phase transition of the fully ordered anorthite (3.3.2), and then the influence of Al/Si disorder on the phase transition (3.3.3) are discussed in this chapter. Finally, Ca 'split' position is discussed in section 3.3.4.

3.3.1 Order of the $P\bar{1}$-$I\bar{1}$ phase transition

Redfern and Salje (1987) and Redfern et al. (1988) reported that the $P\bar{1}$-$I\bar{1}$ phase transition is a tricritical transition in pure anorthite, and Ghose et al. (1988) suggested that this transition is actually the first order (nearly second order) transition. In the present study, the discontinuous jumps of the volume and $I_{MD}^{foAn}(025)$ of the MD-simulated foAn are observed at the transition temperature (Figs. 3-1b, 3-2). These jumps indicate that this phase transition of the MD-simulated foAn is the first order (not nearly second order) transition, clearly differing from the order of the phase transition of real anorthite. On the other hand, the jumps of the volume and $I_{MD}^{pdAn}(025)$ of the MD-simulated pdAn at Tc are not remarkably observed than that in the MD-simulated foAn (Figs. 3-1c, 3-2). This result indicates that the phase transition of the MD-simulated pdAn is a non-first order phase transition. It can be

considered that real anorthite has the local Al/Si disorder violating the *Al-avoidance rule*, more or less. Therefore, it is thought that the order of the phase transition of real anorthite has been tricritical or actually first order (nearly second order). The present MD-simulation suggests that if fully ordered anorthite exists in nature, its phase transition is a first order transition.

3.3.2 Microscopic considerations of the $P\bar{1}$-$I\bar{1}$ phase transition of the fully ordered anorthite

In order to compare the behavior of Ca atoms with those of Al, Si and O atoms constructing the framework during the phase transition, structure factors are calculated from only Ca atoms (F_{Ca}) and from the other atoms except for Ca atoms (F_{oth}) of MD-simulated foAn in the heating experiments. The values of $|\langle F_{Ca}(025)\rangle|$ and $|\langle F_{oth}(025)\rangle|$ are selected as examples and are plotted against temperature (Fig. 3-3). Fig. 3-3 indicates that the amplitudes of the structure factors decrease gradually with increasing temperature up to Tc. At Tc, both of these values suddenly fall down to zero at the same time. To investigate the temporal variations of the structure factors at around the transition temperature in detail, MD simulation of further 30000 steps were calculated at 500K. The temporal variations of the real parts of the structure factors of $F_{Ca}(025)$ and $F_{oth}(025)$, whose imaginary parts are almost zero, are given in Fig. 3-4. The behavior of the real part of $F_{Ca}(025)$ (defined as $Re_{Ca}(025)$) is similar to that of the real part of $F_{oth}(025)$ (defined as $Re_{oth}(025)$). The values of the real parts of both structure factors are ranging between -35 ~ -45 until 10ps, then rapidly change to zero at the same time at around 13.5ps and finally become almost zero until 18ps. If the coupling between the Ca movement and the behavior of the framework is weak or loose like the models by Czank et al. (1973b) and by Redfern and Salje (1992), there may be possible cases such that the arrangement of Ca atoms keeps the $P\bar{1}$ symmetry but the framework changes to the $I\bar{1}$ structure, or vice versa. However, the present MD simulation reveals that the arrangement of Ca atoms and the framework transform simultaneously to $I\bar{1}$ structure at Tc. The present result suggests that the coupling between the Ca atoms motion and the

behavior of the framework is strongly operated during the transition.

In the fpci-simulation of the cooling experiments both Ca atoms and the framework have $I\bar{1}$ symmetry, while in ficp-simulations both have $P\bar{1}$. These results suggest the framework is more movable than Ca atoms. That is, in reverse experiments to low temperature the inflexible Ca atoms dominate the system because the coupling between the behavior of the framework and the Ca atoms motion is strong.

Fig. 3-5 shows the temperature dependencies of the standard deviations of x-, y- and z-atomic coordinates which are indexes of the magnitude of atomic vibration for each element (O, Si, Al, and Ca) in real space. The standard deviations for O, Si, and Al atoms obtained by the MD simulation increase gradually with temperature up to 1000K. In contrast, the standard deviations for Ca atom abruptly jump up to large values at Tc. These suggest that Ca atoms become to vibrate strongly at around the transition temperature and that the average positions of Ca atoms by this thermal vibration are shifted to those in the $I\bar{1}$ structure.

If the $I\bar{1}$ structure is a statical dynamical average of the $P\bar{1}$ type domains with ordered and anti-ordered Ca configurations as proposed by Van Tendeloo et al. (1989), the structure factors of c type reflections should have a repeat between the plus and minus values. However, such a repeat was not observed in the present study, although the repeats by the thermal vibrations are observed. The existence of the antiphase domain in a MD cell at each moment was not also confirmed. We conclude that the driving force for the phase transition is the coupling of a lattice distortion with the Ca motions similar to the model proposed by

Adlhart et al. (1980) and that the transition occurs displacively as proposed by Redfern and Salje (1992).

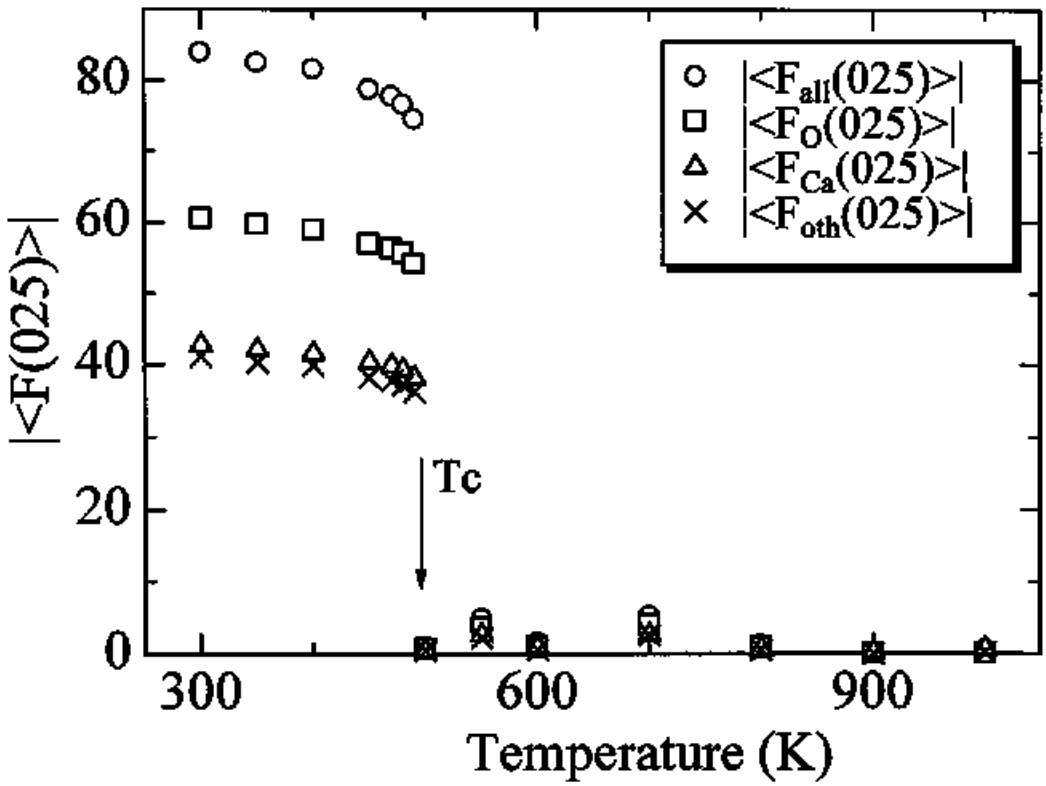

Fig. 3-3. Temperature dependencies of amplitudes of the structure factors; $|\langle F_{all}(025)\rangle|$, $|\langle F_{Ca}(025)\rangle|$, $|\langle F_{oth}(025)\rangle|$, and $|\langle F_{O}(025)\rangle|$, of the MD-simulated foAn. Tc; transition temperature.

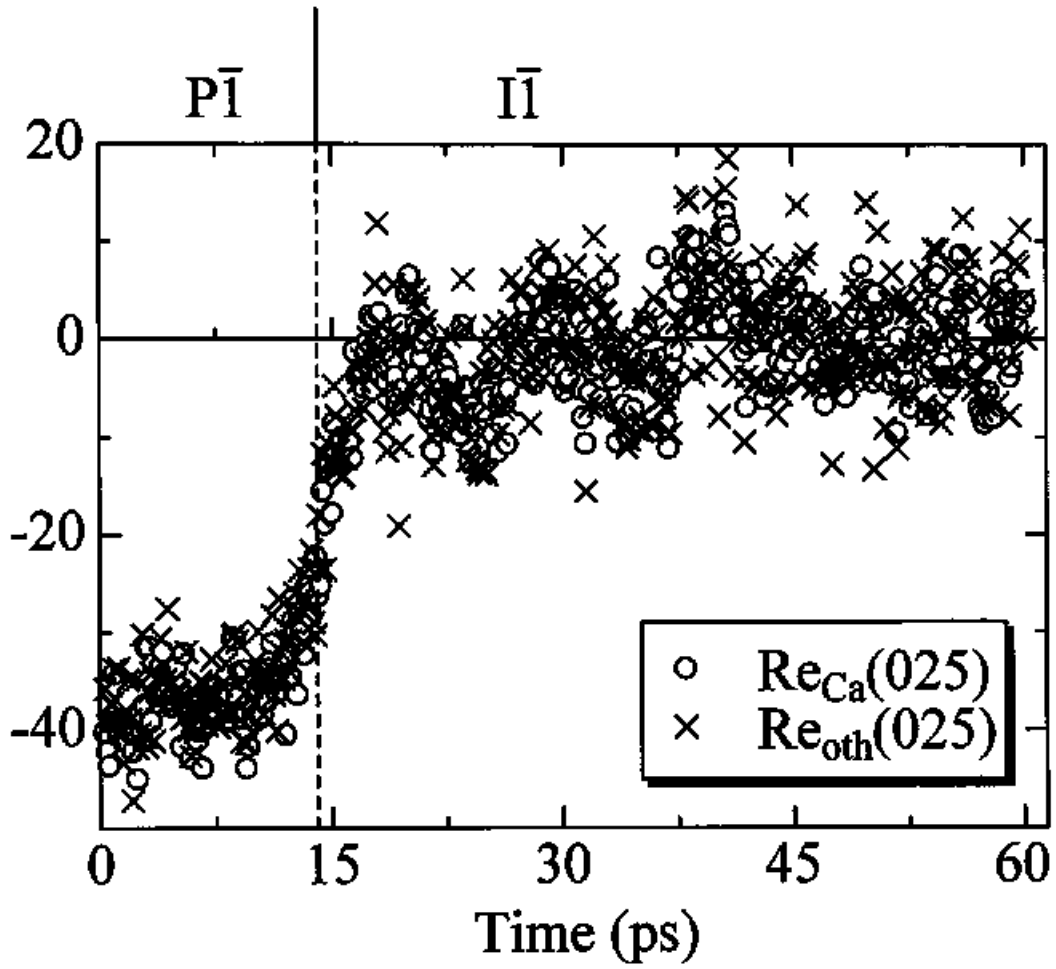

Fig. 3-4. Temporal variations of $Re_{ca}(025)$ and $Re_{oth}(025)$ of an MD-simulated foAn at 500K.

(For clarity every fourth sampling point of the data (300 samples) has been plotted.)

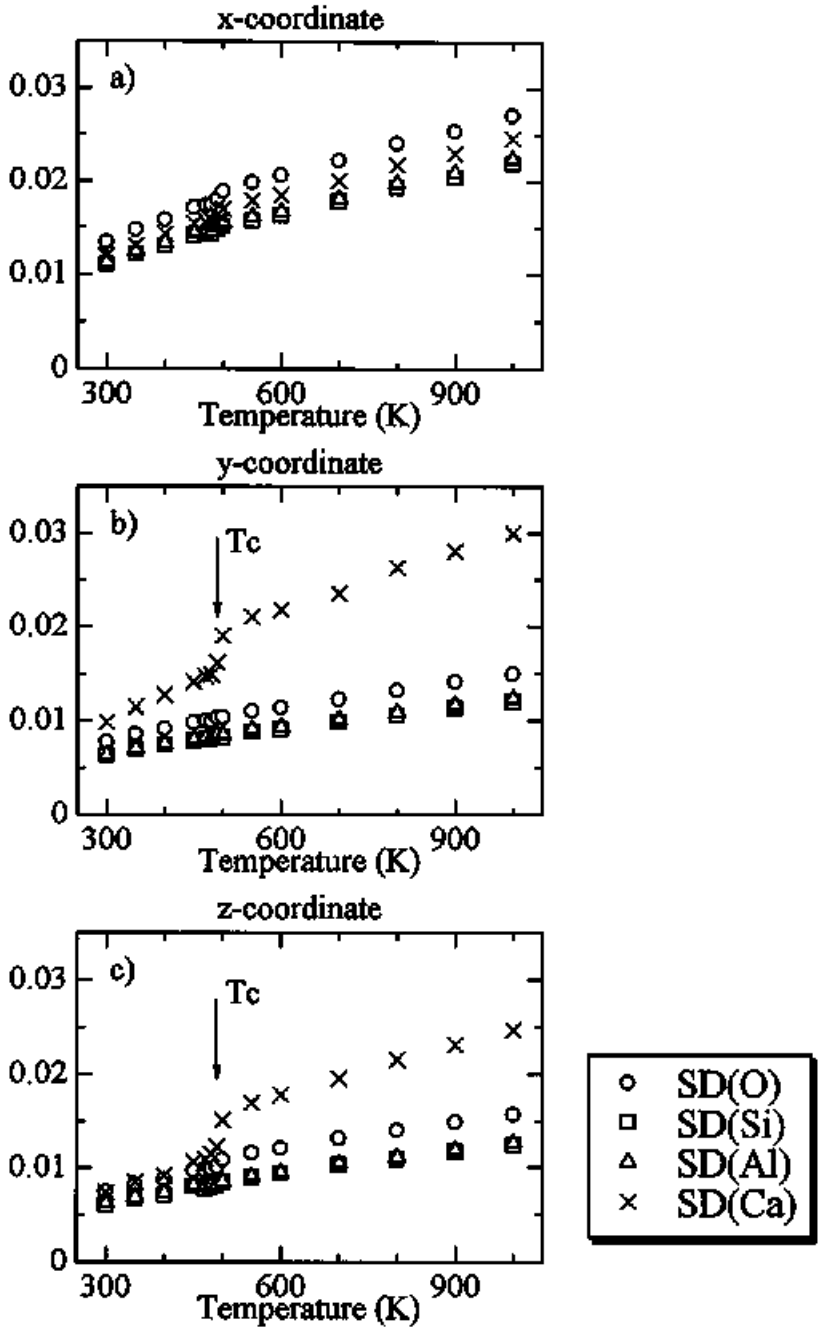

Fig. 3-5. Temperature dependencies of the standard deviation (SD) of a) x-, b) y- and c) z-atomic coordinates of O, Si, Al, and Ca atoms in the MD-simulated foAn. Tc; transition temperature.

3.3.3 The influence of Al/Si disorder on the $P\bar{1}$-$I\bar{1}$ phase transition

In order to investigate the influence of Al/Si disorder on the $P\bar{1}$-$I\bar{1}$ phase transition, the behavior of MD-simulated foAn with temperature change is compared with that of the MD-simulated pdAn. The MD-simulated pdAn has rather higher transition temperature (about 550K) than the MD-simulated foAn (Fig. 3-1b and 2). Furthermore, the discontinuity around transition temperature of the MD-simulated pdAn is not observed, while the MD-simulated foAn shows the discontinuity clearly. In order to clarify the continuous transition, structure factors of the MD-simulated pdAn are calculated in detail. Although the real part of <F(025)> has the negative sign below 500K, it changes to the positive sign at the range from 500K to about 550K (Table 3-6). This indicates that the structure in the temperature range from 500K to about 550K has the antiphase-shifted structure (the displacement vector **R** = 1/2[111]) as compared with the structure at 300K.

A special projection, described below, is employed to study the behavior of Ca atoms in the antiphase-shifted structure. There are four crystallographically non-equivalent positions of Ca atoms (Ca1, Ca2, Ca3, and Ca4) in the $P\bar{1}$ structure. First, the position of each Ca atom in a MD cell is projected on the position of its equivalent Ca atom in a unit cell. There are two crystallographically non-equivalent positions in the $I\bar{1}$ structure. In order to show the deviation of the positions in the $P\bar{1}$ structure from those in the $I\bar{1}$ structure, the projected positions of Ca atoms in a unit cell are further projected on two crystallographic positions by using the symmetry operation of 1/2[111] of the I-lattice. In the projection, each

Ca atom in a MD cell must be plotted on one of the two crystallographically non-equivalent positions, when the atoms are arranged following the symmetry operations of $I\bar{1}$, i.e., Ca1 and Ca3, and Ca2 and Ca4 overlap respectively. Figs. 3-6a~c show the histograms of the projected x-, y- and z-coordinates of Ca atoms in the MD-simulated pdAn. At 300K, the peaks of Ca1 and Ca3 and those of Ca2 and Ca4 appear separately. The relative positions of the peaks of Ca1 and Ca3, and Ca2 and Ca4 at 500K are exchanged from those at 300K (especially y- and z-coordinates in Figs. 6b and 6c). This result supports the formation of the antiphase-shifted structure at 500K.

The mechanism of the formation of the antiphase-shifted structure can be considered as below. Let assume a case where the whole structure tends to be the $I\bar{1}$ structure by both the thermal vibration of Ca atoms and the distortion of the framework. In the structure, some Ca atoms are attracted by and then localized around the oxygen atoms forming Al-O-Al linkages, because the thermal vibration of Ca is weaker than the bonding force between Ca and the O atoms. This localization of Ca atoms must distort the framework to have the $P\bar{1}$ symmetry, resulting in the formation of the antiphase-shifted structure. When the vibration becomes large enough to overcome the localization of Ca atoms at higher temperature than Tc, the whole structure will transform to the $I\bar{1}$ structure. Therefore, the formation of this antiphase-shifted structure can be considered to result in the shift of Tc to higher temperature.

As described above, the partly disordered anorthite does not show the behavior of a first order transition. The antiphase-shifted structure (the $P\bar{1}$ structure) and the $I\bar{1}$ structure coexist in the partially disordered anorthite at temperatures from 500K to 550K (Fig. 3-6).

The $P\bar{1}$ structure is more predominant than the $I\bar{1}$ structure at 500K and vice verse at 550K, as seen in the change of Ca positions in the MD-simulated pdAn at 500 and 550K (Fig. 3-6c). The change of relative abundance of the coexisting two structures with temperature can be considered to result in rather continuous structural change during the transition of the MD-simulated pdAn. This implies the possibility that anorthite with more disordered arrangement of Al/Si will show a tricritical or second-order phase transition.

Table 3-6. Real part of the structure factor of 025 reflection (defined as <Re(025)>) of the MD-simulated pdAn. <Re(025)> below 500K takes a negative sign and <Re(025)> from 500K to 550K takes a positive sign. Furthermore, <Re(025)> at 900K takes a value of about 10.

Temperature (K)	300	400	450	500	550	600	700	800	900	1000
<Re(025)>	-83.55	-79.17	-76.46	58.81	16.82	-1.31	-1.48	1.50	9.38	0.55

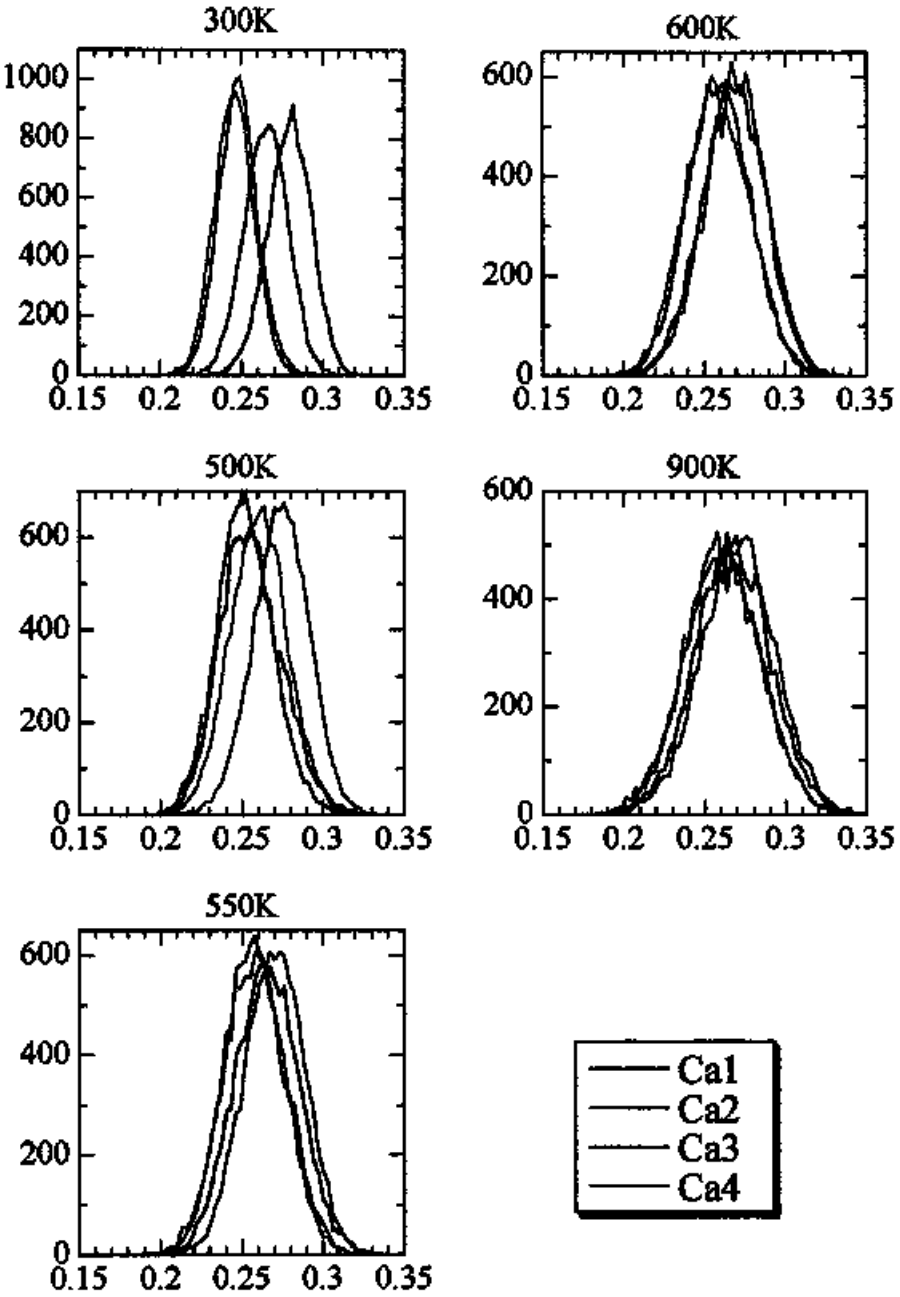

Fig. 3-6a. Histograms of projected x-coordinates of Ca atoms in the MD-simulated pdAn at 300, 500, 550, 600, and 900K.

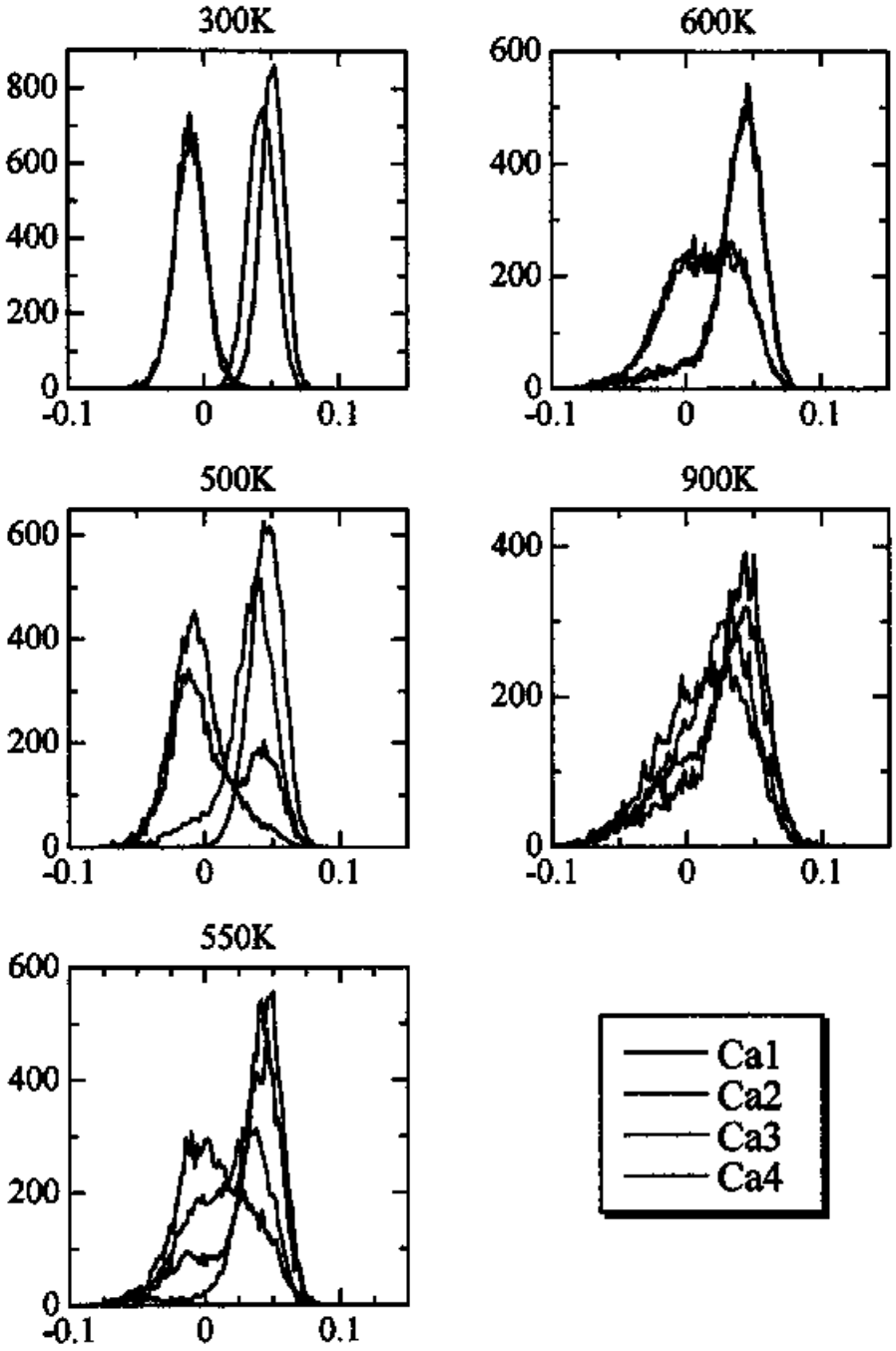

Fig. 3-6b. Histograms of projected y-coordinates of Ca atoms in the MD-simulated pdAn at 300, 500, 550, 600, and 900K.

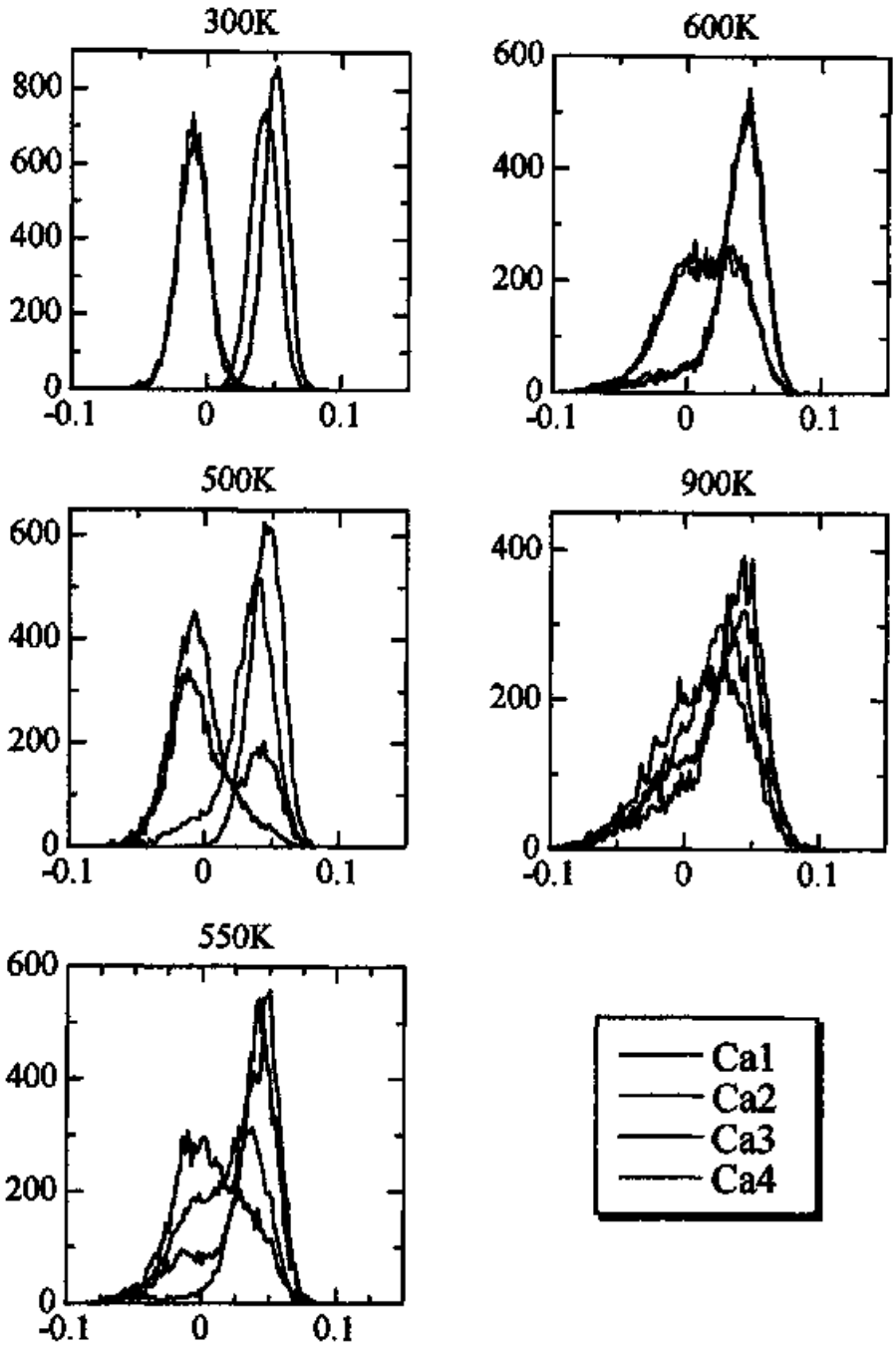

Fig. 3-6c. Histograms of projected z-coordinates of Ca atoms in the MD-simulated pdAn at 300, 500, 550, 600, and 900K.

3.3.4 Ca 'split' position

Czank et al. (1973b) considered a double well potential for the occupancy of Ca^{2+} ion in the structure of anorthite. In contrast, Van Tendeloo et al. (1989) proposed that above Tc, the $I\bar{1}$ structure is a statistical dynamical average of the $P\bar{1}$ type domains with ordered and anti-ordered Ca configurations, and considered that in the average structure above Tc, the framework atoms conform closely to the body-centered symmetry and the Ca atoms appear in split positions. In order to answer the question on the Ca 'split' position, the distribution of the Ca positions in the MD-simulated anorthite is investigated. And, the influence of Al/Si disorder on the Ca motion is discussed.

The histogram of the x-, y- and z-coordinates of Ca positions in the MD-simulated foAn (Fig. 3-7) was obtained by using the same projection method as described above. The fact that four peaks appear in different positions indicates that Ca atoms distribute at the four crystallographically non-equivalent sites at 300K. Above 500K where the stable phase has the $I\bar{1}$ structure, Ca1 and Ca3, and Ca2 and Ca4 overlap each other, respectively, and the shape of every peak is sharp (e.g., Fig. 3-7 at 600K). This means that there are no observable Ca 'split' positions. Furthermore, so far as we observed the time distribution of any Ca atom, two split peaks and the elongated peaks are not observable. The distribution of the time-averaged coordinate of Ca atoms at 600K (Fig. 3-8) indicates that the time-averaged position of Ca atoms keeps at the Ca site in the $I\bar{1}$ structure.

In the MD-simulated pdAn, on the other hand, positions of Ca1 and Ca3, and Ca2 and Ca4 overlap with each other, respectively (Fig. 3-6), as same as the MD-simulated foAn.

However, both peaks of Ca2 and Ca4 are flattened on the top or elongated at 600K. The distribution of the time-averaged coordinate of Ca atoms in the MD-simulated pdAn at 600K shows the split positions of the average coordinates, especially z-coordinate of Ca2 atoms (Fig. 3-9).

Averaged standard deviations of the movement of each Ca atom (Table 3-7) in the MD-simulated pdAn and foAn are almost the same, indicating the similar thermal vibration of Ca atoms in both structures. On the other hand, averaged standard deviation of the time-averaged coordinate of Ca atoms in the MD-simulated pdAn is larger than that in the MD-simulated foAn (Table 3-8). This means that Ca atoms in the MD-simulated pdAn and foAn occupy the multiple-sites and single site, respectively.

Furthermore, at 900K <Re(025)> is about 10 (Table 3-6) and Ca2 has slightly different peaks from Ca4. The elongated shapes of the peaks or slight difference in the peaks suggest the Ca 'split' positions. Existence of such Ca 'split' positions will explain the appearance of c-type reflections at higher temperature beyond Tc reported by Czank et al. (1973b) and Van Tendeloo (1989), and also implies the existence of oxygen atoms forming the Al-O-Al linkages, because the localization of Ca ions caused by the oxygen results in the elongated distribution of Ca atoms in the histogram (Fig. 3-6).

Table 3-7. Time-averages of standard deviation of coordinates of Ca atoms at 600K.

	X	Y	Z
fully ordered An	1.85×10^{-2}	2.18×10^{-2}	1.78×10^{-2}
partly disordered An	1.90×10^{-2}	2.28×10^{-2}	1.86×10^{-2}

Table 3-8. Standard deviations of time-averaged coordinates of a) Ca1 and Ca3, and b) Ca2 and Ca4 atoms at 600K.

a) Ca1 and Ca3

	X	Y	Z
fully ordered An	1.72×10^{-3}	3.92×10^{-3}	3.59×10^{-3}
partly disordered An	3.69×10^{-3}	1.28×10^{-2}	1.00×10^{-2}

a) Ca2 and Ca4

	X	Y	Z
fully ordered An	1.13×10^{-3}	3.42×10^{-3}	3.12×10^{-3}
partly disordered An	4.25×10^{-3}	9.94×10^{-3}	9.52×10^{-3}

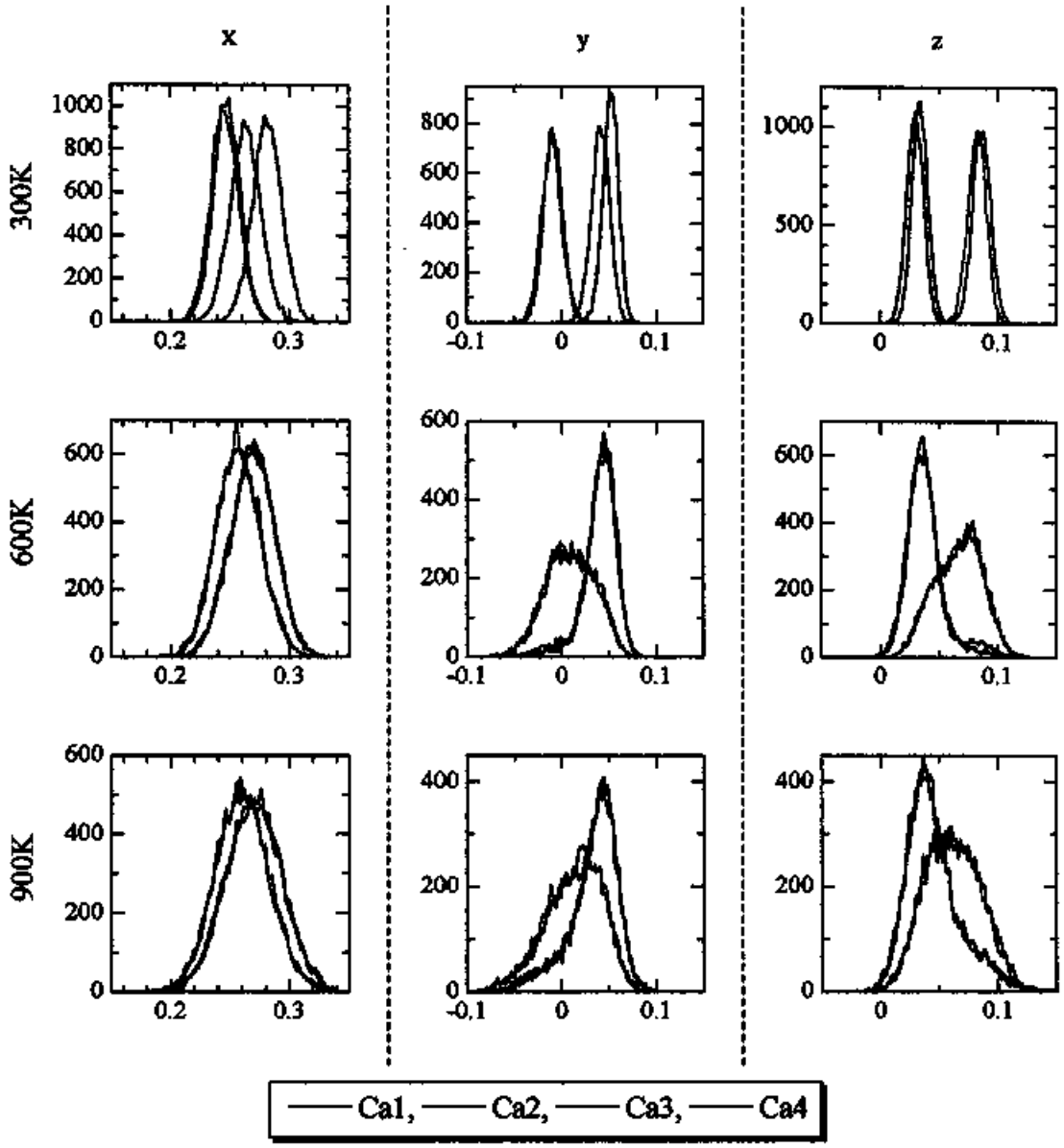

Fig. 3-7. Histograms of projected x-, y- and z-coordinates of Ca positions in the MD-simulated foAn at 300, 600 and 900K.

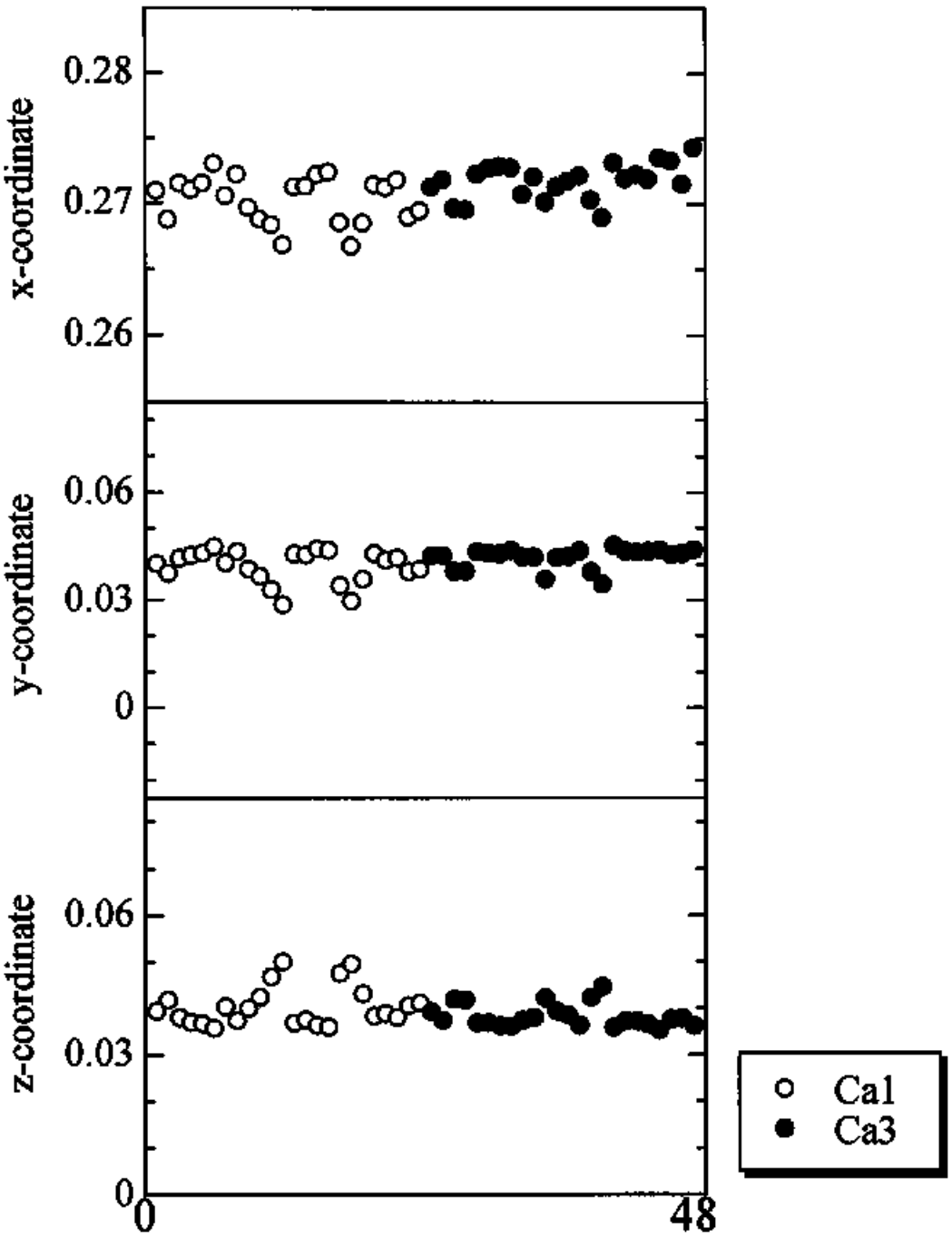

Fig. 3-8a. Time-averaged coordinate of Ca1 (24atoms) and Ca3 (24atoms) in the MD-simulated foAn at 600K. Horizontal axis is arbitrary scale and shows sampling number of Ca.

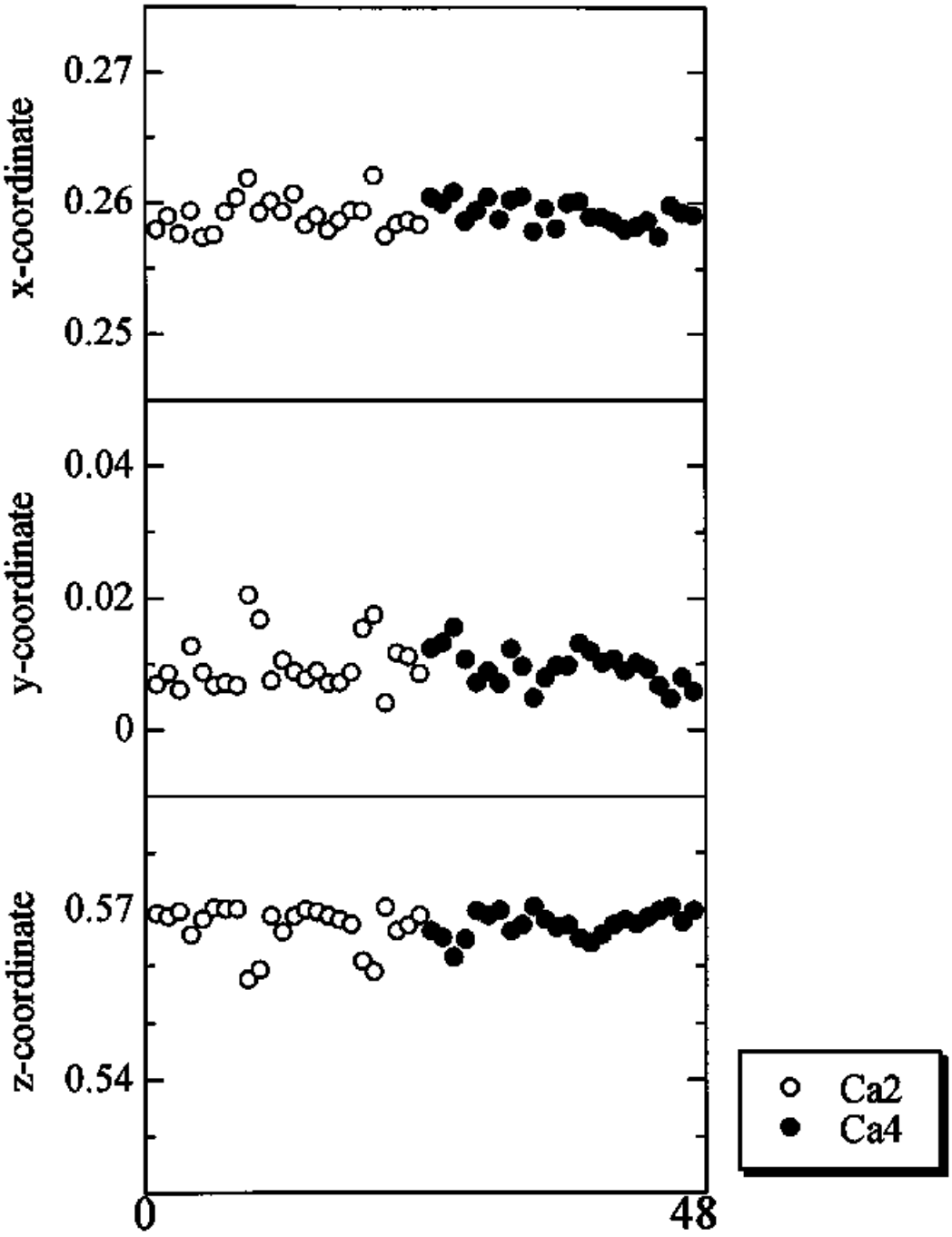

Fig. 3-8b. Time-averaged coordinate of Ca2 (24atoms) and Ca4 (24atoms) in the MD-simulated foAn at 600K. Horizontal axis is arbitrary scale and shows sampling number of Ca.

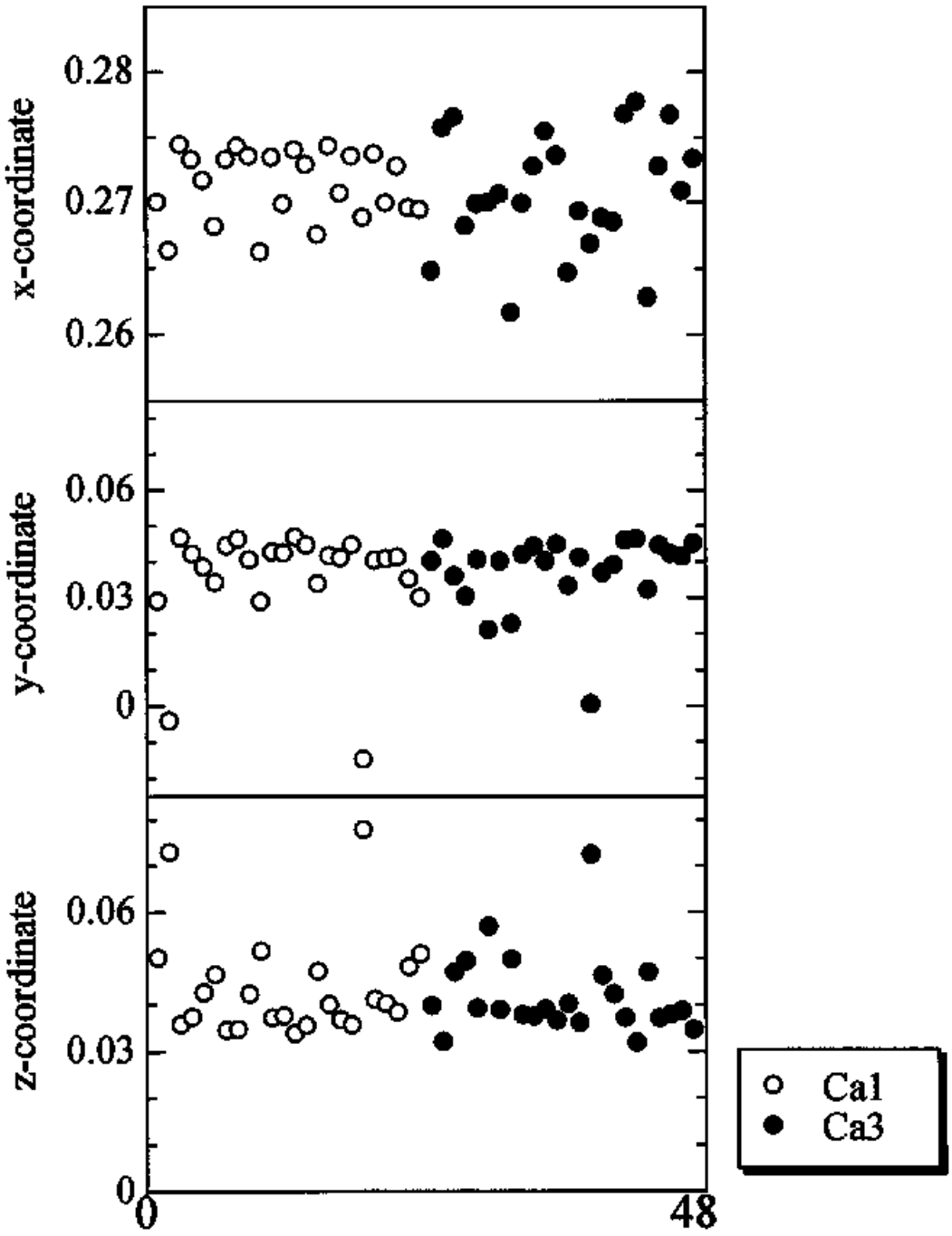

Fig. 3-9a. Time-averaged coordinate of Ca1 (24atoms) and Ca3 (24atoms) in the MD-simulated pdAn at 600K. Horizontal axis is arbitrary scale and shows sampling number of Ca.

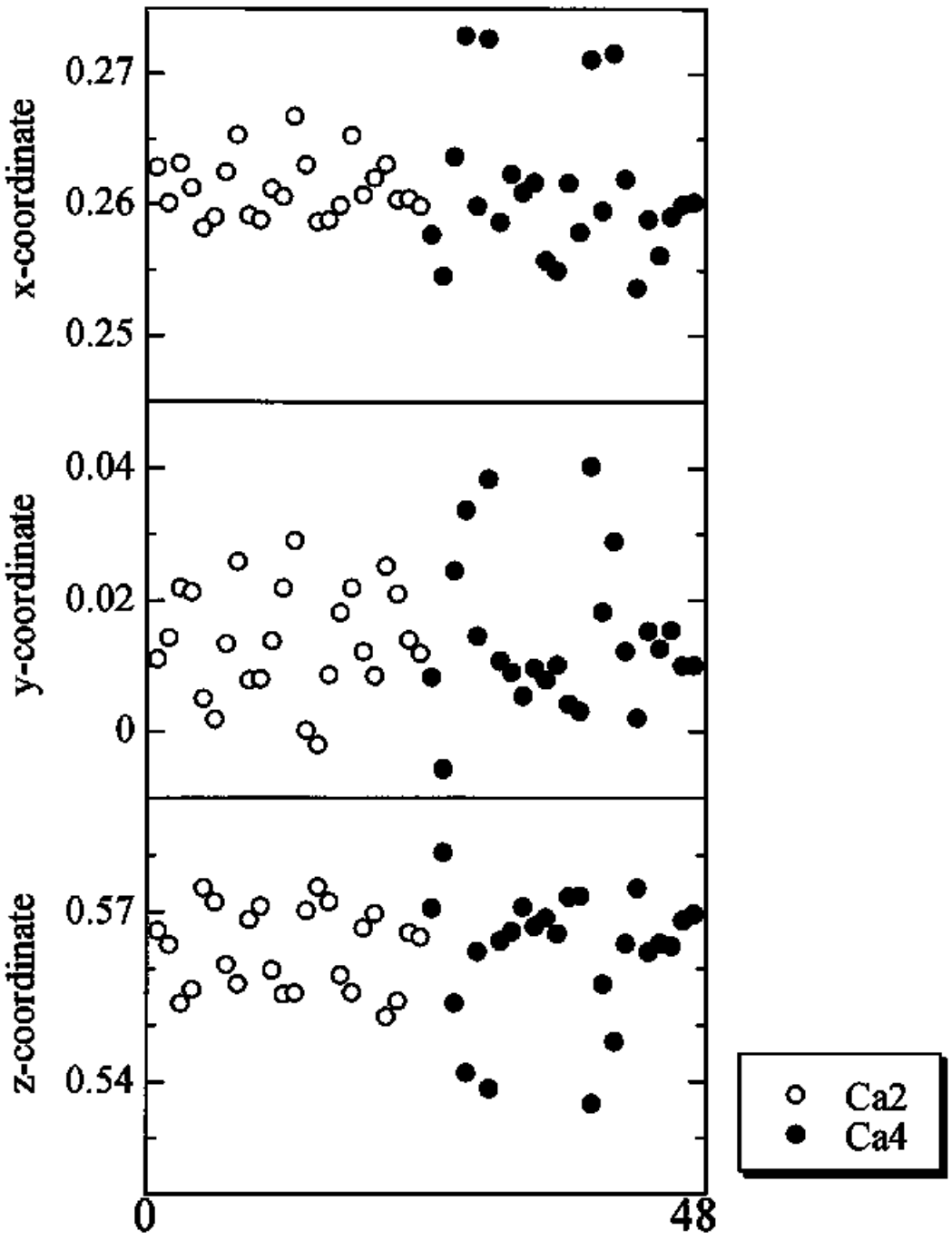

Fig. 3-9b. Time-averaged coordinate of each Ca2 (24atoms) and Ca4 (24atoms) in the MD-simulated pdAn at 600K. Horizontal axis is arbitrary scale and shows sampling number of Ca.

4. Pure Albite

4.1 Introduction

Pure albite has been thought to have four polymorphs; low-albite, high-albite, analbite and monalbite. Low-albite has the space group of $P\bar{1}$ with the ordered arrangement of Al/Si in tetrahedral sites. High-albite also has the space group of $P\bar{1}$ but the disordered arrangement of Al/Si. Both low- and high-albites do not become monoclinic even when they are heated at high temperature in laboratories. Analbite has the same space group and the similar ordering of Al/Si to high-albite, but becomes monoclinic (C2/m) at high temperature. Analbite has been thought to be a metastable phase formed by cooling of monalbite. Monalbite is a high temperature form of albite and has the space group of C2/m and the disordered arrangement of Al/Si.

Numerous attempts have been made to clarify the phase relation and phase transitions among four polymorphs (for a historical review, see Smith, 1974; Ribbe, 1983; Smith and Brown, 1988). Until the mid 1980's, two processes have been related with the phase transitions among four polymorphs; the displacement of atomic positions and the Al/Si ordering in tetrahedral sites. These two processes have been considered to operate independently: the displacement of atomic positions causes the structural collapse of the high temperature monoclinic C2/m structure to the triclinic $C\bar{1}$ structure (monalbite ⇒ high albite), and the sluggish Al/Si ordering process causes the transition from high- to low albite without changing the triclinic symmetry.

Many high temperature experiments of natural and synthetic albite have been made on the phase transitions of natural and synthetic crystals of albite, especially the displacive phase transition from monalbite to high albite (e.g., Grundy and Brown, 1969; Prewitt et al., 1976; Winter et al., 1979; Kroll et al., 1980). The experimental results show that only albite with the highly disordered arrangement of Al/Si undergoes a monalbite - high albite transition at around 1223-1253K.

In contrast, the phase transition related with the Al/Si ordering process can not be studied experimentally in laboratories because of the sluggishness of the process. The transitions have then been studied by theoretical approaches such as the Bragg-Williams approximation. As well-known, indicates that the phase transition of a A_3B_1 compound caused by the ordering of A/B atoms in one crystallographic site is of a first order. Therefore, when the phase transition between low- and high-albites is caused only by the ordering of $AlSi_3$ in four T-sites, it must be of a first order. The equilibrium distribution of Al/Si in the albite framework was calculated by using the quasi-chemical method similar to the Bragg-Williams approximation (Senderov, 1980). The result shows that the equilibrium degree of order between low- and high-albites changes abruptly within a narrow temperature range, suggesting a first order transition. Then, a first order transition has been stressed on the phase transition between low- and high-albites (Ribbe, 1983; Smith, 1983).

Salje (1985) and Salje et al. (1985) first studied the effect of coupling of the displacive transition and the Al/Si ordering process to the phase transitions among polymorphs of albite. In their studies, the thermodynamic properties of Na-rich feldspars are expressed by a Landau-type free energy expansion with two order parameters; Q and Q_{od}. Q represents the rapid lattice distortion, which is observed in the monalbite analbite transition, and Q_{od} the

very sluggish Al/Si ordering. Based on the Landau theory, they showed that both order parameters are involved in the structural phase transition monalbite albite near 1250K. Furthermore, they present that the phase transition (thermal crossover) between high- and low-albites is found to be a non-first order transition and the thermal crossover is a smooth function of temperature similar to a structural phase transition although the symmetry is the same for both $C\bar{1}$. Non-first order transition between low- and high-albites is also supported by the fact that the degree of Al/Si order estimated by the parameter $2\theta(131)$-$2\theta(1\bar{3}1)$ in the powder X-ray diffraction (Goldsmith and Jenkins, 1985).

Salje et al. (1985) calculated a Landau-type free energy expansion using the data of cell parameters of albite with the only low degree of Q_{od} (Q_{od} = 0 ~ 0.25). It is necessary to discuss using the data of albite with high degree of Q_{od}. The starting material controlled the degree of Q_{od} can not been made and it is difficult for Q_{od} to arrive at the equilibrated degree in the laboratories, because the diffusion of Al and Si is extreme sluggishness. And the important point is whether there is the phase transition (thermal crossover) between high- and low-albite or not, although space group keeps $C\bar{1}$ through the phase transition. On the other hand, any degree of Q_{od} can be chosen at an initial stage of MD simulation and Al atoms and Si atoms through the calculation of MD simulation are not exchanged. Therefore, MD simulations of albite with nine kinds of different Q_{od} (Q_{od} = 0 ~ 1) were carried out to investigate thermodynamic behaviour of albite, the correlation between the lattice distortion and Al/Si disordering through both phase transitions, and whether there is the phase transition (thermal crossover) or not. The results of MD simulations were analysed using Landau-type free energy expansion with two order parameter proposed by Salje et al. (1985).

One of the persistent questions related with the crystal structure of albite has been on the behaviour of Na atom. Ferguson et al. (1958) reported that albite shows the positional disorder of Na at room temperature quantified by 'half-atoms' separated by ~0.1 Å in low-albite and ~0.6 Å in high-albite. Quareni and Taylor (1971) concluded that the Na in low-albite was a single atom subject to thermal vibration. This conclusion was confirmed by Smith et al. (1986), who found that the electron density distribution of Na atoms in low-albite was slightly anisotropic at 13 K, and its isotropic temperature factor extrapolated to 0 K was 0.5 $Å^2$ Using other near-zero-Kelvin neutron studies, Smith et al. (1986) argued that zero-point motion is the preferred cause rather than multiple centeres of motion in low albite.

However, it has been decided which is the positional disorder or the thermal disorder, because the motion of Na atoms can not be observed directly in the experiments using natural and synthetic specimens. Because it is difficult to make fully ordered albite with $Q_{od} = 1$ and the natural and synthetic specimens has Al/Si disorder, it must consider the influence of Al/Si order on the nature of Na atoms at low temperature. Therefore, MD simulations of not only a fully ordered albite but disordered albite were carried out to investigate the nature of Na atoms at low temperature and the influence the Al/Si order on the nature of Na atoms, because it can be observed the motion of Na atoms at the atomistic level.

4.2 Thermodynamic behaviour of MD-simulated albite

4.2.1 Procedure

In the present study, several kinds of crystal structures of pure albite by changing the Al/Si order were simulated to investigate their thermodynamic properties. Al and Si atoms are distributed in tetrahedral sites (T-sites) of initial structure of MD crystals by assuming two basic regulations. One is the *Al-avoidance rule* and another is the relation of the number of Al in four T-sites; T1o≥T1m=T2o=T2m (Ribbe, 1994). The order parameter for the Al/Si ordering is Q_{od}=(T1o-T1m)/(T1o+T1m) defined by Salje (1985). MD simulations of the crystal structures with nine different order parameters; Q_{od}=0 (fully disordered albite; fdAb), 0.080, 0.222, 0.400, 0.500, 0.588, 0.737, 0.909, and 1 (fully ordered albite; foAb), were carried out in the present study. Starting from the atomic positions of albite experimentally determined by Winter et al. (1977), an MD-simulated albite was annealed for 20ps (10000 steps) at 300K so as to obtain an initial configuration in each MD-simulated albite with the different Q_{od}. These MD-simulated albite were used as starting structures for further MD calculations at all other temperatures. After heating each starting structure up to a desired temperature, the resulting structure was 'annealed' for at least 20ps (10000 steps), to obtain an equilibrium atomic configuration. After attaining equilibration, a production run of 20ps (10000 steps) was performed, and various properties and atomic positions were, then, evaluated. In the present study, a temperature range of 300-1800K was investigated, while pressure was maintained at 1atm throughout the MD calculations. The unit cell used in the present MD calculation (MD cell) is parallelepiped and the number of

atoms in the system was 1248 (containing 24 crystallographic unit cells of albite; $a_{MD}=3a_{ab}$, $b_{MD}=2b_{ab}$, $c_{MD}=4c_{ab}$). Table 4-1 shows MD simulations of albite carried out in the present study.

Table 4-1. MD simulations of albite carried out in the present study to investigate thermodynamics behavior are tabulated as follow;

MD simulation	fully ordered Ab	disordered Ab	full disordered Ab
Abbreviation	foAb		fdAb
Al/Si ordering parameter (Q_{od})	1	0.080, 0.222, 0.4 0.5 0.588 0.737, and 0.909	0
Al-avoidance rule	O	O	O
Pauling rule	O	O	O
Temperature	300K 1800K	300K 1800K	300K 1800K
Purpose	Thermodynamics behavior	Thermodynamics behavior	Thermodynamics behavior
number of atoms	1248	1248	1248

4.2.2 Result

Cell parameter of MD-simulated albite

Cell parameters obtained from the MD-simulated foAb (Q_{od} = 1) at 300K show good agreement with those of a real crystal of albite determined by Winter et al. (1977) (Table 2-2 or Table 4-2). The temperature dependencies of the cell parameters of the MD-simulated foAb are compared with those of a real albite measured by an X-ray method (Winter et al., 1977) (Figs. 4-1). The lengths of a-, b-, and c-axes by MD simulations increase gradually with temperature up to 1800K. The α, β, and γ angles decrease gradually with temperature up to 1800K. These tendencies are similar to those of a real albite.

The temperature dependencies of the cell parameters of the MD-simulated disordered albite with different Q_{od} are shown in Fig. 4-2. The lengths of a-, b-, and c-axes of all MD-simulated disordered albite increase gradually with temperature up to 1800K as same as those of MD-simulated foAb. The β angles of all MD-simulated disordered albite decrease gradually with temperature up to 1800K as same as that of the MD-simulated foAb. The α angles of all MD-simulated disordered albite except for the MD-simulated fdAb decrease gradually with temperature up to 1800K. That of the MD-simulated fdAb decreases gradually with temperature up to about 1000K and has constant value, 90°, above this temperature. The γ angles of the MD-simulated disordered albite with Q_{od} =1, 0.909, 0.737, and 0.588 decrease gradually with temperature up to 1800K, those with Q_{od} =0.5, and 0.4 are almost constant, and those with Q_{od}=0.222 and 0.080 increase gradually with temperature up to certain temperature and are constant value above these temperature. That of the MD-

simulated fdAb increases gradually with temperature up to about 1000K and has constant value, 90°, above this temperature.

Crystal symmetry and structure factor of MD-simulated albite

Space group of real albite in the fully ordered state is $C\bar{1}$. The conditions for possible reflections, the extinction rule, for *hkl* reflections are *h+k=even*. Structure factors of the MD-simulated foAb simulated at 300K were calculated. The result shows that $|\langle F_{MD}(hkl)\rangle|$ with *h+k=odd* are negligible small, indicating the extinction rule described above. The behaviour of the structure factors indicates that the space group of an MD-simulated foAb is $C\bar{1}$.

The space group of real albite in the fully disordered state at high temperature is C2/m. The condition for possible reflections, the extinction rule, for *hkl* reflections are *h+k=even*, too. And further, two structure factors with indices of *hkl*, and $h\bar{k}l$ are symmetrically equivalent. Structure factors of the MD-simulated fdAb calculated above 1000K show that $|\langle F_{MD}(hkl)\rangle|$ with *h+k=odd* are negligible small and $|\langle F_{MD}(hkl)\rangle|$ with *h+k=even* is not negligible, indicating the extinction rule described above. One of the examples is shown in Fig. 4-3, where $F_{MD}(131)$ and $F_{MD}(1\bar{3}1)$ at 300 and 1300 K are plotted. And $|\langle I_{MD}(131)\rangle - \langle I_{MD}(1\bar{3}1)\rangle|$ (defined as $\Delta I(131)$) is plotted against temperature in Fig. 4-4, because $\langle I_{MD}(131)\rangle$ is not equal to $\langle I_{MD}(1\bar{3}1)\rangle$ in $C\bar{1}$ and $\langle I_{MD}(131)\rangle$ is exactly equal to $\langle I_{MD}(1\bar{3}1)\rangle$ in C2/m as described above. As seen in the figure, the two structure factors have the same amplitude and are plotted in same regions at 1300K (Fig. 4-3). $\Delta I(131)$ decreases abruptly around 900K and then becomes almost zero above 1000K (Fig. 4-4). The behaviour of structure factors indicates that an MD-simulated fdAb has C2/m structure. Transition temperature (T_c^{od}) from

$C\bar{1}$ to C2/m of an MD-simulated albite is estimated to be about 950K, while T_c^{od} of a real albite is about 1250K (Kroll et al., 1980). Structure factors of the MD-simulated disordered albite with the other Q_{od} show that they do not transformed to monoclinic phase.

Table 4-2. Lattice parameters of natural low-albite obtained by an X-ray method (Winter et al., 1977) and those by the MD-simulated foAb at 300K, 1atm.

	a (Å)	b (Å)	c (Å)	α (°)	β (°)	γ (°)	ρ (g/cm^3)
X-ray	8.152	12.784	7.165	94.28	116.67	87.74	2.621
simulation	8.055	13.089	7.323	95.509	117.554	88.194	2.557

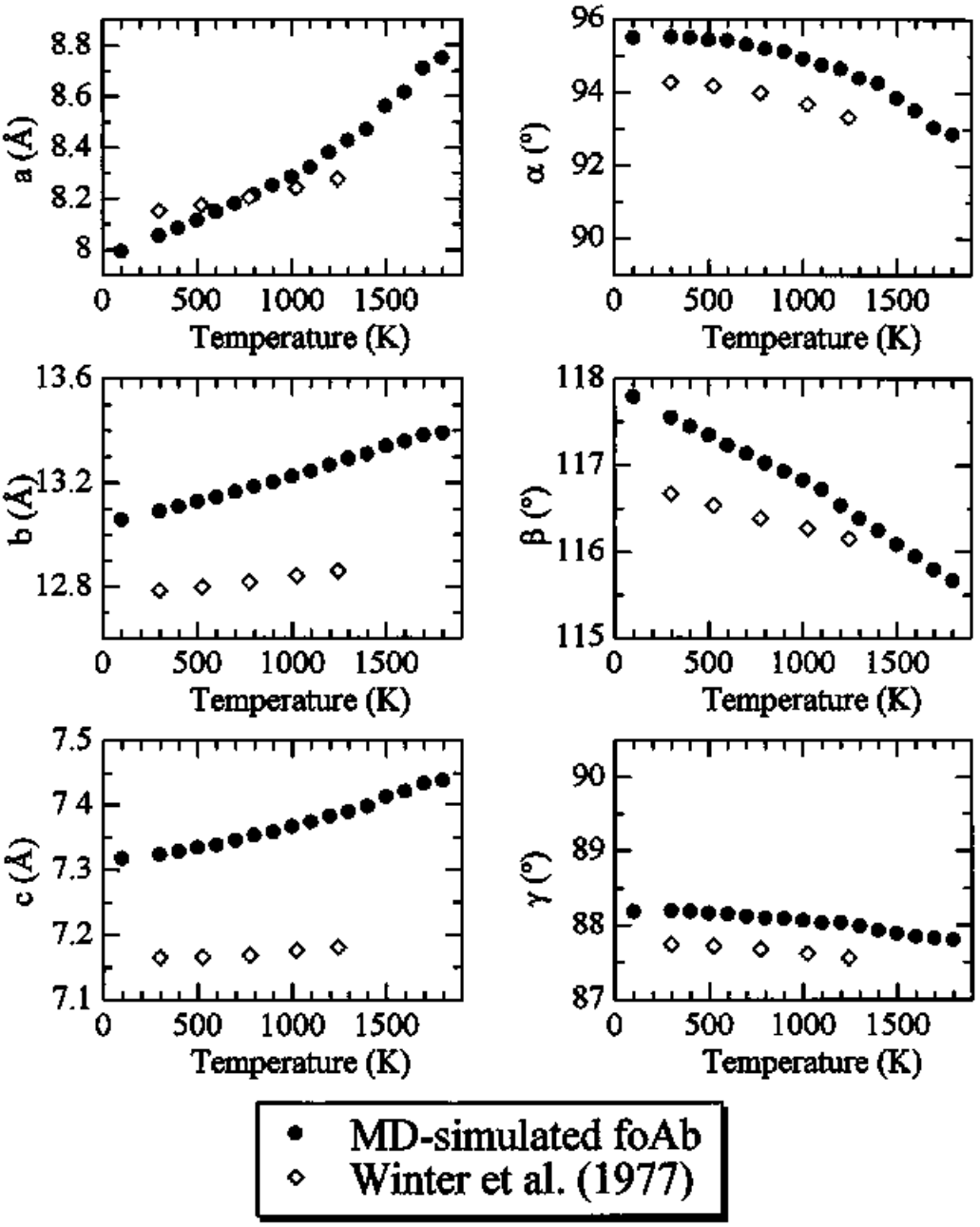

Fig. 4-1. Temperature dependencies of cell parameters of natural low-albite (Winter et al., 1977) and an MD-simulated foAb.

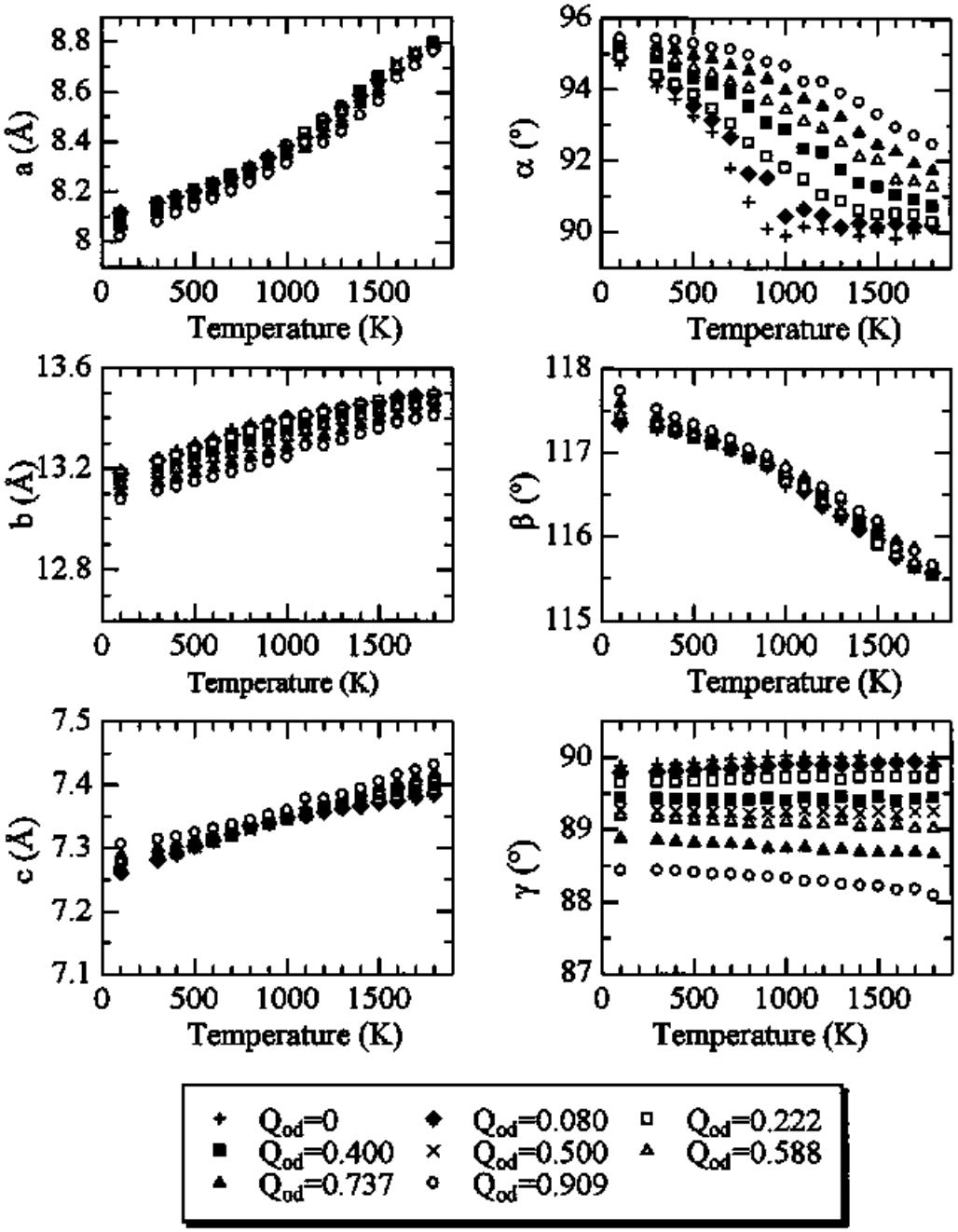

Fig. 4-2. Temperature dependencies of cell parameters of the MD-simulated disordered crystals of albite with different degrees of an order parameter Q_{od} for the Al/Si ordering.

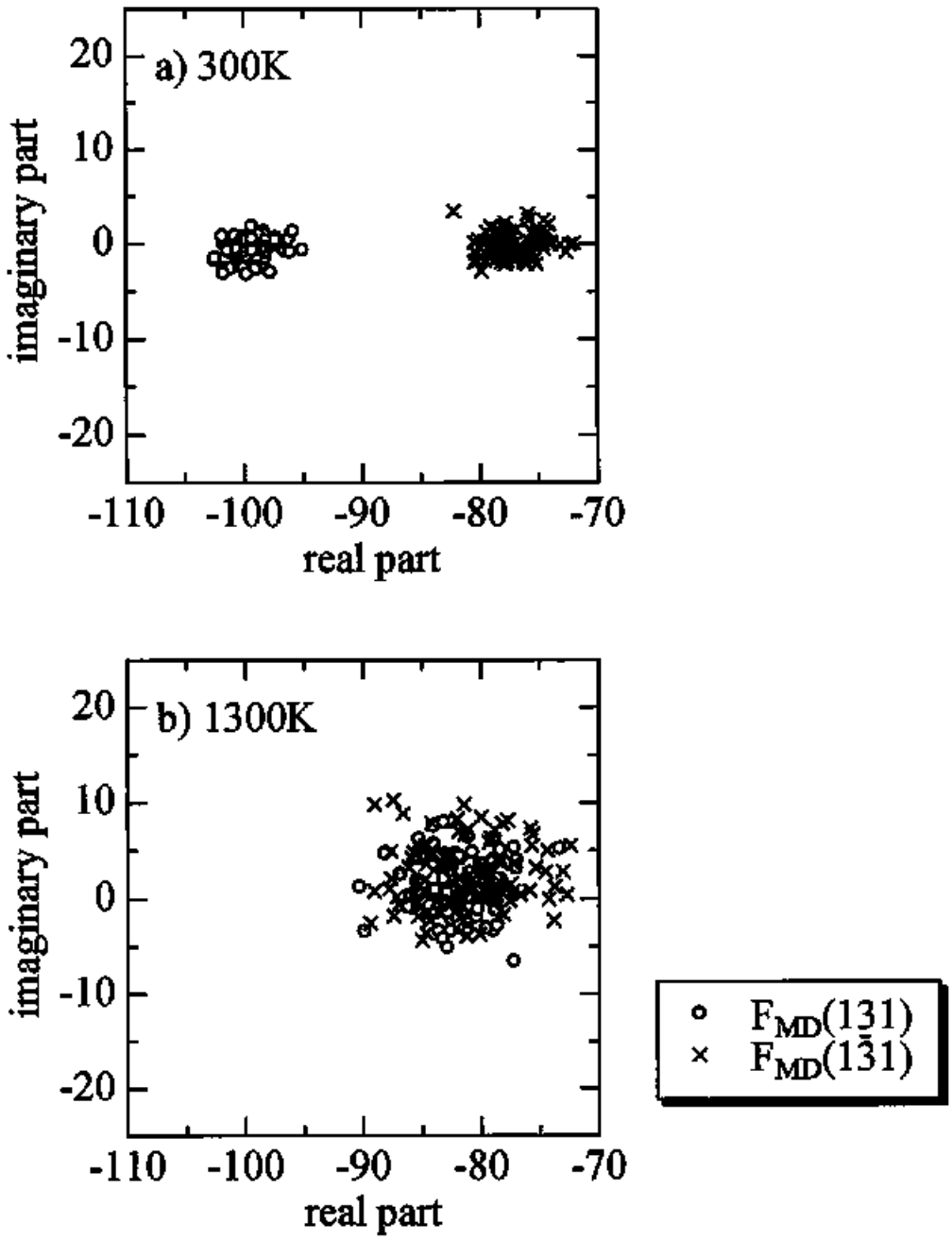

Fig. 4-3. Two structure factors $F_{MD}(131)$, and $F_{MD}(1\bar{3}1)$, plotted in the Gaussian coordinates, at a) 300, and b) 1300 K. For clarity the factors in every fourth sampling point of the data (50 samples) are plotted.

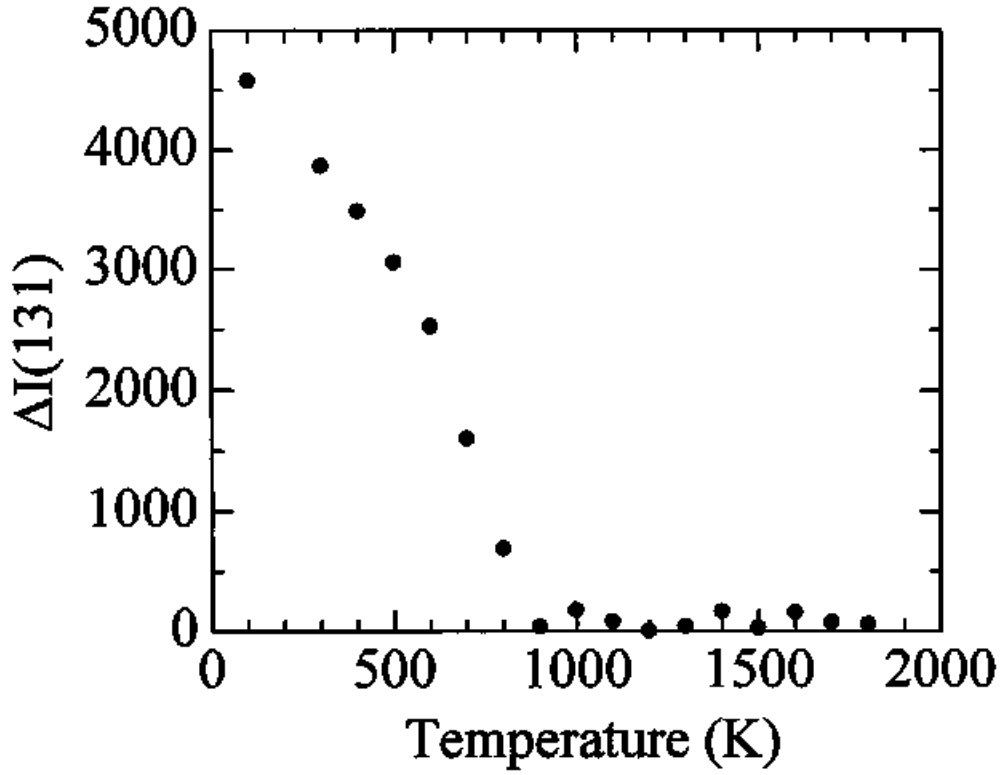

Fig. 4-4. Temperature dependence of the difference of amplitudes of two structure factors; $\Delta I(131)$ ($= |\langle I_{MD}(131)\rangle - \langle I_{MD}(1\bar{3}1)\rangle|$).

4.2.3 Discussion

Thermodynamics behaviour of MD-simulated albite

In general, the spontaneous strain associated with the phase transition C2/m-C$\bar{1}$ has only two components (Salje, 1985; Salje et al., 1985):

$$x_4 = -\frac{c}{c_0}\cos\alpha^* \qquad (1)$$

and $$x_6 = -\frac{b}{b_0}\cos\gamma, \qquad (2)$$

where the parameters with the subscript 0 are those predicted by extrapolation of the high symmetry phase and the parameters without subscript are those of the low symmetry phase. Salje et al. (1985) used the cell parameters of the monoclinic phase at temperature just above the transition temperature as c_0 and b_0, because temperature dependencies of the cell parameters of the monoclinic phase can not obtained in the experiments using the natural and synthetic albite. In the present study, the lattice parameters of the monoclinic phase can obtained and c_0 and b_0 are estimated using the data above 1000K in the MD-simulated fdAb (Q_{od}=0):

$$b_0 = 1.218\times10^{-4}T + 13.287 \qquad (3)$$

$$c_0 = 4.702\times10^{-5}T + 7.299 \qquad (4)$$

The values of x_4 and x_6 are determined by using the equations (1) ~ (4). The temperature dependencies of the strain parameters x_4 and x_6 for different degrees of order (Q_{od}) are shown in Fig. 4-5.

Both spontaneous strain tensors depend explicitly on the order parameters. In the case of albite, there is a linear dependence (Salje, 1985; Salje et al., 1985):

$$x_4 = AQ + BQ_{od} \qquad (5)$$

$$x_6 = CQ + DQ_{od} \qquad (6)$$

The coefficients *A, B, C,* and *D* are determined as below.

At absolute zero temperature, the order parameter of the lattice distortion Q, is 1 and we can rewrite equations (5) and (6) as

$$x_4 = A + BQ_{od} \qquad (5')$$

$$x_6 = C + DQ_{od} \qquad (6')$$

The values of x_4 and x_6 at absolute zero temperature can be obtained by extrapolating the data for each Q_{od} in Fig. 4-5. The coefficients *A, B, C,* and *D* are determined from the Q_{od} dependence of these values by the least square method using equation (5') and (6') as;

$$A = -1.02\times10^{-1}$$

$B = 6.23\times10^{-3}$

$C = -2.87\times10^{-5}$

$D = 2.79\times10^{-2}$

For the calculation of the order parameters from the strain components x_4 and x_6, we use the inverse relation;

$$Q = -9.80x_4 + 2.19x_6 \qquad (7)$$

$$Q_{od} = -1.01\times10^{-2}x_4 + 35.84x_6 \qquad (8).$$

The order parameter of the lattice distortion, Q, depends strongly on x_4 whereas the order parameter of the Al, Si ordering, Q_{od}, is largely determined by x_6. Two order parameters are able to be determined directly from the measured lattice parameters. In the present study, Q_{od} is already known because we chose an Al/Si distribution in the initial structure for the MD simulations. Therefore, only Q is estimated by using equation (7).

The temperature dependencies of Q for different Q_{od} estimated from the present MD simulation (Fig. 4-6a) show similar tendency of those of Salje et al. (1985) (Fig. 4-6b). Q values in the MD-simulated albite with fixed Q_{od}=0 decrease continuously with temperature up to about 900K and then become to be zero above 900K. This shows that the phase transition from monoclinic to triclinic phase of albite, as far as Q_{od} is maintained to be zero (i.e., analbite monalbite phase transition), is a nearly 2nd order phase transition. This transition temperature is estimated to be about 900K, while it is lower than 1251K estimated by the heating experiments (Kroll et al., 1980).

To know which MD-simulated polymorph is stable under a certain condition, it is necessary to estimate the free energy, G, of the MD-simulated structures. In general, entropy of a system in a given state is given by a combination of the configurational entropy, the vibrational entropy, the spin entropy, and the others. Unfortunately, the spin entropy can not be estimated in the MD simulation method, and the vibrational entropy is also difficult to be estimated because temperature and pressure of a system in MD simulations are controlled by scaling particle velocities and the cell lengths. Therefore, only the configurational entropy, $S_{conf}^{Al/Si}$, of MD-simulated crystals is calculated in the present study. It is difficult to evaluate $S_{conf}^{Al/Si}$ when the distribution of Al/Si satisfies *Al-avoidance rule*. In the present study, therefore, $S_{conf}^{Al/Si}$ of MD-simulated crystal with the Al/Si configuration violating the *Al-avoidance rule* is calculated as below;

$$S_{conf}^{Al/Si} = aR\{3\cdot(N_{T1m}\ln N_{T1m} - T1m\ln T1m - (N_{T1m} - T1m)\ln(N_{T1m} - T1m)) + (N_{T1o}\ln N_{T1o} - T1o\ln T1o - (N_{T1o} - T1o)\ln(N_{T1o} - T1o))\},$$

where R is the gas constant (8.31 $Jmol^{-1}K^{-1}$), a the scaling factor in the present MD simulations, N_{T1m} and N_{T1o} the number of T1m- and T1o-sites in MD cell respectively, and $T1m$ and $T1o$ the number of Al atoms in T1m- and T1o-sites respectively. The enthalpy of the MD-simulated albite, H, is estimated as;

$$H = U + K + PV,$$

where U is the potential energy, K the kinetic energy, P pressure of the MD simulation, and V the volume of the MD-simulated albite.

The free energy (G) of the MD-simulated albite is then assumed to be $G = H - TS_{conf}^{Al/Si}$ in the present study. Table 4-3 shows temperature dependencies of G for different degrees of the Al/Si order (Q_{od}). The values of G under thermal equilibrium conditions must have the minimum value at each temperature (shaded in Table 4-3). The values of Q_{od} under thermal equilibrium conditions are determined numerically from the table, and further the values of Q are also estimated numerically from Fig. 4-6. The temperature dependencies of Q and Q_{od} at equilibrium are plotted separately in Fig. 4-7a. Above the transition temperature, 1400K, only a stable phase has $Q = Q_{od} = 0$ and must be the monoclinic phase (C2/m). The temperature for the transition between phases in thermal equilibrium states is much higher than the transition temperature between phases with the fully disordered Al/Si distribution, i.e., the transition between analbite and monalbite (about 900K in the present study).

With decreasing temperature, the symmetry is reduced to triclinic $C\bar{1}$ ($Q \neq 0$, $Q_{od} \neq 0$). Below the transition temperature, the temperature dependencies of Q and Q_{od} have the similar tendency. However, the inflection point at ca. 950K showed by Salje et al. (1985) (Fig. 4-8a) is not found in the present study (Fig. 4-7a). The coupling behaviour between two order parameters is depicted in the order parameter vector space (Fig. 4-7b). This equilibrium line is linear and thus a rounded corner in the thermal crossover between high- and low-albites reported by Salje et al. (1985) (Fig. 4-8b) is not found in the present study. The free energy is given as the function of T, Q, and Q_{od} by Salje et al. (1985):

$$\Delta F = \frac{1}{2}aQ^2 + \frac{1}{4}bQ^4 + \frac{1}{6}cQ^6 + \frac{1}{2}a_{od}Q_{od}^2 + \frac{1}{4}b_{od}Q_{od}^4 + \frac{1}{6}c_{od}Q_{od}^6$$

$$+ (d_0 + d_1T + d_2T^2 + d_3T^3)QQ_{od}$$

$$= f(T, Q(T), Q_{od}(T)),$$

where, a, b, c, a_{od}, b_{od}, c_{od}, d_0, d_1, d_2, and d_3 are the coefficients. Salje et al. (1985) calculate the free energy, internal energy (U), entropy (S) and specific heat (C) for a sodium feldspar under thermal equilibrium conditions by using this equation (Fig. 4-9). The calculated free energy shows an abrupt change with temperature around 950K. Salje et al. (1985) conclude that the abrupt energy change is associated with the thermal crossover between high- and low-albites, and that the energy change is large relative to that due to the C2/m-C$\bar{1}$ phase transition. This abrupt energy change around 950K has been considered to be related strongly to the change of Q_{od} around 950K (Fig. 4-7b). In the present study, on the other hand, both Q_{od} and Q change abruptly only around the transition temperature of C2/m-C$\bar{1}$ phase transition and no other abrupt change is not observed even around 950K (Fig. 4-7a). This suggests that the energy change reported by Salje et al. (1985) which associated the thermal crossover between high- and low-albites does not exist, and that the energy change due to the C2/m-C$\bar{1}$ phase transition is large. It can be therefore suggested that the symmetry reduction from C2/m to C$\bar{1}$ is dominated by 2nd order transition due to both the displacement of atoms (Q) and the Al/Si ordering (Q_{od}), and that there is not the thermal crossover between high- and low-albites.

Table 4-3. Temperature dependence of the value of G (KJ/mol) for different degrees of Al/Si ordering (Q_{od}).

	Q_{od}=0.000	Q_{od}=0.080	Q_{od}=0.222	Q_{od}=0.400	Q_{od}=0.500	Q_{od}=0.588	Q_{od}=0.737	Q_{od}=0.909	Q_{od}=1.000
100K	-12527.620	-12528.712	-12527.468	-12529.845	-12531.302	-12531.964	-12534.537	-12538.057	
200K									
300K	-12465.664	-12466.782	-12465.492	-12467.692	-12469.060	-12469.544	-12471.546	-12473.707	
400K	-12434.376	-12435.557	-12434.227	-12436.388	-12437.647	-12438.033	-12439.769	-12441.264	
500K	-12402.967	-12404.105	-12402.756	-12404.796	-12406.055	-12406.375	-12407.787		-12407.958
600K	-12371.318	-12372.476	-12371.149	-12373.066	-12374.288	-12374.524	-12375.728		-12374.483
700K	-12339.200	-12340.573	-12339.155	-12341.110	-12342.271	-12342.369		-12342.981	-12340.697
800K	-12307.189	-12308.315	-12306.896	-12308.666	-12309.800	-12309.643		-12309.873	-12306.766
900K	-12274.780	-12275.446	-12274.624	-12276.455	-12277.180	-12277.228		-12276.310	-12272.666
1000K	-12242.397	-12243.356	-12242.064	-12243.755	-12244.532	-12244.068		-12241.955	-12238.161
1100K	-12210.313	-12210.987	-12208.666	-12210.508		-12210.714	-12211.371	-12172.063	-12203.293
1200K	-12175.925	-12176.488	-12175.375	-12176.944		-12174.565	-12176.594	-12172.808	-12166.305
1300K	-12141.299	-12142.876	-12142.061	-12141.761		-12140.454	-12141.876	-12138.704	-12130.822
1400K	-12107.982		-12106.620	-12106.743	-12107.498	-12106.250	-12106.865	-12101.897	-12094.500
1500K		-12074.516	-12072.048	-12071.630	-12073.503	-12073.408	-12070.936	-12066.001	-12054.731
1600K		-12039.637	-12038.286	-12037.705	-12036.706	-12035.796	-12035.618	-12026.590	-12018.542
1700K		-12005.192	-12003.448	-12003.066	-12001.937	-12000.351	-12000.736	-11991.131	-11979.607
1800K		-11971.159	-11969.319	-11968.021	-11967.610	-11966.587	-11963.053	-11955.455	-11943.438

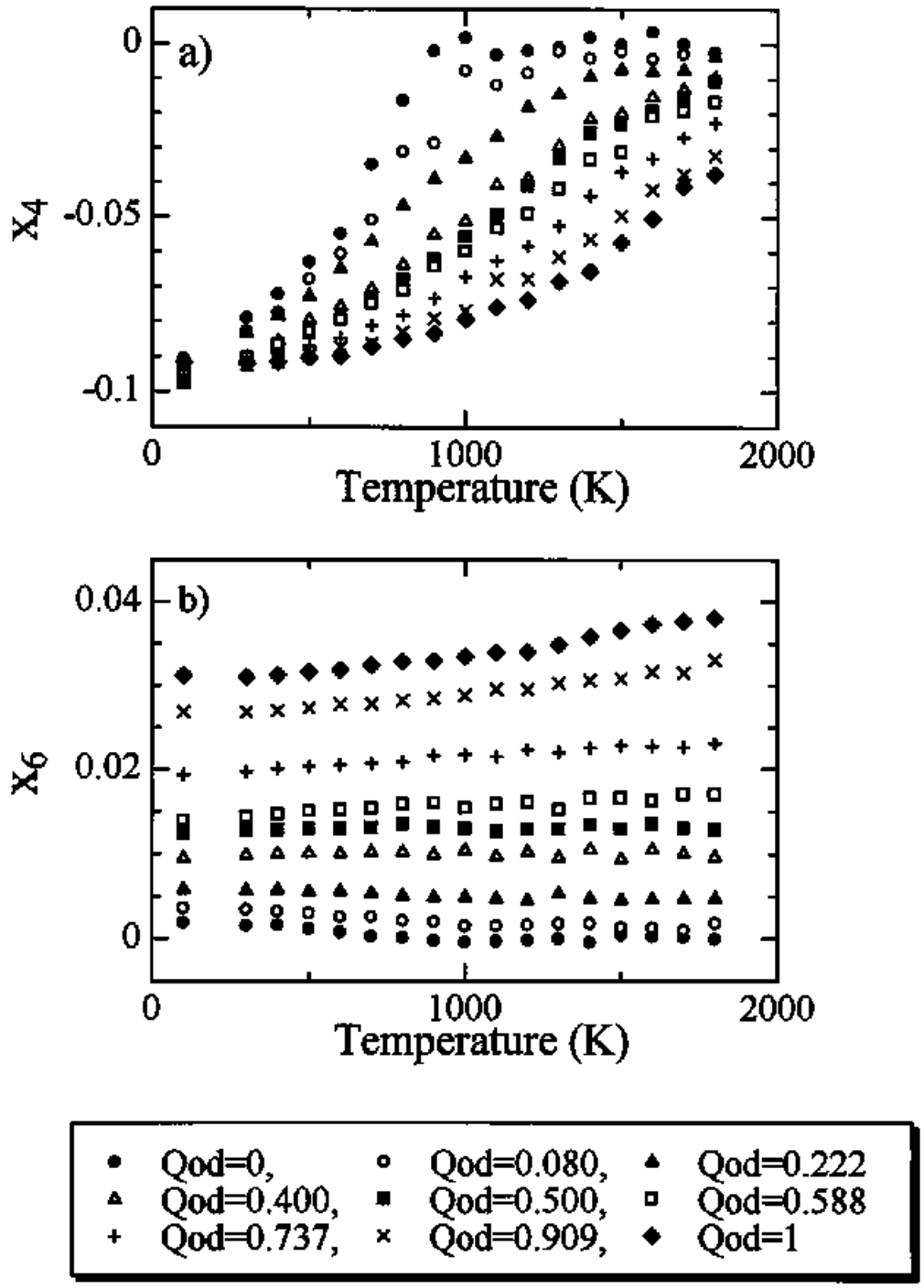

Fig. 4-5. Temperature dependencies of the strain parameters, a) x_4 and b) x_6, for different degrees of an order parameter Q_{od} for the Al/Si ordering.

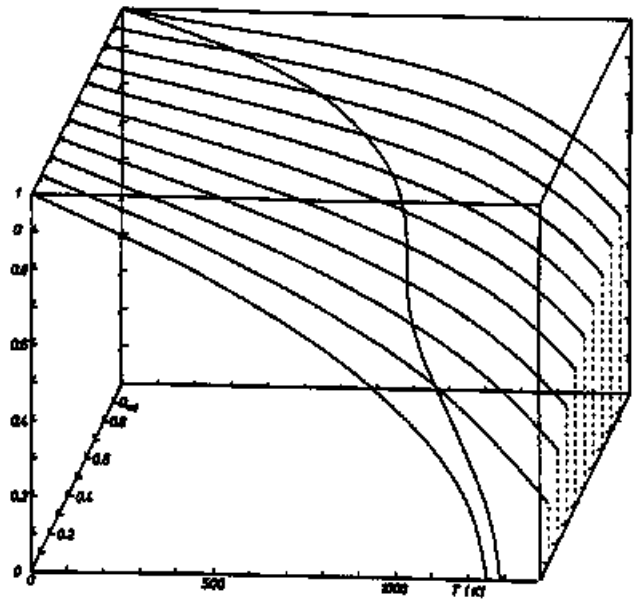

Fig. 4-6a. Temperature dependence of the displacive order parameter Q for different degrees of Al/Si order ordering order parameter Q_{od} for natural albite (Salje et al., 1985).

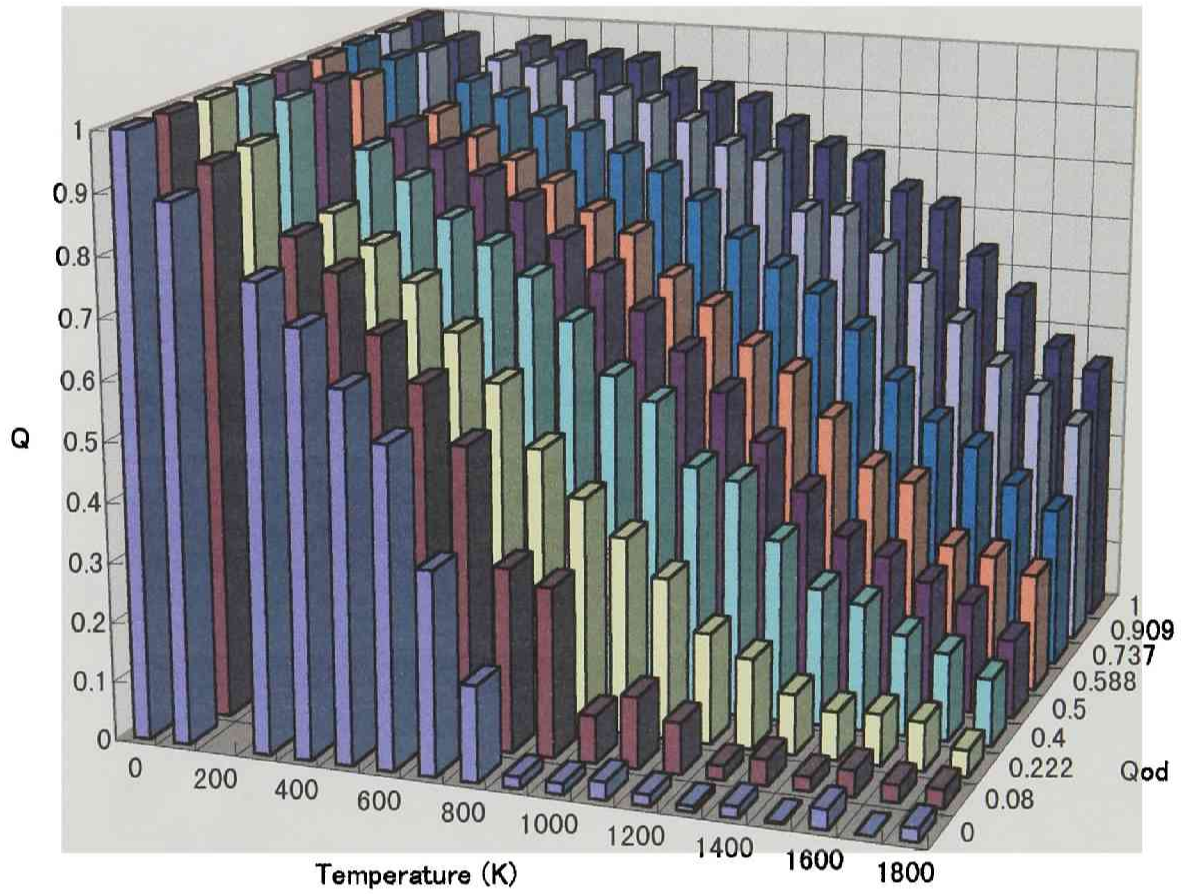

Fig. 4-6b. Temperature dependencies of the displacive order parameter Q for different degrees of Al/Si order ordering order parameter Q_{od} for MD-simulated albite.

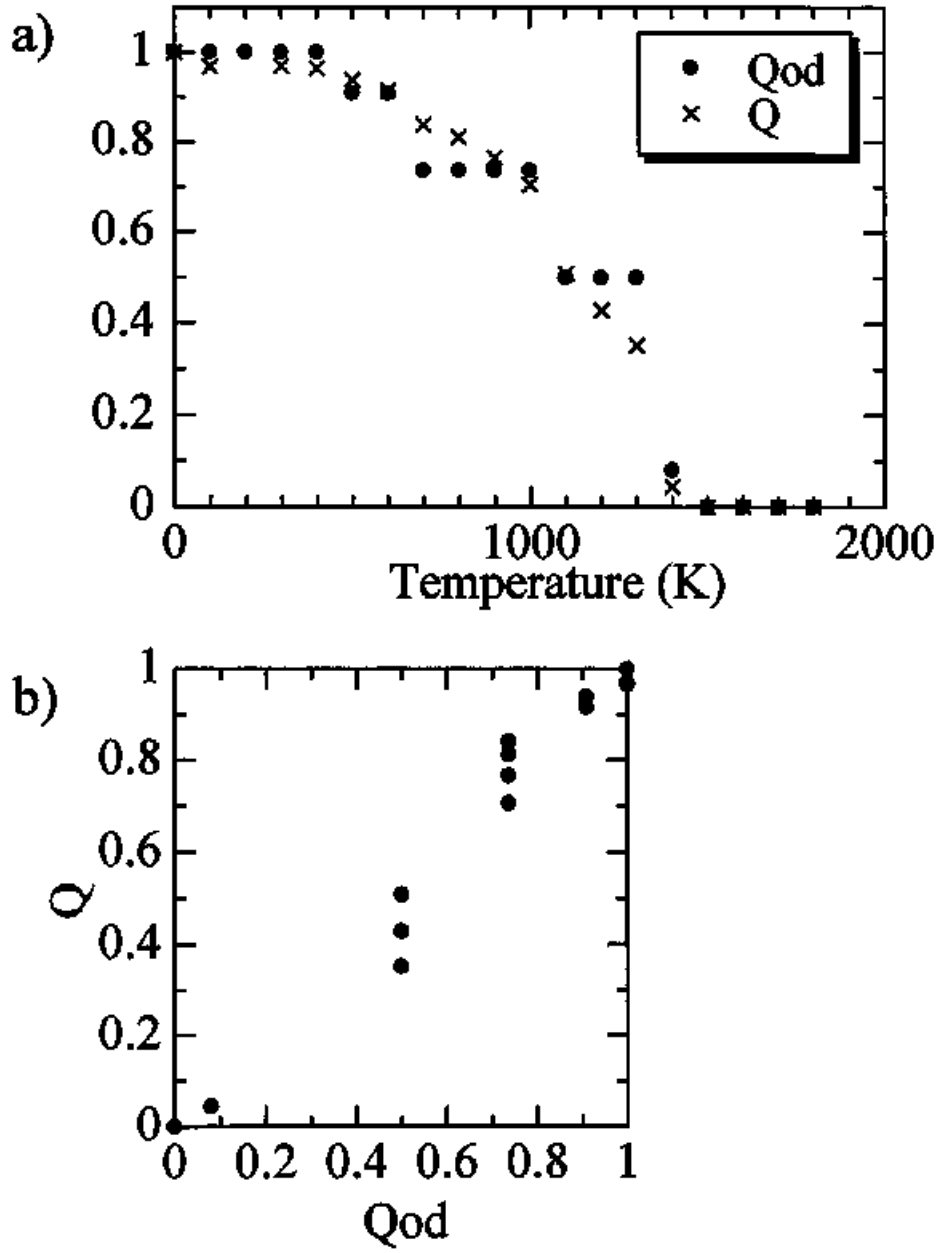

Fig. 4-7. a) Temperature dependencies of a displacive order parameter Q and an order parameter Q_{od} for the Al/Si ordering at thermodynamic equilibrium and b) an order parameter vector space diagram of MD-simulated albite under thermodynamic equilibrium conditions representing the values of Q and Q_{od} at various temperatures.

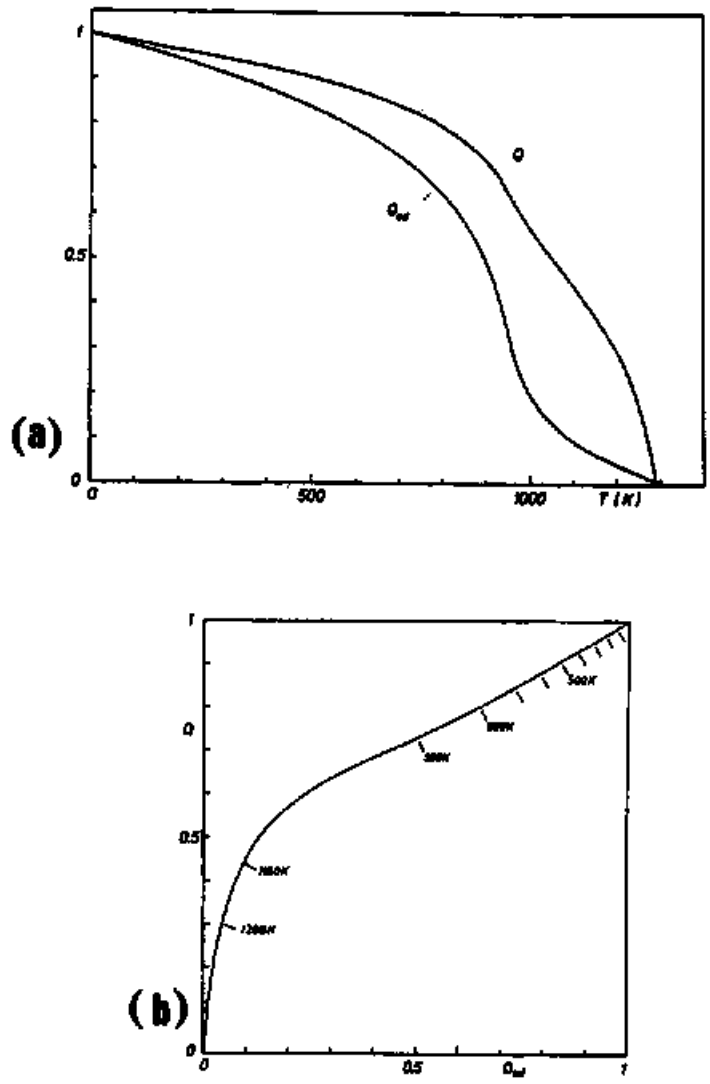

Fig. 4-8. a) Temperature dependencies of a displacive order parameter Q and an order parameter Q_{od} for Al/Si ordering at thermodynamic equilibrium and b) an order parameter vector space diagram of natural albite under thermodynamic equilibrium conditions representing the values of Q and Q_{od} at various temperatures. (Salje et al., 1985).

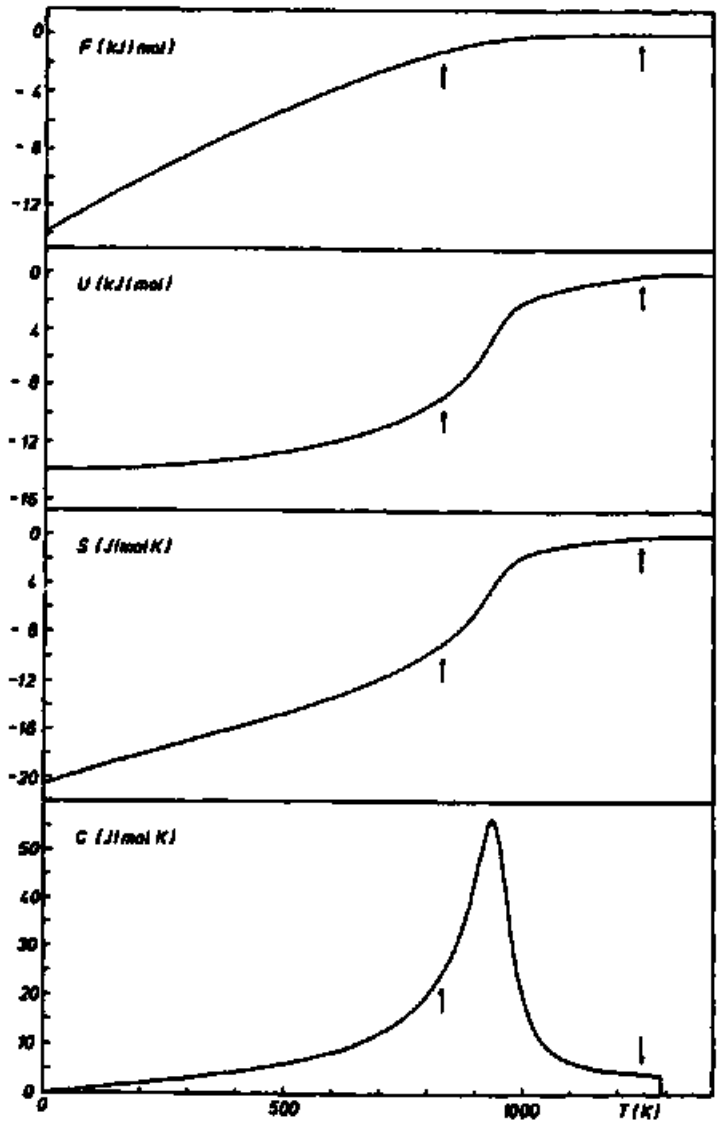

Fig. 4-9. Temperature dependencies of the excess free energy ΔF, excess internal energy ΔU, excess entropy ΔS, and excess specific heat ΔC of natural albite under thermodynamic equilibrium conditions (Salje et al., 1985).

4.3 The behaviour of Na atom in MD-simulated albite at low temperature

4.3.1 Procedure

MD simulation was carried out to investigate the behaviour of Na atoms in fully ordered albite (Q_{od}=1) at low temperature. Partially disordered albite (pdAb), which has Q_{od}=0.933 and includes Al-O-Al linkages in the MD cell, was also simulated at low temperature to investigate the influence of the Al/Si disorder on the Na motion. The number of atoms in a MD cells was 1664 (containing 32 crystallographic cells of albite; $a_{MD}=4a_{ab}$, $b_{MD}=2b_{ab}$, $c_{MD}=4c_{ab}$). Two kinds of initial structures were annealed for 20ps (10000 steps) at 300K so as to obtain an equilibrium atomic configuration. These MD-simulated albite were used as each starting MD-simulated albite. After falling the temperature of the system to 5K using each starting MD simulated albite, the resulting MD-simulated albite was 'annealed' for at least 20ps (10000 steps), to obtain an equilibrium atomic configuration. After attaining equilibration, a production run 20ps (10000 steps) was performed, and various properties and atomic positions were, then, evaluated. The interval of sampling was fixed at every 25 MD steps (50 fs). In the matter of these simulations at 5K, it is necessary to consider quantum mechanical effect. However, these MD simulations were carried out under the classical MD method in the present study. Table 4-4 shows MD simulations of albite carried out in the present study.

Table 4-4. MD simulations of Albite carried out in the present study to investigate the nature of Na atom at low temperature are tabulated as follow;

MD simulation	fully ordered Ab	partly disordered Ab
Abbreviation	foAb	pdAb
Al/Si ordering parameter (Q_{od})	1	0.933
Al-avoidance rule	O	O
Pauling rule	O	×
Temperature	5K	5K
Purpose	Nature of Na atom at low temperature	Nature of Na atom at low temperature
number of atoms	1664	1664

4.3.2 Result and Discussion

A projection, described below, is employed to study the behavior of Na atoms at low temperature. Because there is only one crystallographic position of Na atoms in the $C\bar{1}$ structure, each Na atom in a MD cell is projected on one position in a unit cell. The histograms of the x-, y- and z-coordinates of projected Na positions in the MD-simulated foAb and pdAb are shown in Fig. 4-10 and 4-11, respectively. The shape of every peak of Na atoms in the MD-simulated foAb is very sharp and has small variance (Fig. 4-10). On the other hand, every peak in the MD-simulated pdAb has wider variance than that of the MD-simulated foAb and has a few small peaks around main peak (Fig. 4-11). The histograms indicate that there are peaks with wider variance but no observable two- or multiple-peaks of Na atoms in both MD simulations. It can not be decided directly from the histograms whether the wider variance of peaks is resulted from the positional disorder or the thermal disorder.

In order to clarify the origin of the wider variance of peaks, the time-averaged coordinates in both MD simulations are calculated and plotted in histograms (Fig. 4-12). The shapes of the peaks of the MD-simulated foAb are very sharp (solid line in Fig. 4-12) and the standard deviations are very small (Table 4-5). In the MD-simulated pdAb, on the other hand, the shapes have wider variance (broken line in Fig. 4-11) and the standard deviations are much larger than that of the MD-simulated foAb. Secondly, to investigate the thermal vibration, the averaged standard deviation of the movement of Na atoms is calculated (Table 4-6). As seen in the table, the averages in the MD-simulated pdAb are smaller than those in the MD-simulated foAb. This fact suggests that Na atoms in the MD-simulated foAb keep

the same position in $C\bar{1}$ structure on the time average and vibrate by thermal vibration, and that those in the MD-simulated pdAb occupy in multiple sites breaking the $C\bar{1}$ symmetry and vibrate weaker than that in the MD-simulated foAb. The behaviour of Na atoms can be interpreted to be caused by the existence of oxygen atoms forming Al-O-Al linkage in the MD-simulated pdAb, *i.e.*, some Na atoms are attracted by the oxygen atoms.

To discuss on the behaviour of Na atom in reciprocal space, structure factors from (1) all atoms (all elements), (2) only Na atoms, and (3) atoms other than Na (Si, Al and O) constructing the framework, are calculated from the MD-simulated crystals. In the MD-simulated foAb, every $|\langle F_{MD}(hkl)\rangle|$ with $h+k=2n$ has a non-negligible value, and the other $|\langle F_{MD}(hkl)\rangle|$ and the structure factors with non integer are negligible small. This fact suggests that the phase transformation does not occur from $C\bar{1}$ to the other space group at low temperature, 5K. In the MD-simulated pdAn, on the other hand, the structure factors with non-integer and $h+k\neq 2n$ are stronger than those of the MD-simulated foAb. The ratios of the maximum value of the structure factors with $h+k\neq 2n$ to the maximum value of that with $h+k=2n$ or non-integer ($0\leq 4h_{MD}\leq 12$, $-8\leq 2k_{MD}\leq 8$, $-8\leq 4l_{MD}\leq 8$) are calculated. The ratios of structure factors from all atoms, only Na atom and atoms other than Na are about 2.4%, about 8.7% for $|\langle F(2.75, 3, -1.75)\rangle|$ and about 1.9% for $|\langle F(0.25, 4\ 0)\rangle|$ (Table 4-7). These ratios are a little larger than those in the MD-simulated foAb. And, the ratio of only Na atom in the MD-simulated pdAn is larger than that of other atoms composing the framework. This fact supports that Na atoms in the MD-simulated pdAn occupy in multiple sites breaking the $C\bar{1}$ symmetry, and implies the possibility that the reflections with non-integer and $h+k\neq 2n$

appear at very low temperature in the case of more disordered albite.

Table 4-5. Standard deviations of averaged coordinates of Na atoms in two simulations on albite with Q_{od}=1 and 0.933.

	X	Y	Z
Q_{od}=1	5.02×10^{-3}	3.45×10^{-3}	6.76×10^{-3}
Q_{od}=0.933	9.20×10^{-3}	1.32×10^{-2}	1.77×10^{-2}

Table 4-6. Average of standard deviations of the movement of Na atoms in two simulations on albite with Q_{od}=1 and 0.933.

	X	Y	Z
Q_{od}=1	4.28×10^{-3}	3.22×10^{-3}	5.95×10^{-3}
Q_{od}=0.933	2.59×10^{-3}	2.35×10^{-3}	3.83×10^{-3}

Table 4-7. Maximum value of the structure factors with $h+k=2n$, $h+k\neq 2n$, and non-integer from all atom, Na atom, and other atoms in the MD-simulated pdAb.

	all	Na atom	other atoms
F(hkl) with $h+k=2n$	(002)	(002)	(002)
ratio (%)	100	100	100
F(hkl) with $h+k\neq 2n$	(34-2)	(14-2)	(34-2)
ratio (%)	1.11	3.91	0.48
F(hkl) with no integer	(0.25 4 0)	(2.75 3 -1.75)	(0.25 4 0)
ratio (%)	2.4	8.7	1.9

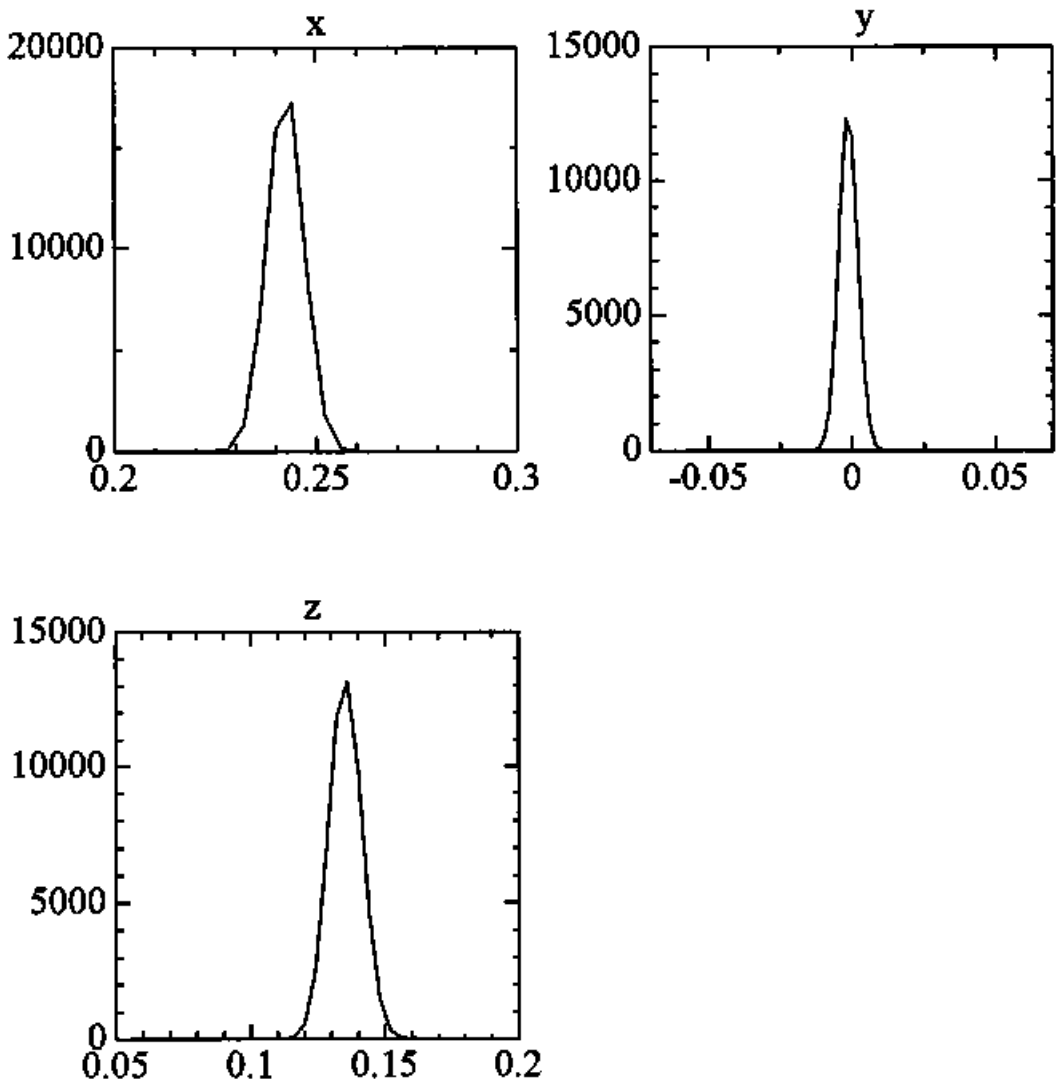

Fig. 4-10. Histograms of x-, y- and z-coordinates of Na positions in the MD-simulated foAb at 5K.

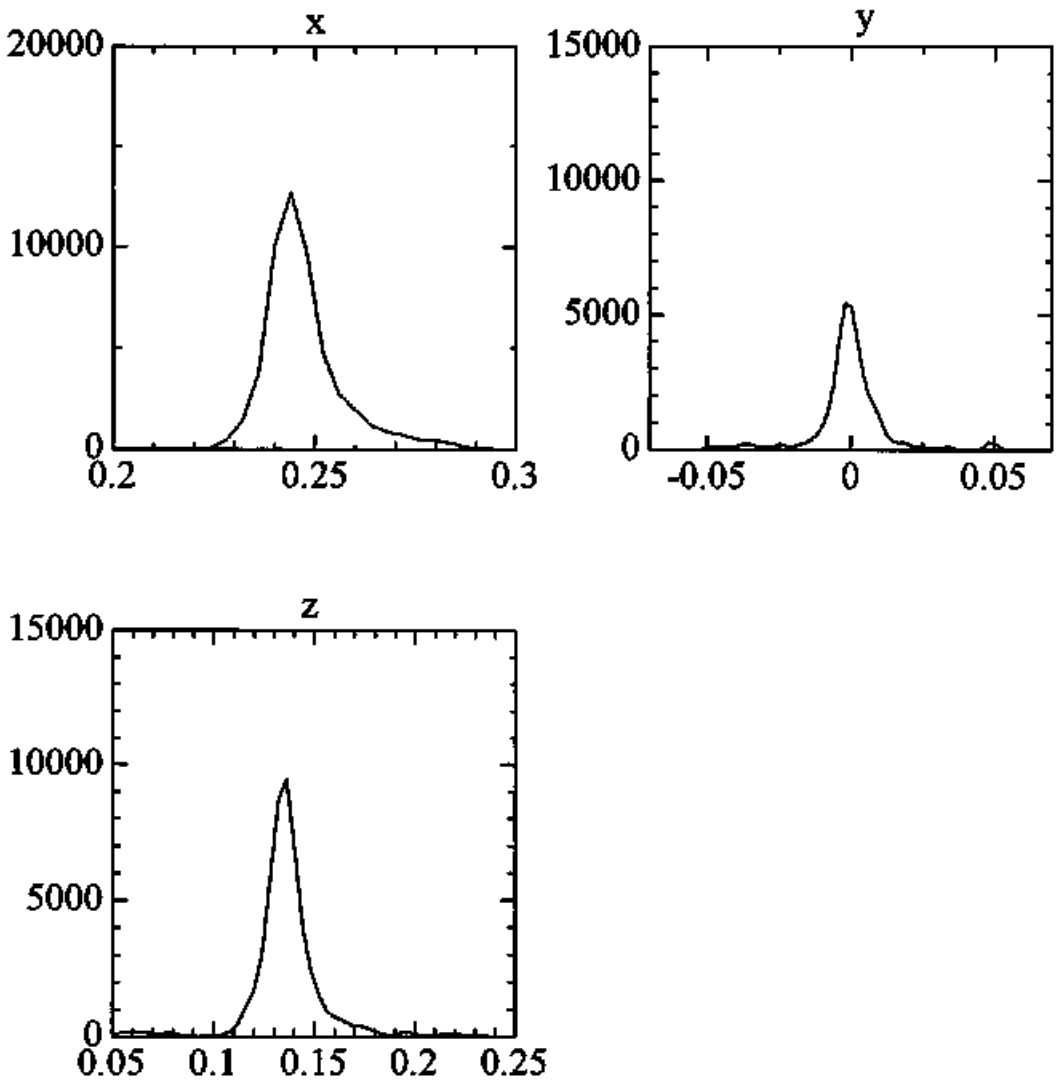

Fig. 4-11. Histograms of x-, y- and z-coordinates of Na positions in the MD-simulated pdAb at 5K.

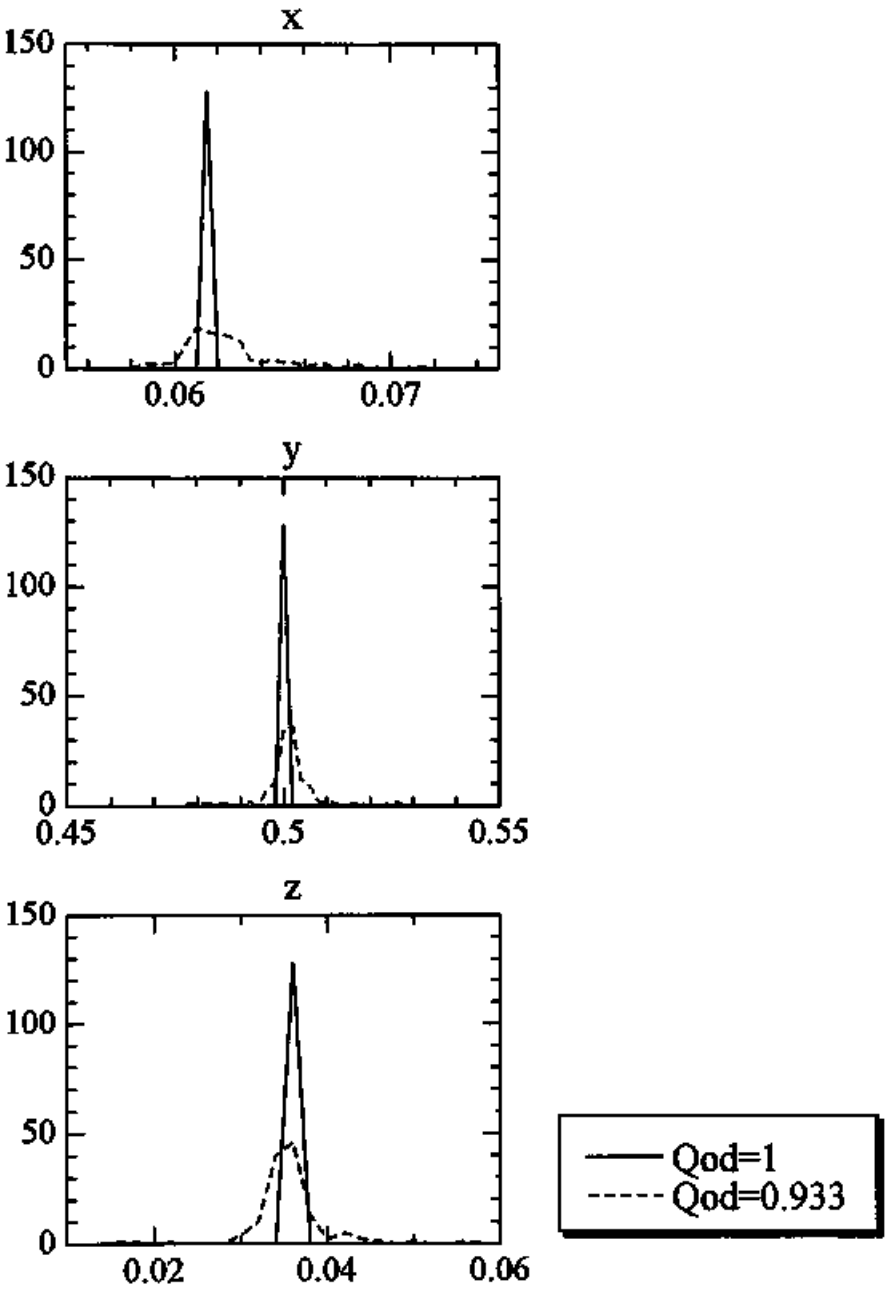

Fig. 4-12. Histograms of time-averaged coordintes of Na atoms in MD simulated albite with Q_{od} = 1 and 0.933.

5. Plagioclase Feldspar Solid Solution

5.1 Introduction

There have been known three commensurate structures (space groups of $C\bar{1}$, $I\bar{1}$ and $P\bar{1}$) for plagioclase feldspar. `e' plagioclase has been observed in the composition range between -An25 and -An75. Plagioclase feldspar has a wide range of solid solution at high temperature. On the other hand, in the intermediate composition range, three miscibility gaps (peristerite gap, Bøggild gap and Huttenlocher gap) have been recognized. The phase relations have not been precisely established, except for several tentative ones (e.g., Smith, 1974; Carpenter, 1994).

If pure albite and pure anorthite are the only two fully ordered structures possible, it could be argued that the most stable state for a plagioclase at any intermediate composition might be to unmix into intergrowth of albite + anorthite, as suggested in a few tentative phase diagrams (e.g., Smith, 1974; Carpenter, 1994). This phenomena has not been observed in natural plagioclase. This must be due to the extreme sluggishness, even on a geological time scale, of such a complete reconstruction of the Al, Si framework and the diffusion of Al and Si at temperature below 900K. Therefore, MD simulation method is applied to the problem of this unmixing.

Peristerite miscibility gap has been studied extensively more than the other two

miscibility gaps in plagioclase, probably because plagioclase in the composition range of peristerite commonly occur in metamorphic rocks. Coexistence of two sodic plagioclase feldspars, albite and oligoclase, appear in many greenschist and amphibolite facies rocks (Maruyama et al., 1982; Grove et al., 1983; Grapes and Otsuki, 1983; Ashworth and Evirgen, 1985; Ishizuka, 1985; see Goldsmith, 1982, for older references). This coexisting two plagioclase is called peristerite. The maximum extent of the peristerite two phase field is generally taken to be ~An1 to ~An25, as summarized by Smith and Brown (1988). Previous proposals for the peristerite miscibility gap fall into three groups: those favouring a "solvus" (Ribbe, 1962; Crawford, 1966; Nord et al., 1978; Maruyama et al., 1982), those preferring a binary loop associated with a first order transition in albite (Smith, 1972, 1974; Orville, 1974; Ishizuka, 1985), and those favouring a conditional spinodal with higher than the first order transition in character (Carpenter, 1981; Carpenter, 1994).

The exsolution microstructures observed with transmission electron microscopy and some of exsolution lamellae are consistent with those having developed by a spinodal decomposition mechanism (e.g., Nord et al., 1978; Appendix in the present study). It has been so far thought that the sodic component is ordered low albite while the oligoclase appears to be less well ordered. In some cases the oligoclase has the incommensurate structure, as implied by the presence of diffuse 'e' reflections in single crystal diffraction patterns (Bown and Gay, 1958; Appendix in the present study). The currently accepted hypothesis is that the driving force for exsolution is due primarily to the free energy of ordering in albite, and that the existence of the miscibility gap is conditional upon the Al/Si ordering taking place.

Although Al/Si ordering process at whole composition make progress with decreasing temperature and with increasing An composition, in the "conditional spinodal" model Al/Si ordering process in the Ab-rich plagioclase make progress with increasing Ab composition. The correlation between peristerite gap and 'e'-plagioclase has never been discussed.

5.2 Thermodynamics behavior of MD-simulated plagioclase feldspar solid solution

5.2.1 Procedure

MD simulations were carried out on MD-crystals of solid solution of plagioclase feldspar with 25 different compositions (Table 5-1) and different degrees of ordering. Each MD-crystal was simulated in the temperature range of 300-1500K and under 1atm. A unit cell used in the present MD calculation (MD cell) was parallelepiped and the number of atoms in the system was 1248 (containing 24 crystallographic unit cells of albite; $a_{MD}=3a_{ab}=3a_{an}$, $b_{MD}=2a_{ab}=2a_{an}$, $c_{MD}=4c_{ab}=2c_{an}$).

Four different ordering schemes were employed in MD-crystals of plagioclase. In the crystal structure of plagioclase, there are two different sites; tetrahedral (T-site) and polyhedral sites (M-site). In the present study, it is assumed that ordering and disordering of Al and Si in tetrahedral sites can occur satisfying the *Al-avoidance rule*. There can be two different ways to distribute Ca and Na in M sites, depending upon whether local charge valance is maintained (*Pauling rule*) or not. In addition, lamella structure which consists of albite and anorthite was simulated to investigate the enthalpy change due to phase separation. Therefore, in the present study, four different structures were simulated; (1) fully ordered structure, (2) Al/Si disordered structure coupled with Ca/Na distribution, (3) Al/Si disordered structure not coupled with Ca/Na distribution and (4) lamella structure.

(1) *Fully ordered plagioclase (foPl)* : The initial structure was constructed by putting the structure of anorthite with the size of half unit cell, that called "An-cluster" in the present

study, into the MD cell of albite at random satisfying the *Al-avoidance rule*. The number of An-clusters put into a MD cell changes from 1 to 23 depending upon to chemical composition. In the resultant structure, the number of Al atom in four non-equivalent T-sites (T1o, T1m, T2o and T2m) of $C\bar{1}$ structure is in the order of T1o ≥ T1m = T2o = T2m (Table 5-1).

(2) *Al/Si disordered plagioclase coupled with Ca/Na (coupled-Pl)*: In the case of Al/Si disordered plagioclase, Al and Si atoms were distributed into four non-equivalent T-sites at random in each composition ($Ab_{66.67}An_{33.33}$ ~ $Ab_{95.83}An_{4.17}$) satisfying the *Al-avoidance rule*. In the resulting structure, the number of Al atoms in four non-equivalent T-sites are the same, *i.e.*, T1o = T1m = T2o = T2m (Table 5-1). Ca atoms were then distributed into M-site depending upon the number of Al atoms in T-sites surround the M-site to satisfy the *Pauling rule*.

(3) *Al/Si disordered plagioclase decoupled with Ca/Na (decoupled-Pl)*. In the structure with this type of disordering, the distribution of Al and Si atoms in tetrahedral sites is the same as that of Al/Si disordered plagioclase. However, in the structure, Ca and Na atoms were distributed randomly into M-sites ignoring the *Pauling rule*.

(4) *Lamella structure*: The lamella structure with the composition of $An_{22.22}Ab_{77.78}$ was constructed by using pure albite and pure anorthite. Initial atomic positions of the lamella structure were given based on the Megaw cell (Megaw, 1960) with a_M, b_M, and c_M. The

relation between Megaw cell and albite unit cell is as follows;

$a_M = a_{Ab}$

$b_M = 1/2 \cdot (a_{Ab} + b_{Ab})$

$c_M = 3/2 \quad a_{Ab} + 1/2 \cdot b_{Ab} + c_{Ab}$.

The number of atoms in the system was 5850 containing 225 crystallographic unit cells of Megaw cell; $a_{MD}=5a_M$, $b_{MD}=9a_M$, $c_{MD}=5c_M$. The interface of lamella is parallel to $(010)_M$. This MD-simulated plagioclase were used as an initial MD-simulated plagioclase for MD calculation of the lamella structure.

Starting from each initial MD-simulated plagioclase, each MD-simulated plagioclase was annealed for 20ps (10000steps) at 300K so as to obtain an equilibrium atomic configuration at the particular temperature. These MD-simulated plagioclase were used as starting MD-simulated plagioclase in each case. After raising the temperature of the system to the required level using each starting MD-simulated plagioclase, the resulting MD-simulated plagioclase was 'annealed' for at least 20ps (10000steps), to obtain an equilibrium atomic configuration. After attaining equilibration, a production run of 20ps (10000steps) was performed, and various properties and atomic positions were, then, evaluated. Table 5-2 shows MD simulations of plagioclase carried out in the present study.

Table 5-1. Numbers of Si, Al, Ca, and Na atoms of the MD-simulated plagioclase feldspar and the number of Al atom in four non-equivalent T-sites (T1o, T1m, T2o and T2m) in the MD-simulated foPl and the MD-simulated coupled-Pl. The MD-simulated foPl; T1m = T2o = T2m, the MD-simulated coupled-Pl; T1o = T1m = T2o = T2m.

					foPl		coupled-Pl
	Si	Al	Ca	Na	T1o	T1m	T1o
Ab_{0}	192	192	96	0	48	48	48
$Ab_{4.17}$	196	188	92	4	50	46	47
$Ab_{8.33}$	200	184	88	8	52	44	46
$Ab_{12.50}$	204	180	84	12	54	42	45
$Ab_{16.67}$	208	176	80	16	56	40	44
$Ab_{20.83}$	212	172	76	20	58	38	43
$Ab_{25.00}$	216	168	72	24	60	36	42
$Ab_{29.17}$	220	164	68	28	62	34	41
$Ab_{33.33}$	224	160	64	32	64	32	40
$Ab_{37.50}$	228	156	60	36	66	30	39
$Ab_{41.67}$	232	152	56	40	68	28	38
$Ab_{45.83}$	236	148	52	44	70	26	37
$Ab_{50.00}$	240	144	48	48	72	24	36
$Ab_{54.17}$	244	140	44	52	74	22	35
$Ab_{58.33}$	248	136	40	56	76	20	34
$Ab_{62.50}$	252	132	36	60	78	18	33
$Ab_{66.67}$	256	128	32	64	80	16	32
$Ab_{70.83}$	260	124	28	68	82	14	31
$Ab_{75.00}$	264	120	24	72	84	12	30
$Ab_{79.17}$	268	116	20	76	86	10	29
$Ab_{83.33}$	272	112	16	80	88	8	28
$Ab_{87.50}$	276	108	12	84	90	6	27
$Ab_{91.67}$	280	104	8	88	92	4	26
$Ab_{95.83}$	284	100	4	92	94	2	25
Ab_{100}	288	96	0	96	96	0	24

Table. 5-2. MD simulations of plagioclase feldspar carried out in the present study to investigate the nature of Na atom at low temperature are tabulated as follow;

MD simulation	fully ordered Pl	Al/Si disordered Pl coupled with Ca/Na	Al/Si disordered Pl decoupled with Ca/Na	Pl of lamella structure
Abbreviation	foPl	coupled-Pl	decoupled-Pl	
Initial position	put An-cluster into MD cell at random	CaAl/NaSi random	Ca/Na, Si/Al random	$(010)_M$ lamella in MD cell
Al-avoidance rule	O	O	O	O
Pauling rule	O	O	×	O
Temperature	300 - 1500K	300 - 1500K	300 - 1500K	300 - 900K
Composition	whole plagioclase	$Ab_{66.67}An_{33.33}$ ~ $Ab_{95.83}An_{4.17}$	$Ab_{66.67}An_{33.33}$ ~ $Ab_{95.83}An_{4.17}$	$Ab_{77.78}An_{22.22}$

5.2.2 Result and Discussion

Cell parameters of MD-simulated fully ordered plagioclase

Composition dependencies of the cell parameters of the MD-simulated foPl at 300K are shown in Fig. 5-1. In this figure, the length of c-axis of albite was doubled to match with that of the primitive anorthite cell. The length of a-axis of the MD-simulated foPl is almost constant through whole composition. The lengths of b- and c-axes decrease gradually with increasing the anorthite component (An-component). The α angle is constant with increasing the An-component from $Ab_{100}An_0$ to about $Ab_{60}An_{40}$ and from $Ab_{60}An_{40}$ decreases gradually with increasing An-component. The β angle decreases gradually with increasing the An-component from $Ab_{100}An_0$ to about $Ab_{25}An_{75}$ and from $Ab_{25}An_{75}$ becomes to be almost constant. The γ angle increases gradually with increasing the An-component from $Ab_{100}An_0$ to about $Ab_{25}An_{75}$ and from $Ab_{25}An_{75}$ becomes to be almost constant. Although the cell parameters of the MD-simulated foPl can not be directly compared with those of real plagioclase with various order degrees, these tendencies are similar to those of a real plagioclase except for the length of b-axis.

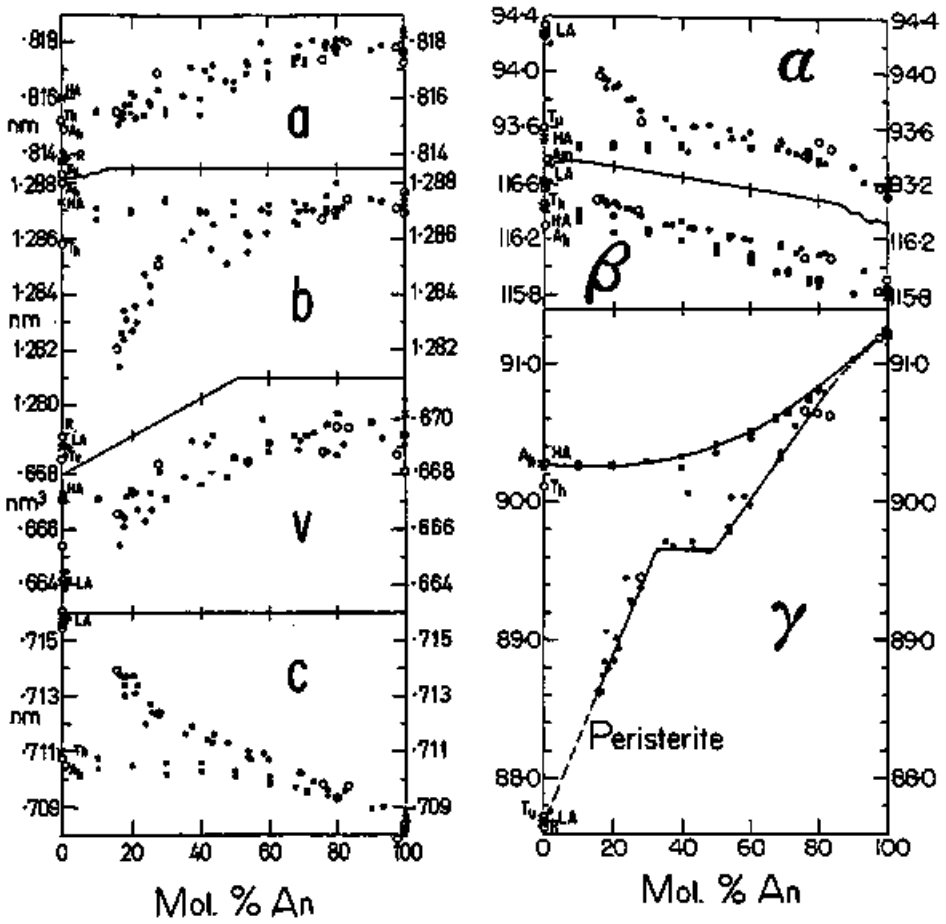

Fig. 5-1a. Variation of cell parameters of natural plagioclase with An component (Smith and Brown,1988).

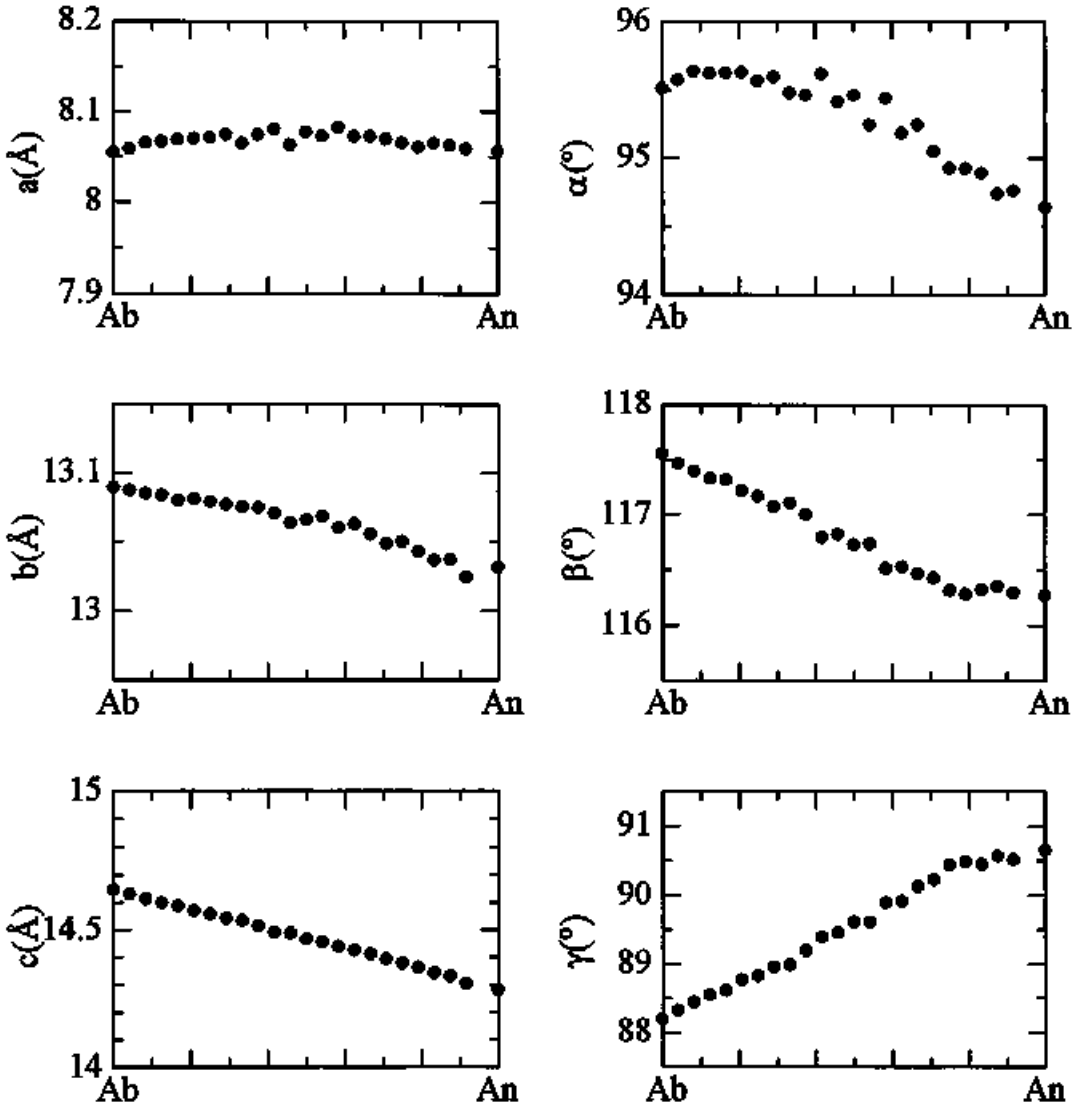

Fig. 5-1b. Variations of cell parameters of the MD-simulated foPl with the An component at 300K.

Crystal symmetry and structure factor of MD-simulated fully ordered plagioclase

Space groups of plagioclase feldspar are $P\bar{1}$, $I\bar{1}$ and $C\bar{1}$. The conditions for possible reflections for *hkl* reflections are none for $P\bar{1}$, $h+k+l=2n$ for $I\bar{1}$, and $h+k=2n$ *and* $l=2n$ for C $\bar{1}$. Structure factors of the MD-simulated foPl at 300K were calculated. As an example, the composition dependencies of the values of $I_{MD}(025)$ and $I_{MD}(1\bar{2}1)$ are shown in Fig. 5-2. The value of $I_{MD}(025)$ is negligible from $Ab_{100}An_0$ to about $Ab_{30}An_{70}$ and from $Ab_{30}An_{70}$ increase gradually up with increasing An-component. On the other hand, the value of $I_{MD}(1\bar{2}1)$ is negligible from $Ab_{100}An_0$ to about $Ab_{60}An_{40}$ and from about $Ab_{60}An_{40}$ increase gradually with the An-component. The behavior of these structure factors indicates that the phase of the MD-simulated foPl at 300K is $C\bar{1}$ from $Ab_{100}An_0$ to $Ab_{60}An_{40}$, $I\bar{1}$ from $Ab_{60}An_{40}$ to $Ab_{30}An_{70}$, and $P\bar{1}$ from $Ab_{30}An_{70}$ to Ab_0An_{100}. Such a phase change of the MD-simulated foPl with the composition is consistent with the change of the cell parameters such as the α angle is almost constant within the composition range that the stable phase is $C\bar{1}$, and the β and γ angles are almost constant within the composition range that the stable phase is $P\bar{1}$.

The $P\bar{1}$-$I\bar{1}$ phase transition of foPl with composition is of a second order, because of the continuous change of the cell parameters and structure factors with composition. On the other hand, the $P\bar{1}$-$I\bar{1}$ transition of fully ordered pure anorthite with temperature is of a first order. These results suggest that the nature of the $P\bar{1}$-$I\bar{1}$ phase transition changes from first in pure anorthite to second order with increasing the albite component. This is very similar to

the nature of the $C\bar{1}$-$I\bar{1}$ phase transition discussed by Carpenter (1992).

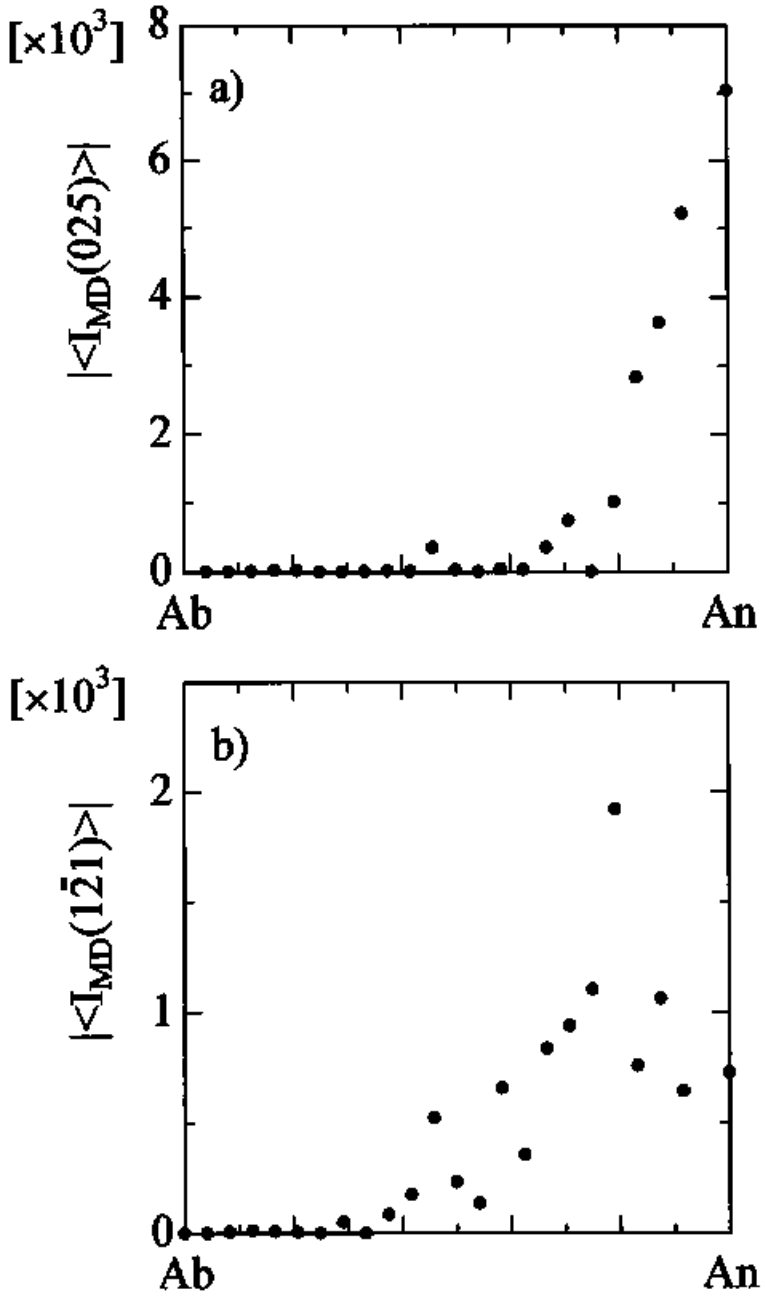

Fig. 5-2. Variation of the amplitudes of structure factors, a) $|\langle I_{MD}(025)\rangle|$ and b) $|\langle I_{MD}(1\bar{2}1)\rangle|$ of MD-simulated foPl with the An component at 300K.

Thermodynamics behavior of MD-simulated plagioclase

The excess enthalpies of mixing of the MD-simulated foPl, the MD-simulated coupled-Pl, and the MD-simulated decoupled-Pl are calculated as the difference from the straight line between the MD-simulated foAb and the MD-simulated foAn (Fig. 5-3). Below 1100K, the excess enthalpy of the MD-simulated foPl is concaved upward. The excess enthalpy of the MD-simulated coupled-Pl decreases gradually with increasing the An-component toward that of fully ordered anorthite. On the other hand, the excess enthalpy of the MD-simulated decoupled-Pl increases with increasing An-component.

To discuss the phase relation among the MD-simulated foPl, the MD-simulated coupled-Pl, and the MD-simulated decoupled-Pl, it is necessary to estimate the free energy, G, of the MD-simulated plagioclase. Entropy, S, of system in a given state is necessary to consider the configurational entropy, the vibrational entropy, the spin entropy, and the others. However, the spin entropy can not be estimated in the MD simulation method, and the vibrational entropy is difficult to calculate to control temperature and pressure of MD simulations by scaling particle velocities and simulation cell lengths. Therefore, only the configurational entropy is considered in the present study. The configurational entropy of three kinds of the MD-simulated plagioclase; the MD-simulated foPl, the MD-simulated coupled-Pl, and the MD-simulated decoupled-Pl, is described as below.

MD-simulated fully ordered plagioclase

Because the MD-simulated foPl was constructed by putting An-cluster into the MD cell, it can be considered only the configurational entropy due to the distribution of An-

clusters in a MD cell, S_{conf}^{An}. In the present study, S_{conf}^{An} is calculated as below

$$S_{conf}^{An} = aR\{N \ln N - N_{An} \ln N_{An} - (N - N_{An}) \ln(N - N_{An})\},$$

where R is the gas constant (8.31 $Jmol^{-1}K^{-1}$), a the scaling factor in the present MD simulations, N the number of albite unit cell in MD cell, and N_{An} the number of An-clusters. The free energy in the MD-simulated foPl, G_{order}, is defined as $G_{order} = \Delta H - TS_{conf}^{An}$.

MD-simulated Al/Si disordered plagioclase coupled with Ca/Na

In case of disordered plagioclase, it should be considered two kinds of configurational entropy; one is due to Al and Si atoms distributed over four non-equivalent T-sites ($S_{conf}^{Al/Si}$) and the other due to Ca and Na atoms distributed over M-sites ($S_{conf}^{Ca/Na}$). In the MD-simulated coupled-Pl, it is not necessary to consider $S_{conf}^{Ca/Na}$, because Ca atoms are put into M-site in order of the number of Al atoms in T-sites surrounding M-site to satisfy the *Pauling rule*. Therefore, it is consider only $S_{conf}^{Al/Si}$ as the configurational entropy in the present study. $S_{conf}^{Al/Si}$ must satisfy both Q_{od}=0 (T1o = T1m = T2o = T2m) and the *Al-avoidance rule*. It is difficult to estimate such $S_{conf}^{Al/Si}$. Therefore, in the present study, $S_{conf}^{Al/Si}$ satisfies only Q_{od}=0, because the number of Al atoms is smaller than that of Si atoms near albite end-member. Then, $S_{conf}^{Al/Si}$ is given by:

$$S_{conf}^{Al/Si} = aR(N_T \ln N_T - N_{Al} \ln N_{Al} - N_{Si} \ln N_{Si}),$$

where N_T, N_{Al}, and N_{Si} are the total number of T-site, Al atoms, and Si atoms in MD cell respectively. The true configurational entropy which satisfies the *Al-avoidance rule* is smaller than $S_{conf.}^{Al/Si}$. The free energy of the MD-simulated coupled-Pl, $G_{Qod=0}$, is defined as $G_{Qod=0} = \Delta H\text{-}TS_{conf.}^{Al/Si}$.

MD-simulated Al/Si disordered plagioclase decoupled with Ca/Na

In the case of MD-simulated decoupled-Pl, it is necessary to consider both $S_{conf}^{Al/Si}$ and $S_{conf}^{Ca/Na}$ as the configurational entropy, $S_{conf.}^{all}$, due to the distribution of Na, Ca, Al and Si atoms arranged randomly with satisfying the *Al-avoidance rule* but ignoring the *Pauling rule*. S_{conf}^{all} is then given by:

$$S_{conf}^{all} = S_{conf}^{Al/Si} + S_{conf}^{Ca/Na}$$

$$= aR(N_T \ln N_T - N_{Al} \ln N_{Al} - N_{Si} \ln N_{Si} + N_M \ln N_M - N_{Ca} \ln N_{Ca} - N_{Na} \ln N_{Na}),$$

where N_M, N_{Ca}, and N_{Na} are the total number of M-site, Ca atoms, and Na atoms in MD-cell respectively. The true configurational entropy which satisfy the *Al-avoidance rule* is smaller than S_{conf}^{all}. The free energy of the MD-simulated decoupled-Pl, G_{all}, is defined as $G_{all} = \Delta H\text{-}TS_{conf.}^{all}$.

ΔH, -TS, and G of each MD-simulated plagioclase are plotted in the Fig. 5-4. At 300K, the MD-simulated foPl is a stable phase. At high temperatures, the MD-simulated coupled-Pl

or the MD-simulated decoupled-Pl is stable phase. Above 1300K, the MD-simulated decoupled-Pl is a stable phase. In pure anorthite, G of ordered anorthite is smaller than that of fully disordered anorthite below 1500K, that is, ordered anorthite is more stable than fully disordered anorthite. However, fully disordered anorthite becomes to be stable above 1500K because -TS becomes larger value. On the other hand, in case that the MD-simulated foPl is a stable phase in whole composition at low temperature (e.g., 300K), the curve of ΔG concaved upward in the MD-simulated foPl shown in Fig. 5-3 and 5-4 indicates the possibility of the phase separation between albite and anorthite in real case such as that the annealing time is infinite.

To confirm the fall of the excess enthalpy for the phase separation, the excess enthalpy of the MD-simulated lamella structure consisting of pure albite and pure anorthite is shown in Fig. 5-3. The enthalpy of the MD-simulated lamella structure has smaller value than that of the MD-simulated foPl. This result means that the MD-simulated lamella structure is more stable than the MD-simulated foPl with the same composition. This supports that the phase separation between the pure albite and the pure anorthite.

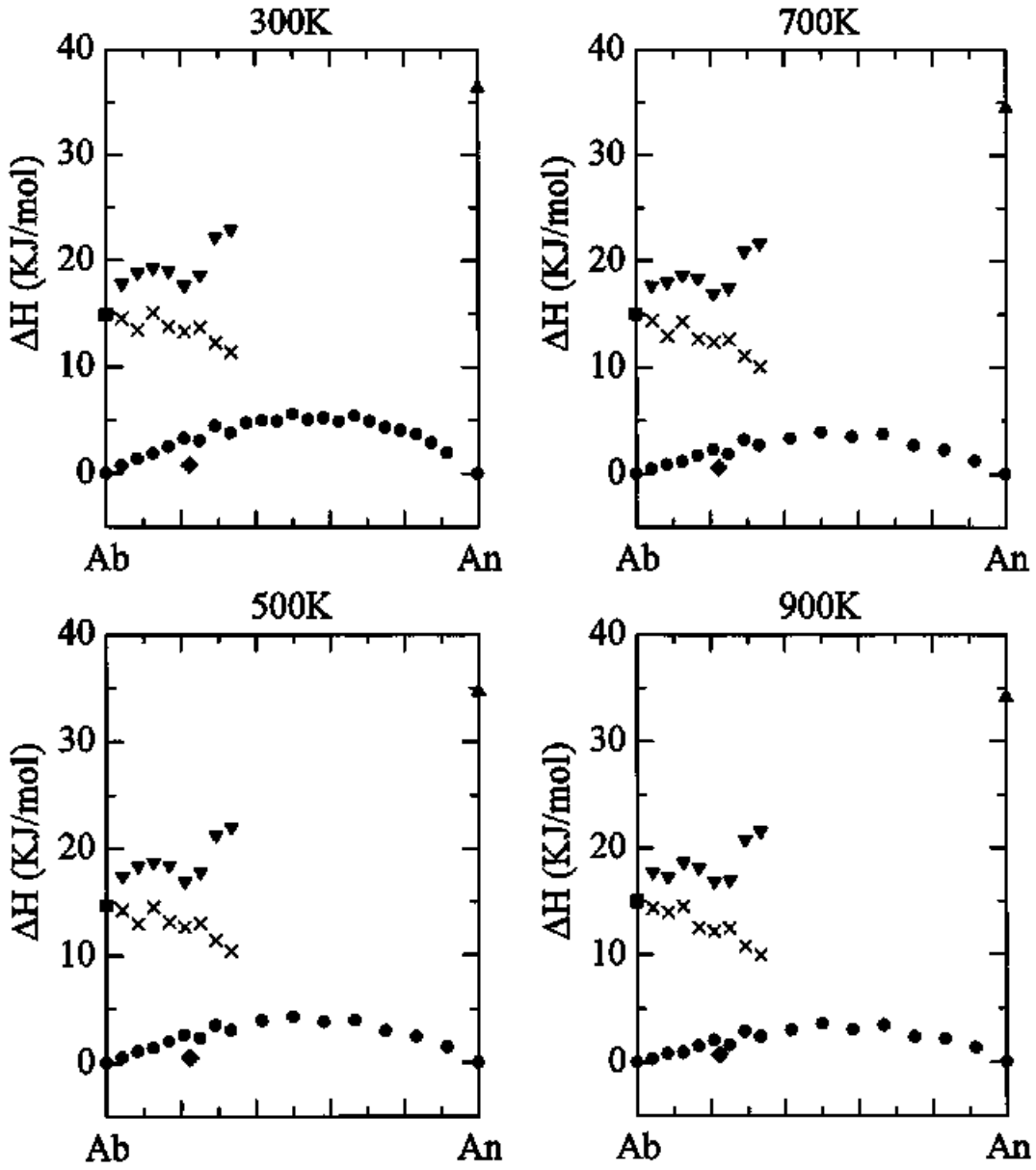
300K
700K
500K
900K
ΔH (KJ/mol)
40
30
20
10
0
Ab
An

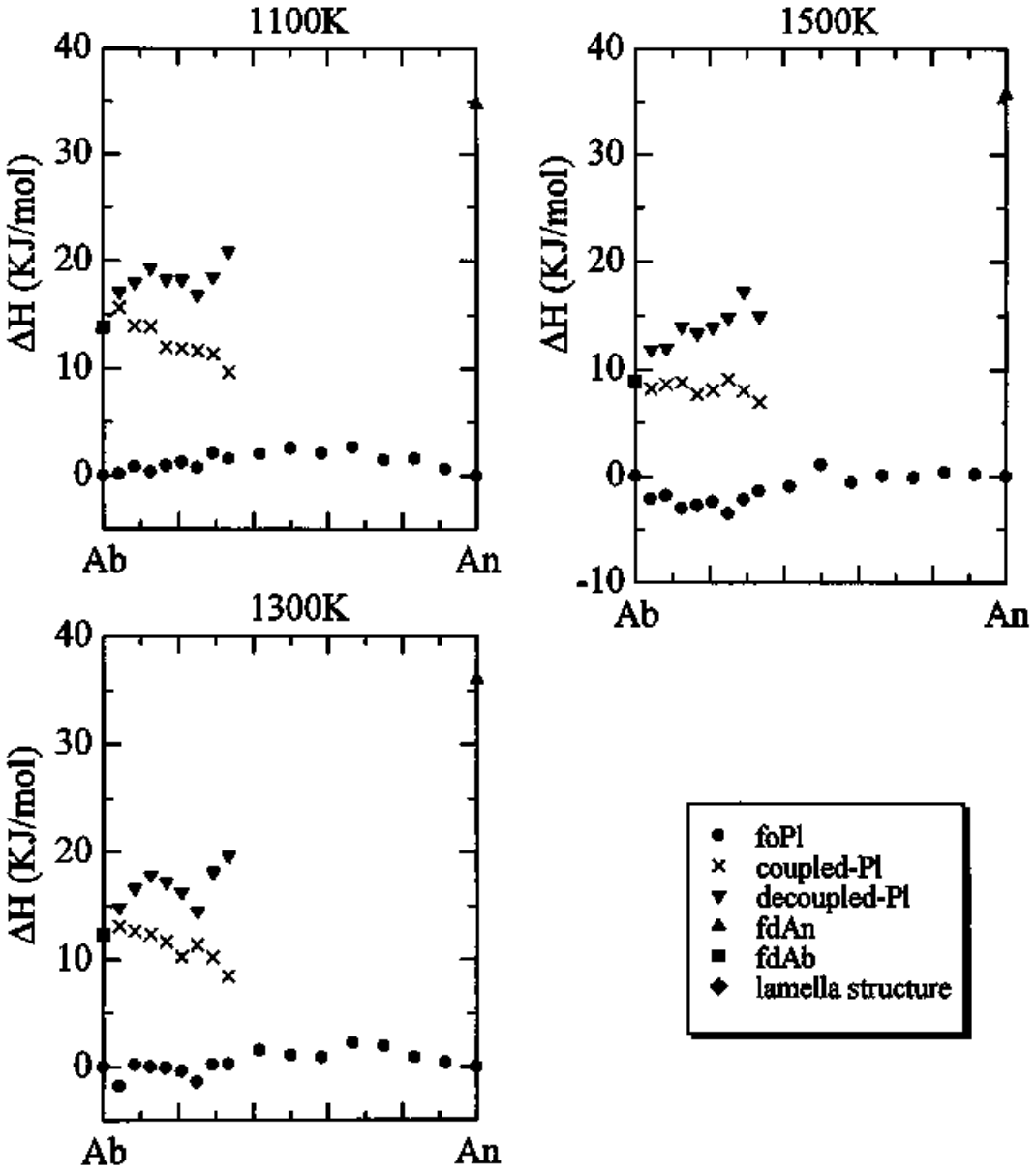

Fig. 5-3. Variations with the An component, of the excess enthalpy ΔH of three kinds of MD-simulated plagioclase, the MD-simulated plagioclase with a lamellae structure, fully disordered MD-simulated albite, and fully disordered MD-simulated anorthite in the temperature range of 300K ~ 1500K.

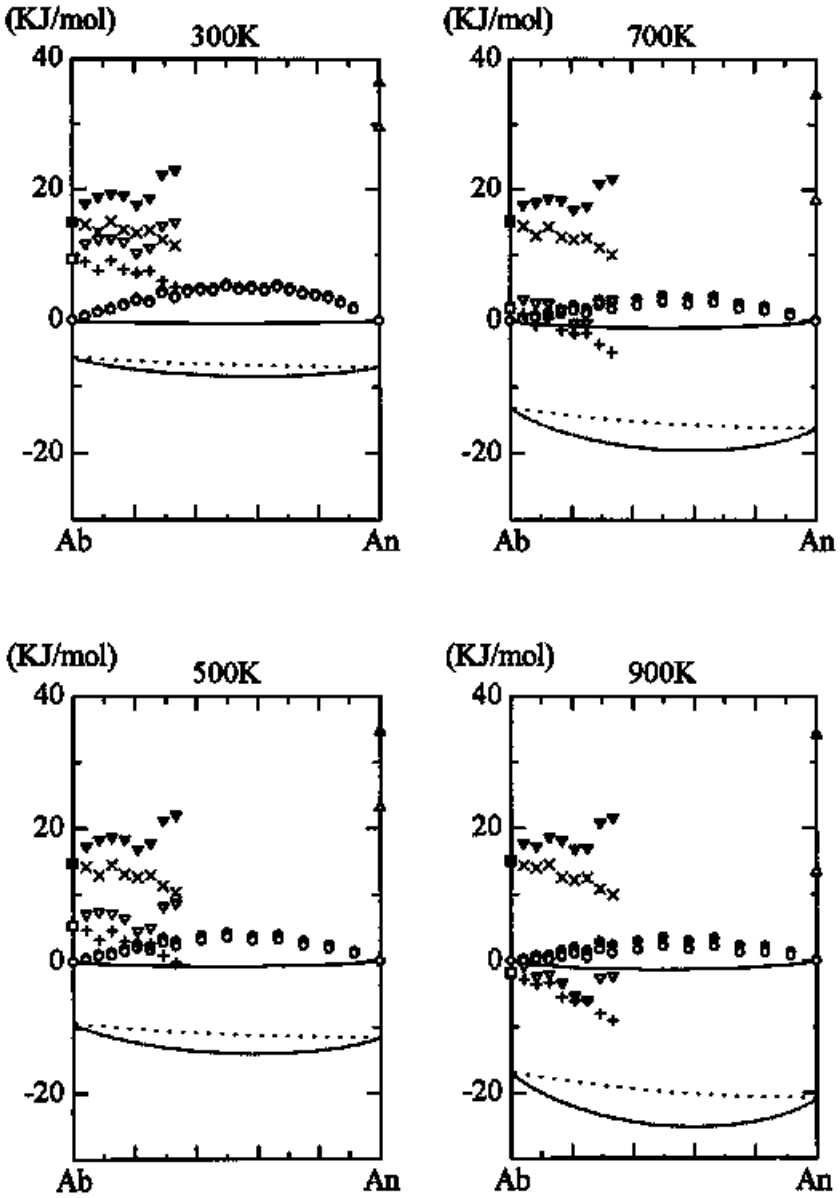
(KJ/mol)
300K
40
20
0
-20
Ab
An
(KJ/mol)
700K
40
20
0
-20
Ab
An
(KJ/mol)
500K
40
20
0
-20
Ab
An
(KJ/mol)
900K
40
20
0
-20
Ab
An

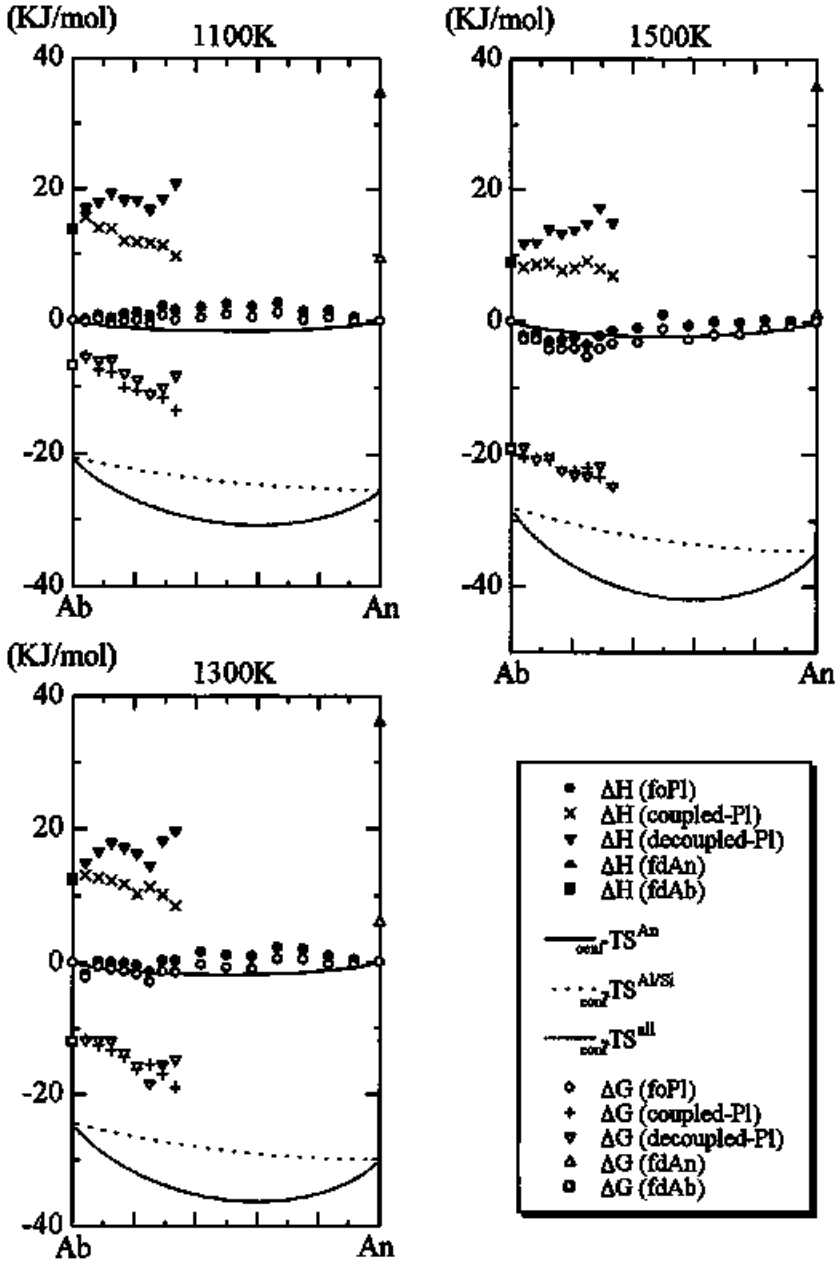

Fig. 5-4. Variations with the An component, of ΔH, $-TS$, and $\Delta G = \Delta H - TS$ of three kinds of MD-simulated plagioclase, MD-simulated fdAb, and MD-simulated fdAn in the temperature of 300K ~ 1500K.

5.3 Peristerite Gap

Three models for the peristerite gap: "solvus", "binary loop" associated with a first order transition in albite, and "conditional spinodal" with higher than the first order transition in character, have been proposed till now. The exsolution lamellae due to spinodal decomposition were observed in some natural specimens under a transmission electron microscope (e.g., Appendix in the present study). Therefore, the origin of the peristerite gap can narrow down to two models; "solvus", and "conditional spinodal" However, it is difficult to determine whether "solvus" or "conditional spinodal" through the observation of natural specimens and the experiments of natural and synthetic specimens. This is because the degrees of Q_{od} in albite and oligoclase are not directly determined in each specimen and can not be controlled by experiments. Therefore, MD simulation where initial atomic positions can be set at will is applied to the origin of the peristerite gap. In the case of fully ordered plagioclase at whole composition at low temperature, the phase separation between pure albite and pure anorthite occurs as described above section, and the peristerite gap between pure albite and oligoclase is not observed.

Composition dependencies of the order parameter Q_{od} for the Al/Si ordering at constant temperature can not be estimated, simply because no detailed phase diagram of plagioclase feldspar has been published. In the present study, we choose two typical cases of MD simulation which have different composition dependencies of the order parameter Q_{od} for the Al/Si ordering; *pitted partly disordered plagioclase (pitted-pdPl)*, and *linear partly disordered plagioclase (linear-pdPl*. It is assumed that Q_{od} in anorthite richer than $Ab_{75}An_{25}$ has constant value, 1, in both simulations. It has been thought that the incommensurate

structure ('e'-plagioclase) has stability fields at intermediate compositions. However, in the present study, the peristerite gap in the system without 'e'-plagioclase is discussed below because of the difficulty of the MD simulation of 'e'-plagioclase.

5.3.1 Procedure

The Al/Si ordering order parameter Q_{od} was defined as $Q_{od} = (T1o-T1m)/(T1o+T1m) \times ((Ca+Na)/Na)$. In a MD-crystal, Al and Si atoms are distributed into four non-equivalent T-sites, satisfying the *Al-avoidance rule*. The number of Al atoms in four non-equivalent T-sites (T1o, T1m, T2o and T2m) is T1o ≥ T1m = T2o = T2m (Table 5-3). Partly disordered structures for Ab-rich plagioclase were constructed to carry out MD-simulations of linear-pdPl and pitted-pdPl; $Ab_{83.33}/Q_{od} = 0.87$, $Ab_{87.5}/Q_{od} = 0.82$, $Ab_{91.67}/Q_{od} = 0.76$, $Ab_{91.67}/Q_{od} = 0.89$, $Ab_{95.83}/Q_{od} = 0.71$, $Ab_{95.83}/Q_{od} = 0.83$, and $Ab_{100}/Q_{od} = 0.63$. Thereafter, Ca atoms were putted into M-sites satisfying the *Pauling rule*. These MD-simulated plagioclase were used as an initial structure for MD-simulations of the partly disordered plagioclase. Table 5-4 shows MD simulations of plagioclase carried out in the present study.

5.3.2 Result and Discussion

Pitted partly disordered plagioclase (pitted-pdPl)

It has been believed that pure albite phase is usually fully ordered but its coexisting oligoclase phase at equilibrium has partly disorder (e.g., Ribbe, 1960; Ribbe, 1962). MD simulations for the pitted-pdPl were carried out by assuming the composition dependency of

Q_{od} given in Fig. 5-5. MD simulation results with $Ab_{83.33}/Q_{od}$ = 0.87, $Ab_{87.5}/Q_{od}$ = 0.82 and $Ab_{91.67}/Q_{od}$ = 0.89 are shown in Fig. 5-5a, and with $Ab_{91.67}/Q_{od}$ = 0.89 in Fig. 5-5b. The excess enthalpies of mixing of the MD-crystals with the composition dependency of Q_{od} shown in Fig. 5-5a and Fig. 5-5b are the deviations from the straight line connecting the enthalpies of fully ordered albite and perfect anorthite, respectively (Fig. 5-6 and 5-7). Thermodynamics of the peristerite gap must be discussed using the free energy. However, at this moment, discussion is possible only based on the excess enthalpy because of the difficulty to estimate the configurational entropy corresponded this composition dependency of Q_{od}. Excess enthalpy has the remarkable curve concaved upward at the albite rich region, indicating the possibility of the peristerite gap. However, even when Q_{od} has the composition dependency shown in Fig. 5-5a, e.g., at 700K, this dependency changes to that shown in Fig. 5-5b at lower temperature, e.g., 500K. At further lower temperature, e.g., 300K, a stable phase is fully ordered plagioclase with Q_{od}=1 in the whole composition range. With changing the composition dependency of Q_{od} with decreasing temperature, for example, the composition dependency of the excess enthalpy change from that at 700K shown in Fig. 5-6 to that at 500K shown in Fig. 5-7. The results show that this remarkable curve concaved upward in the excess enthalpy is smaller, and further the composition of oligoclase phase shifted to the Ab-richer (Fig. 5-6 and 5-7). These results signify that the width of the miscibility gap become narrower with decreasing temperature. Therefore, it can be shown that the assumption that pure albite phase is fully ordered but the oligoclase phase has partly disorder is not correct in the system ignoring the existence of 'e'-plagioclase.

Linear partly disordered plagioclase (linear-pdPl)

Results of the MD simulations for the linear-pdPl carried out by assuming the composition dependency of Q_{od} are shown in Fig. 5-8 ($Ab_{83.33}/Q_{od} = 0.87$, $Ab_{87.5}/Q_{od} = 0.82$, $Ab_{91.67}/Q_{od} = 0.76$, $Ab_{95.83}/Q_{od} = 0.71$, and $Ab_{100}/Q_{od} = 0.63$ in Fig. 5-8a and $Ab_{91.67}/Q_{od} = 0.89$ and $Ab_{95.83}/Q_{od} = 0.83$ in Fig. 5-8b). The excess enthalpies of mixing of the MD-crystals with albite composition dependency of Q_{od} shown in Figs. 5-8a and -8b are the deviations from the straight line connecting the enthalpies of the partly disordered albite and perfect anorthite (Figs. 5-9 and -10). Fig. 5-9a shows that the excess enthalpy has minimum value at about $Ab_{75}An_{25}$ with a small value of Q_{od}. The excess enthalpy in the more Ab-rich area than $Ab_{75}An_{25}$ shows the curve concaved upward, indicating the possibility of the phase separation between pure albite phase and oligoclase phase, that is, peristerite gap. And oligoclase phase has the composition where the excess enthalpy has minimum value. However, if Q_{od} has the composition dependency shown in Fig. 5-8a, e.g., at 700K, this dependency changes to that shown in Fig. 5-8b at lower temperature, e.g., 500K and then becomes the same as fully ordered plagioclase with Q_{od}=1 in the whole compositional range at further lower temperature, e.g., 300K. With changing the composition dependency of Q_{od} with decreasing temperature, for example, the composition dependency of the excess enthalpy change from that at 700K shown in Fig. 5-9 to that at 500K shown in Fig. 5-10. This results in the shift of the composition of oligoclase phase, i.e., that with the minimum value of the excess enthalpy, to more Ab-rich (Fig. 5-9 and 5-10). This result signifies that the width of miscibility gap become narrower with decreasing temperature as same as the case of pitted-pdPl. It is thought that this linear correlation does not have the peristerite gap in the system ignoring the

existence of 'e'-plagioclase.

In the "conditional spinodal" model proposed by Carpenter (1981), which is currently accepted, the existence of peristerite gap is interpreted to be entirely due to the ordering of Al and Si in pure albite, i.e., the phase transition from high-albite to low-albite. In the model, much attention is not paid on the importance of the existence of 'e'-plagioclase. However, the present results of two typical cases of MD simulations on *pitted partly disordered plagioclase,* and *linear partly disordered plagioclase,* imply that the thermodynamic of peristerite gap can not be explained by only the composition dependency of the order parameter Q_{od} in the system even in the case where 'e'-plagioclase is absent. In the previous chapter; "Pure Albite", the existence of the crossover between high- and low-albite is not suggested. Furthermore, 'e'-reflections are found in lamellae in natural specimens (e.g., Appendix in the present study), suggesting coexisting of albite and 'e'-plagioclase in peristerite gap. Therefore, it can be suggested that the consideration about 'e'-plagioclase is indispensable for understanding the origin of the peristerite gap. Therefore, the "conditional spinodal" model is not supported in the present study. On the other hand, it is suggested in the present study that "solvus" can be considered to be a more influential model than the "conditional spinodal" model, since the thermodynamic driving force for "solvus" can be considered to be due to the unmixing between pure albite and 'e'-plagioclase and independent upon the existence of the phase transition from high- to low-albite.

Table 5-3. The number of Al atom in four inequivalent T-sites (T1o, T1m, T2o and T2m) in the MD-simulated pdPl.

	Q_{od}	T1o	T1m	T2o	T2m
$Ab_{83.33}$	0.87	76	12	12	12
$Ab_{87.50}$	0.82	72	12	12	12
$Ab_{91.67}$	0.76	68	12	12	12
$Ab_{91.67}$	0.89	80	8	8	8
$Ab_{95.83}$	0.71	64	12	12	12
$Ab_{95.83}$	0.83	82	6	6	6

Table 5-4. MD simulations of plagioclase feldspar carried out in the present study to investigate Peristerite gap are tabulated as follow;

MD simulation	pitted partly disordered Pl -a			pitted partly disordered Pl -b	linear partly disordered Pl -a					linear partly disordered Pl -b	
Abbreviation	pitted-pdPl			pitted-pdPl	linear-pdPl					linear-pdPl	
Ab component	83.33	87.5	91.67	91.67	83.33	87.5	91.67	95.83	100	91.67	95.83
Q_{od}	0.87	0.82	0.89	0.89	0.87	0.82	0.76	0.71	0.63	0.89	0.83
Al-avoidance rule		O		O			O			O	
Pauling rule		O		O			O			O	
Temperature	300 - 1500K			300 - 1500K	300 - 1500K					300 - 1500K	

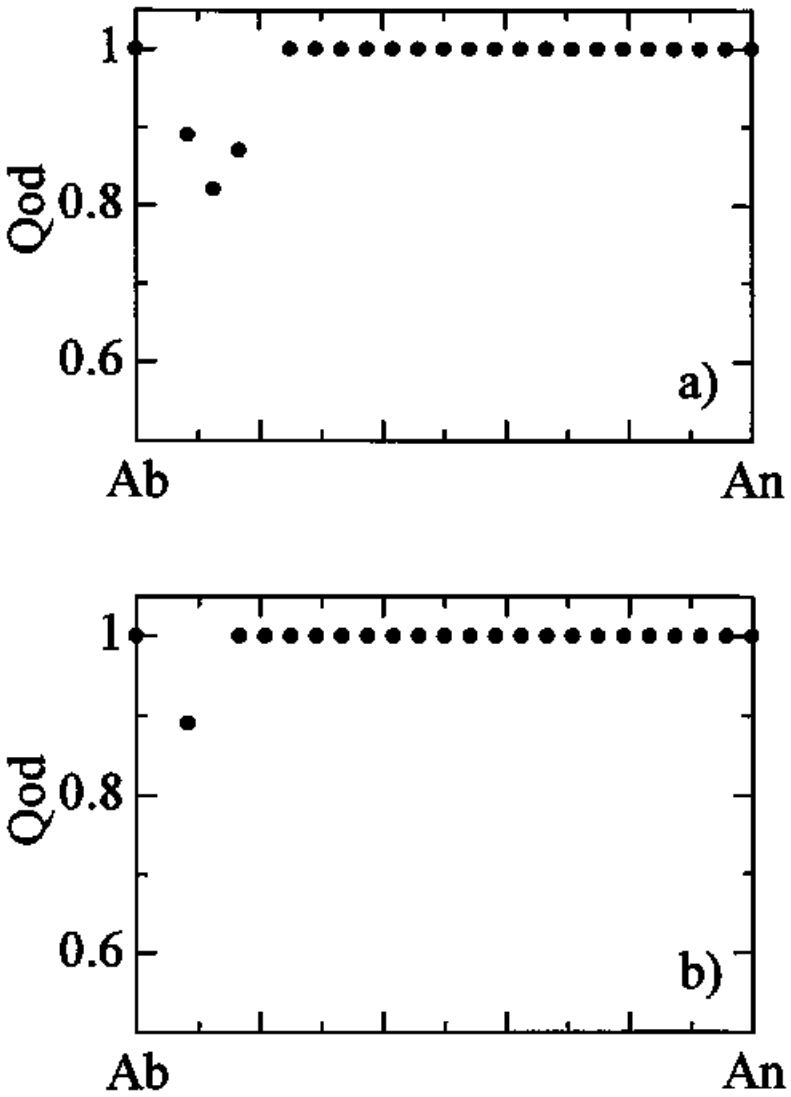

Fig. 5-5. One of the typical cases of composition dependency of Q_{od}, i. e., the MD-simulated pitted-pdPl. The composition dependency of Q_{od} changes from (a) to (b) with decreasing temperature.

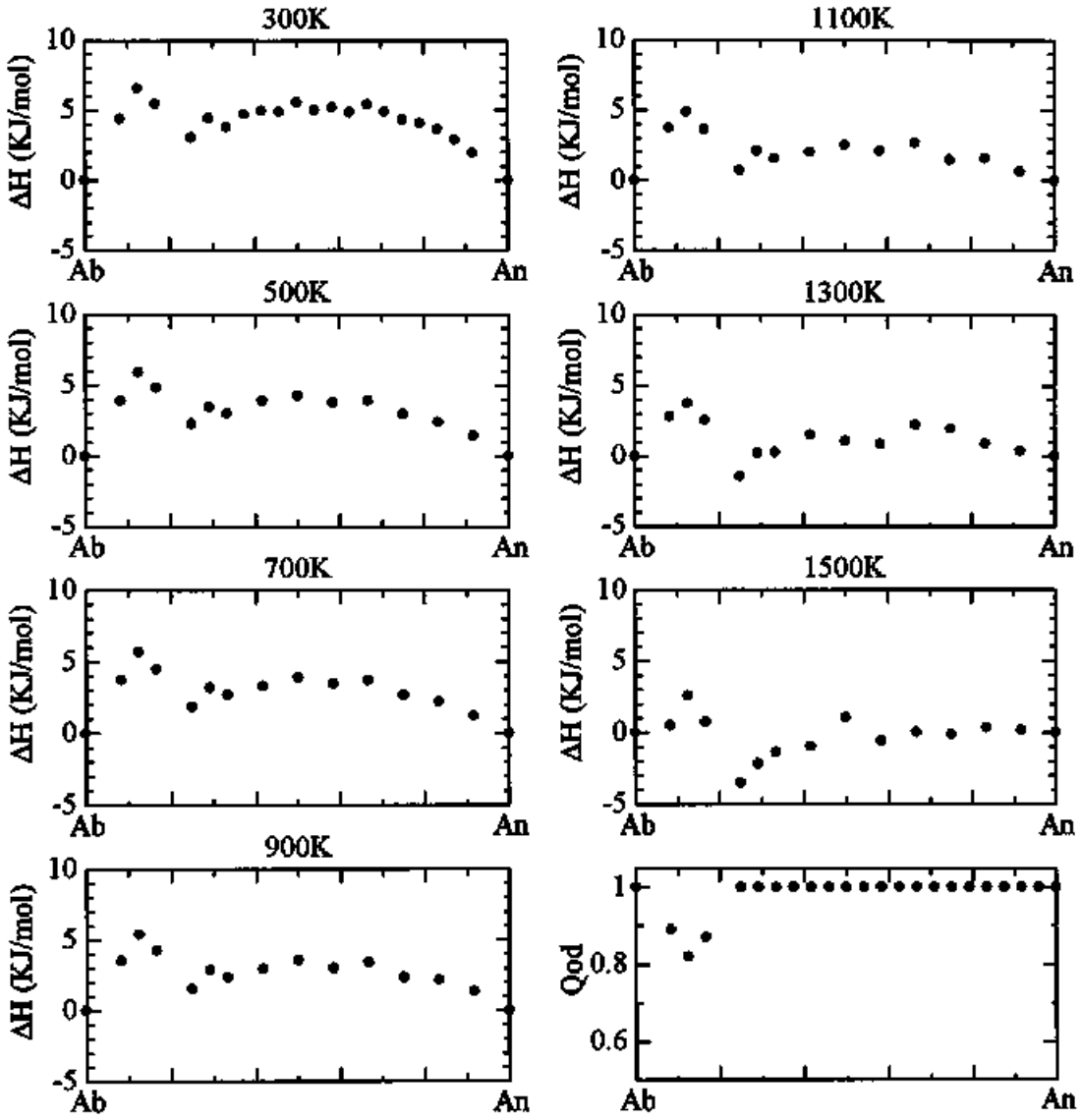

Fig. 5-6. Excess enthalpies of mixing of the MD-simulated pitted-pdPl with the composition dependency of Q_{od} shown in Fig. 5-5a.

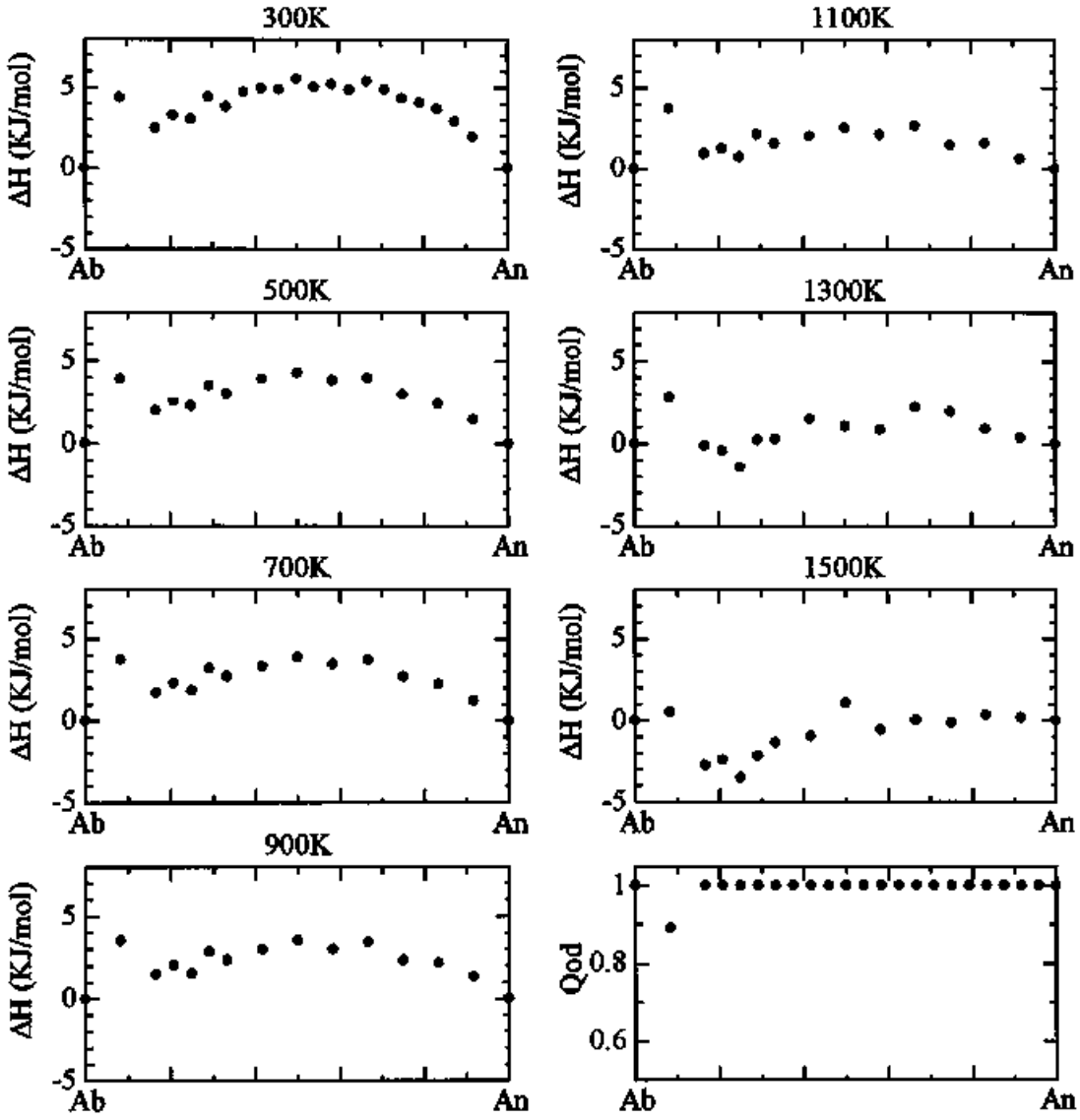

Fig. 5-7. Excess enthalpies of mixing of the MD-simulated pitted-pdPl with composition dependency of Q_{od} shown in Fig. 5-5b.

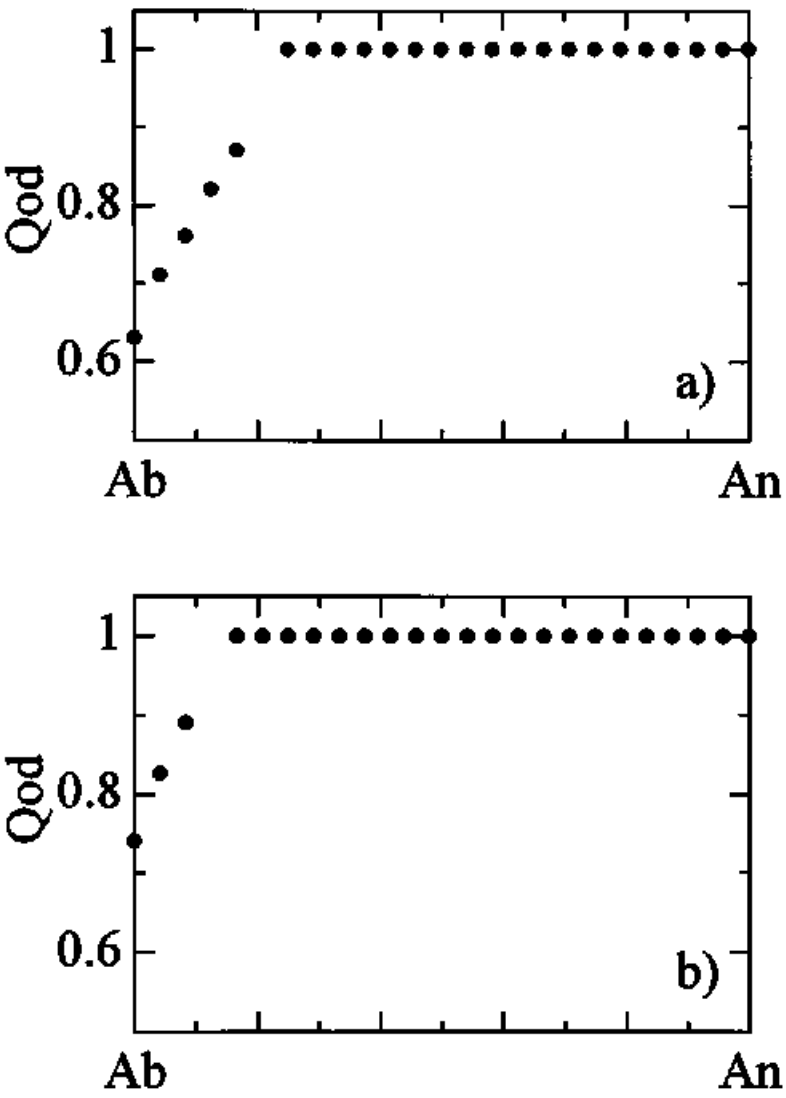

Fig. 5-8. One of the typical cases of composition dependency of Q_{od}, i. e., the MD-simulated linear-pdPl. The composition dependency of Q_{od} changes from (a) to (b) with decreasing temperature.

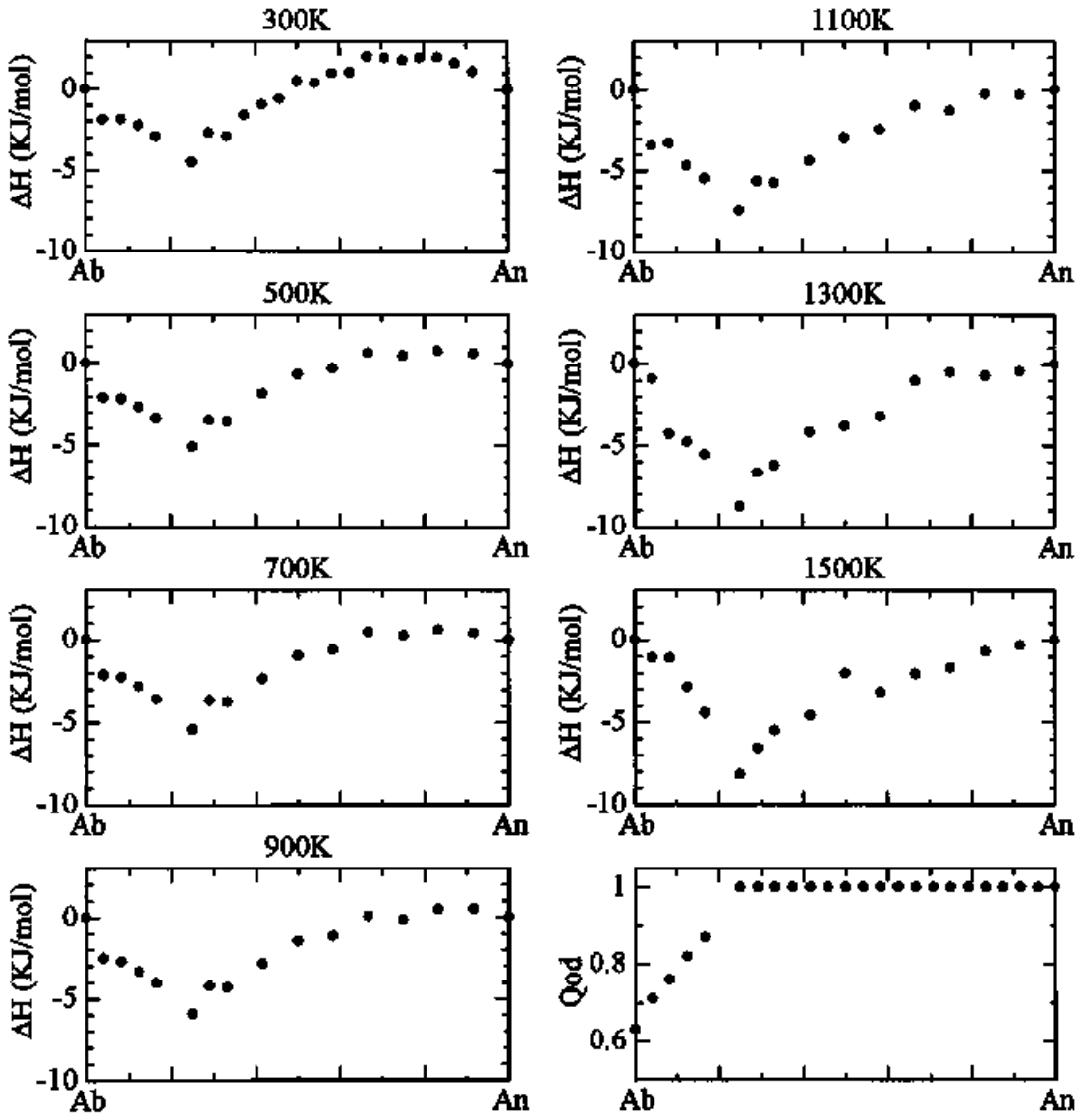

Fig. 5-9. Excess enthalpies of mixing of the MD-simulated linear-pdPl with composition dependency of Q_{od} shown in Fig. 5-8a.

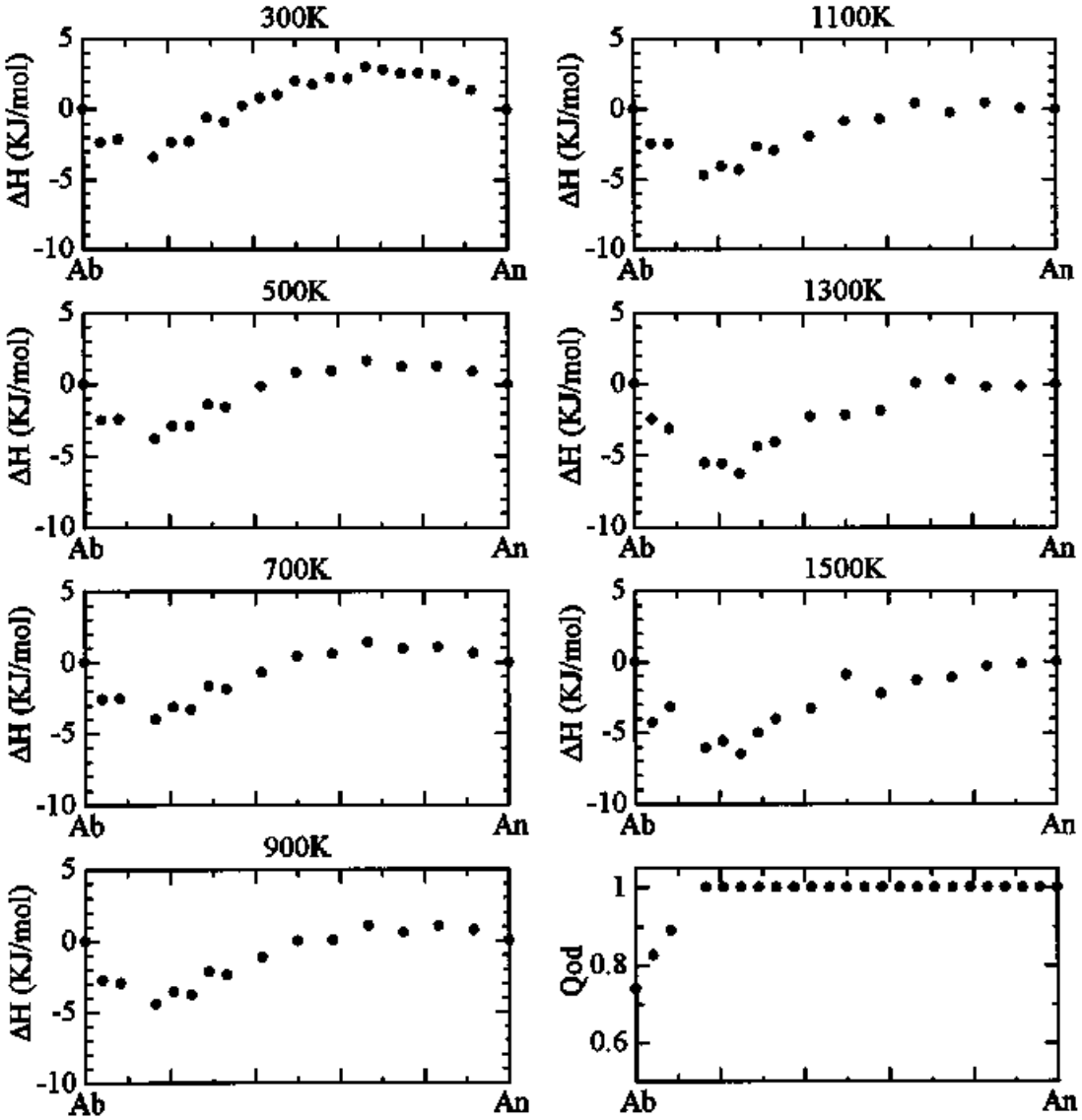

Fig. 5-10. Excess enthalpies of mixing of the MD-simulated linear-pdPl with composition dependency of Q_{od} shown in Fig. 5-8b.

6. Conclusions

(1) Using the newly evaluated parameters of Molecular Dynamics (MD) simulation in the NaO-CaO-MgO-Al_2O_3-SiO_2 system, 21crystals are quite successfully reproduced in the MD simulations. The MD simulations on three kinds of feldspar; pure anorthite, pure albite and plagioclase feldspar solid solution were carried out to investigate the mechanism of the phase transitions and thermodynamic behavior.

Pure Anorthite

(2) The MD simulations of fully ordered anorthite and partly disordered anorthite were carried out to investigate the thermodynamic behaviour of anorthite. The jumps of the volume and the structure factors at the transition temperature are observed in the MD-simulated fully ordered anorthite but not in the MD-simulated partly disordered anorthite. These results show that the $P\bar{1}$-$I\bar{1}$ phase transition of the MD-simulated fully ordered anorthite is first order (not nearly second order) and that of the MD-simulated partly disordered anorthite is non-first order. The correlation between the Ca motions and the behavior of the framework is strong during the $P\bar{1}$-$I\bar{1}$ phase transition in the MD-simulated anorthite. The fact that the transition of real anorthite is tricritical is then interpreted as that real anorthite has locally a slightly disordered arrangement of Al/Si.

(3) Ca atoms in MD-simulated fully ordered anorthite at high temperature where the $I\bar{1}$ structure is stable occupy not the 'split' positions but the positions of the $I\bar{1}$ structure. On the

other hand, Ca atoms in MD-simulated partly disordered anorthite at the same temperature occupy in multiple sites, because some Ca atoms are attracted by the oxygen atoms which bridge between two Al atoms violating the *Al-avoidance rule*, implying the existence of the Ca 'split' position in real anorthite.

Pure Albite

(4) MD simulations of pure albite with different order parameter Q_{od} of the Al/Si ordering were carried out to investigate the thermodynamic properties. The results were analyzed by using the Landau-type free energy expansion with two order parameters, Q and Q_{od} proposed by Salje et al. (1985). The MD-simulated albites show that the symmetry reduction from C2/m to $C\bar{1}$ is dominated by 2nd order transition due to both the displacement of atoms (Q) and the Al/Si ordering (Q_{od}), and that there is no thermal crossover between high- and low-albites.

(5) To investigate the behavior of Na atom, MD simulations of fully ordered and partly disordered albite were carried out at low temperature. Na atoms in the MD-simulated fully ordered albite keep the positions of the $C\bar{1}$ structure and move by thermal vibration. On the other hand, Na atoms in the MD-simulated partly disordered albite occupy multiple sites breaking the $C\bar{1}$ symmetry and vibrate weaker than that in the MD-simulated fully ordered albite, because some Na atoms are attracted by the oxygen atoms which bridge between Al atoms violating the *Al-avoidance rule*.

Plagioclase feldspar solid solution

(6) To investigate the thermodynamic behavior of plagioclase, MD simulations of fully ordered and disordered plagioclase were carried out. MD-simulated fully ordered plagioclase is a stable phase in the whole compositional range at low temperature (300K in the present study). At low temperature the phase separation between pure albite and pure anorthite can be expected, because the excess enthalpy of MD-simulated plagioclase of the lamellae structure between pure albite and pure anorthite is smaller than that of MD-simulated fully ordered plagioclase with the same composition.

(7) In the system without 'e'-plagioclase, MD simulations of plagioclase with different composition dependencies of Q_{od} were carried out to investigate the origin of peristerite miscibility gap. MD-simulated plagioclase with any composition dependencies of Q_{od} in this system can not explain the thermodynamic of peristerite gap. This fact suggests that the existence of 'e'-plagioclase is very important to understand the origin of peristerite gap.

Acknowledgements

The author would like to express his sincere thanks to Professor Masao Kitamura of Kyoto University for supervising him during this study with many valuable advice, encouraging discussions and critical readings of this manuscript.

The author is deeply indebted to Professor Katsuyuki Kawamura of Tokyo Institute of Technology for many important advice and encouraging discussions.

The author is grateful to Dr. Katsutoshi Tomita of Kyoto University for his valuable suggestions and helpful discussions.

The author is grateful to Dr. Norimasa Shimobayashi of Kyoto University for his valuable suggestions and helpful criticism of this manuscript.

The author is grateful to Professor Toshiharu Irisawa of Gakusyuin University, Professor Masanori Matsui of Kyusyu University, Dr. Tadashi Akamatsu of Kochi University for their helpful comments and discussions.

The author is grateful to Professor Kazuhiro Suzuki of Nagoya University, Dr. Hideo Ishizuka of Kochi University, Professor Kazuyuki Shiraishi of National Institute of Polar Research, and Mr. Katsushi Shirahata of Kyoto University for providing with the specimens used in study and their helpful comments.

The author wishes to thank Dr. Naoya Sawaguchi of National Industrial Research Institute of Nagoya, Mr. Hiroyuki Hasegawa of Geographical Survey Institute, Miss Kiiko Matsumoto of Gakusyuin University, and Mr. Kentaro Uesugi of Tokyo Institute of Technology for their discussions and their technical helps with molecular dynamics simulation experiments.

Thanks are due to Dr. Takashi Fujita of Okayama University, Dr. Naoya Imae of National Institute of Polar Research, Mr. Noboru Suda of KYOCERA CORPORATION, and Dr. Mitsuru Fudaki of Yamaguchi University for their kind discussions and helps. Thanks are also due to Mr. Shoichi Toh, Mr. Eiji Miura and many colleagues of Kyoto University for their technical helps.

References

Adlhart W., Frey F. and Jagodzinski H. (1980) X-ray and neutron investigation of the $P\bar{1}$-$I\bar{1}$ transition in pure anorthite. Acta Crystallography, A 36, 450-460.

Akamatsu T., Akiyama K., Fukuhama M., and Kawamura K. (1995) Molecular dynamics simulations of CsCl-type solid solution crystals (in Japanese). Annual Meeting abstracts of Mineralogical Society of Japan, 58.

Akamatsu T., Fukuhama M., Nukui H., and Kawamura K. (1994) Molecular dynamics simulations of NaCl-type solid solution crystals: The first application of molecular dynamics to solid solutions. Molecular Simulation, 12, 431-434.

Akamatsu T., Maeno M., and Kawamura K. (1996) Molecular dynamics simulations of perovskite-type solid solution (in Japanese). The Annual Meeting Abstracts of Mineralogical Society of Japan, 78.

Ashworth J.R. and Evirgen M.M. (1985) Plagioclase relations in pelites, central Menderes Massif, Turkey. I. The peristerite gap with coexisting kyanite. Journal Metamorphic Geology, 3, 207-218.

Belonoshko A.B. and Dubrovinsky L.S. (1995) Molecular dynamics of stishovite melting. Geochimica et Cosmochimica Acta, 59, 1883-1889.

Belonoshko A.B. and Dubrovinsky L.S. (1996a) Molecular and lattice dynamics study of the MgO-SiO_2 system using a transferable interatomic potential. Geochimica et Cosmochimica Acta, 60, 1645-1656.

Belonoshko A.B. and Dubrovinsky L.S. (1996b) Molecular dynamics of NaCl (B1 and B2)

and MgO (B1) melting: two-phase simulation. American Mineralogist, 81, 303-316.

Bown M.G. and Gay P. (1958) The reciprocal lattice geometry of the plagioclase feldspar structures. Zeitschrift für Kristallographie, Bd. 111,S. 1-14.

Brown W.L., Hoffmann W. and Laves F. (1963) Über kontinuierliche und reversible transformationen des anorthits ($CaAl_2Si_2O_8$) zweishen 25 und 350°C. Naturwissenschaften, 50, 221.

Carpenter M.A. (1981) A "conditional spinodal" within the peristerite miscibility gap of plagioclase feldspars. American Mineralogist, 66, 553-560.

Carpenter M.A. (1992) Equilibrium thermodynamics of Al/Si ordering in anorthite. Physics and Chemistry of Minerals, 19, 1-24.

Carpenter M.A. (1994) Subsolidus phase relations of the plagioclase feldspar solid solution. In: Parsons I. (ed.) Feldspars and Their Reactions., NATO ASI series C, 221-269.

Clark J.R., Appleman D.E., and Papike J.J. (1969) Crystal-chemical characterization of clinopyroxenes based on eight new structure refinements. Mineralogical Society of America Special Paper 2, 31-50.

Crawford M.L. (1966) Composition of plagioclase and associated minerals in some schists from Vermont, U.S.A., and South Westland, New Zealand, with inferences about the peristerite solvus. Contributions to Mineralogy and Petrology, 13, 269-294.

Czank M., Schulz H., Laves F., and Gros W. (1972) Investigation of domains in anorthite by electron microscopy. Naturwissenschaften, 59,77-78.

Czank M., Van Landuyt J., Schulz H., Laves F. and Amelinckx S. (1973a) Temperature dependence of domains in anorthite. Naturwissenschaften, 59, 646.

Czank M., Van Landuyt J., Schulz H., Laves F., and Amelinckx S. (1973b) Electron microscopic study of the structural changes as a function of temperature in anorthite. Zeitschrift für Kristallographie, 138, 403-418.

Czaya R. (1971) Refinement of the structure of γ-Ca_2SiO_4. Acta Crystallographica, B27, 848-849.

Ferguson R.B., Traill R.J. and Taylor W.H. (1958) The crystal structure of low-temperature and high-temperature albites. Acta Crystallography, 11, 331-348.

Fischer V.P. (1967) Neutronenbeugungsuntersuchung der strukturen von $MgAl_2O_4$- und $ZnAl_2O_4$-spinellen, in Abhängigkeit von der Vorgeschichte. Zeitschrift für Kristallographie, 124, 275-302.

Foit F.F. and Peacor D.R. (1973) The anorthite crystal structure at 410 and 830 °C. American Mineralogist, 58, 665-675.

Frey F., Jagodzinski H. and Prandal W. (1977) Dynamic character of primitive to body-centered phase transition in anorthite. Physics and Chemistry of Minerals, 1, 227-231.

Fujino K., Sasaki S., Takeuchi Y., and Sadanaga R. (1981) X-ray determination of electron distributions in forsterite, fayalite and tephroite. Acta Crystallographica, B37, 513-518.

Ghose S., McMullan R.K. and Weber H.P. (1993) Neutron diffraction studies of the $P\bar{1} \rightarrow I\bar{1}$ transition in anorthite, $CaAl_2Si_2O_8$, and the crystal structure of the body-centered phase at 514K. Zeitschrift für Kristallographie, 204, 215-237.

Ghose S., Van Tendeloo G. and Amelinckx S. (1988) Dynamics of a second-order phase transition: $P\bar{1}$ to $I\bar{1}$ phase transition in anorthite, $CaAl_2Si_2O_8$. Science, 242, 1539-1541.

Goldsmith J.R. (1982) Review of the behavior of plagioclase under metamorphic conditions. American Mineralogist, 67, 643-652.

Goldsmith J.R. and Jenkins D.M. (1985) The high-low albite relations revealed by reversal of degree of order at high pressures. American Mineralogist, 70, 911-923.

Grapes B. and Otsuki M. (1983) Peristerite compositions in quartzofeldspathic schists, Franz Josef-Fox Glacier Area, New Zealand. Journal Metamorphic Geology, 1, 47-61.

Grove T.L., Ferry J.M. and Spear F.S. (1983) Phase transitions and decomposition relations in calsic plagioclase. American Mineralogist, 68, 41-59.

Grudy H.D. and Brown W. L. (1969) A high-temperature X-ray study of equilibrium forms of albite. Mineralogical Magazine, 37-286, 156-172.

Hatch D.M. and Ghose S. (1989) A dynamical model for the $I\bar{1}$ $P\bar{1}$ phase transition in anorthite, $CaAl_2Si_2O_8$. Physics and Chemistry of Minerals, 16, 614-620.

Hazen R.M. (1976) Effects of temperature and pressure on the cell dimension and X-ray temperature factors of periclase. American Mineralogist, 61, 266-271.

Hazen R.M. and Finger L.W. (1978) Crystal structures and compressibilities of pyrope and grossular to 60kbar. American Mineralogist, 63, 297-303.

Ishizuka H. (1985) Prograde metamorphism of Horokanai ophiolite in the Kamuikotan zone, Hokkaido, Japan. Journal of Petrology; 26, 391-417.

Kawamura K. (1997) MXDTRICL. Japan Chemistry Program Exchange, #077.

Kempster C.J.E., Megaw H.D. and Radoslovich E.W. (1962) The structure of anorthite, $CaAl_2Si_2O_8$. I. Structure Analysis. Acta Crystallographica, 15,1005-1017.

Kroll H., Bambauer H.U. and Schirmer U. (1980) The high albite-monalbite and analbite-

monalbite transitions. American Mineralogist, 65, 1192-1211.

Lager G.A. and Meagher E.P. (1978) High-temperature structural study of six olivines. American Mineralogist, 63, 365-377.

Maruyama S., Liou J.G. and Suzuki K. (1982) The peristerite gap in low-grade metamorphic rocks. Contributions to Mineralogy and Petrology, 81, 268-276.

Matsui M. (1988) Molecular dynamics study of $MgSiO_3$ perovskite. Physics and Chemistry of minerals, 16, 234-238.

Matsui M. (1989) Molecular dynamics study of the structural and thermodynamic properties of MgO crystal with quantum correction. Journal of Chemistry and Physics, 91, 489-494.

Matsui M. and Price G.D. (1992) Computer Simulation of the $MgSiO_3$ polymorphs. Physics and Chemistry of Minerals, 18, 365-372.

Matsumoto T., Tokonami M. and Morimoto N. (1975) The crystal structure of omphacite. American Mineralogist, 60, 634-641.

Meagher E.P. (1975) The crystal structures of pyrope and grossularite at elevated temperatures. American Mineralogist, 60, 218-228.

Megaw H.D. (1960) Order and disorder II. Theory of diffraction effects in the intermediate plagioclase feldspars. Proceedings of the Royal Society of London, A259, 159-183.

Miyake A., Hasegawa H., Kawamura K., and Kitamura M. (1997) Symmetry and its change in reciprocal space of a crystal simulated by molecular dynamics: application to quartz. Acta Crystallographica, Section A, (submitted).

Morimoto N. (1960) The crystal structures of clinoenstatite and pigeonite. Zeitschrift für Kristallographie, 114, 120-147.

Newnham R.E. and deHaan Y.M. (1962) Refinement of the α Al_2O_3, Ti_2O_3, V_2O_3 and Cr_2O_3 structures. Zeitschrift für Kristallographie, 117, 235-237.

Nord G.L. Jr., Hammarstrom J. and Zen E-an (1978) Zoned plagioclase and peristerite formation in phyllites from southwestern Massachusetts. American Mineralogist, 63, 947-955.

Ohashi Y. (1984) Polysynthetically-twinned structures of enstatite and wollastonite. Physics and Chemistry of Minerals, 10, 217-229.

Orville P.M. (1974) The peristerite gap as an equilibrium between ordered albite and disordered plagioclase solid solution. Bulletin de la Scociété française de Minéralogie et de Cristallographie, 97, 386-392.

Peacor D.R. and Prewitt C.T. (1963) Comparison of the crystal structures of bustamite and wollastonite. American Mineralogist, 48, 588-596.

Phillips B.L. and Kirkpatrick R.J. (1995) High-temperature ^{29}Si MAS NMR spectroscopy of anorthite ($CaAl_2Si_2O_8$) and its $P\bar{1}$-$I\bar{1}$ structural phase transition. Physics and Chemistry of Minerals, 22, 269-276.

Prewitt C.T. and Burnham C.W. (1966) The crystal structure of jadeite, $NaAlSi_2O_6$. American Mineralogist, 51, 956-975.

Prewitt C.T., Sueno S. and Papike J.J. (1976) The crystal structures of high albite and monalbite at high temperatures. American Mineralogist, 61, 1213-1225.

Quareni S. and Taylor W.H. (1971) Anisotropy of the sodium atom in low albite. Acta Crystallography, B27, 281-285.

Redfern S.A.T. and Salje E.(1987) Thermodynamics of plagioclase II: Temperature

evolution of the spontaneous strain at the $I\bar{1}$-$P\bar{1}$ phase transition in anorthite. Physics and Chemistry of Minerals, 14, 189-195.

Redfern S.A.T. and Salje E. (1992) Microscopic dynamic and macroscopic thermodynamic character of the $I\bar{1}$-$P\bar{1}$ phase transition in anorthite. Physics and Chemistry of Minerals, 18, 526-533.

Redfern S.A.T., Graeme-Barber A. and Salje E. (1988) Thermodynamics of plagioclase III Spontaneous Strain at the I P phase transition in Ca-rich plagioclase. Physics and Chemistry of Minerals, 16, 157-163.

Ribbe P.H. (1960) An X-ray and optical investigation of peristerite plagioclases. American Mineralogist, 45, 626-644.

Ribbe P.H. (1962) Observations on the nature of unmixing in peristerite plagioclases. Norsk Geologisk Tidsskrift, 42, 2, 138-151.

Ribbe P.H. (1983) Aluminum-silica order in feldspars; domain textures and diffraction patterns. In P.H. Ribbe, Ed., Feldspar Mineralogy, Reviews in Mineralogy, Vol. 2, 2nd Edition, 21-55.

Ribbe P.H. (1994) The crystal structures of the aluminum-silicate feldspars. In: Parsons I. (ed.) Feldspars and Their Reactions., NATO ASI series C, 1-49.

Salje E., (1985) Thermodynamics of sodium feldspar I: Order parameter treatment and strain induced coupling effects. Physics and Chemistry of Minerals, 12, 93-98.

Salje E. (1987) Thermodynamics of plagioclase I: Theory of the $I\bar{1}$-$P\bar{1}$ phase transition in anorthite and Ca-rich plagioclases. Physics and Chemistry of Minerals, 14, 181-188.

Salje E., Kuscholke B., Wruck B., and Kroll H. (1985) Thermodynamics of sodium feldspar II: Experimental results and numerical calculations. Physics and Chemistry of Minerals, 12, 99-107.

Senderov E.E. (1980) On the theory of Al, Si ordering in albite. Physics and chemistry of minerals, 6, 251-268.

Shirahata K. and Hirajima T. (1995) Chemically sector-zoned garnet in Sanbagawa schists; its mode of occurrence and growth timing. Jouranl of Mineralogy, Petology and Economic geology, 90, 69-79.

Smith J.V (1972) Critical review of synthesis and occurrence of plagioclase feldspars and a possible phase diagram. Journal of Geology 80, 505-525.

Smith J.V (1974) Feldspar minerals, v1. Springer Verlag, Berlin Heidelberg New York.

Smith J.V (1983) Phase euilibria of plagioclase. In P.H. Ribbe, Ed., Feldspar Mineralogy, Reviews in Mineralogy, Vol. 2, 2nd Edition, 223-239.

Smith J.V., Artioli G., and Kvick A. (1986) Low albite, $NaAlSi_3O_8$: neutron diffraction study of crystal structure at 13K. American Mineralogist, 71, 727-733.

Smith J.V and Brown W.L. (1988) Feldspar minerals. 1. Springer, Berlin Heidelberg New York.

Staehli J.L. and Berinkmann D. (1974) A nuclear magnetic resonance study of the phase transition in anorthite, $CaAl_2Si_2O_8$. Zeitschrift für Kristallographie, 140, 360-373.

Stein D.J. and Spera F. (1995) Molecular dynamics simulations of liquids and glasses in the system $NaAlSiO_4$-SiO_2: Methodology and melt structures. American Mineralogist, 80, 417-431.

Suzuki K. (1975) On some unusual bands and veins metasomatically developed in the contact aureole in Kasugamura, Gifu-ken. J Geol Soc Jpn, 81, 487-504.

Tsuneyuki S., Aoki H., Tsukada M. and Matsui Y. (1990) Molecular-dynamics study of the α to β structural phase transition of quartz. Physical review letters, 64, 776-779.

Van Tendeloo G.V., Ghose S. and Amelinckx S. (1989) A dynamic model for the $P\bar{1}$-$I\bar{1}$ phase transition in anorthite, $CaAl_2Si_2O_8$; 1. Evidence from electron microscopy. Physics and Chemistry of Minerals, 16, 311-319.

Wainwright J.E. and Starkey J. (1971) A refinement of the structure of anorthite. Zeitschrift f ür Kristallographie, Bd 133 S, 75-84.

Wentzovitch R.M., Martins J.L., and Price G.D. (1993) Ab initio molecular dynamics with variable cell shape: application to $MgSiO_3$. Physical Review Letters, 70, 3947-3950.

Winter J.K. and Ghose S. (1979) Thermal expansion and high-temperature crystal chemistry of the Al_2SiO_5 polymorphs. American Mineralogist, 64, 573-586.

Winter J.K., Ghose S., and Okamura F.P (1977) A high-temperature of the thermal expansion and the anisotropy of the sodium atom in low albite. American Mineralogist, 62, 921-931.

Winter J.K., Okamura F.P., and Ghose S. (1979) A high temperature structural study of high albite, monalbite and the analbite-monalbite phase transition. American Mineralogist, 64, 921-931.

Wright A.F and Lehmann M.S. (1981) The structure of quartz at 25 and 590°C determined by neutron diffraction. Journal of solid state chemistry, 36, 371-380.

Wyckoff R.W.G. (1963) *Crystal Structures*, John Wiley & Sons, New York.

Appendix. Observation of natural specimens

Texture of albite-rich plagioclase feldspar in metamorphic rocks from four different areas was observed in the present study: Kasugamura, Horokanai, East Antarctica and Sanbagawa areas. Chemical compositions of plagioclase which occurs in Kasugamura and Horokanai areas have been studied in relation to peristerite miscibility gap by Maruyama et al. (1982) and Ishizuka (1985), respectively. Crystals of plagioclase in polished thin sections of metamorphic rocks from Kasugamura and Horokanai area were studied under an optical microscope, a scanning electron microscope (SEM; HITACHI S-530) with a detector for back-scattered electrons (GW Type 30) and an energy dispersed spectrometer (EDS; Kevex Delta Series) for X-ray microanalyses, and a transmission electron microscope (TEM; HITACHI H-8000K). Internal texture of plagioclase from East Antarctica and Sanbagawa areas were studied under TEM.

Kasugamura area

The geological and petrographic characters of constituent rocks in Kasugamura area were reported by Suzuki (1975) and the peristerite gap in this area was studied by Maruyama et al. (1982). The samples used in the present study were collected from the locality and their polished thin sections were observed under SEM. Both grains of albite and oligoclase can be found in several rock samples. However, it could not be decided in the present study whether this coexistence is formed under an equilibrium condition or not, because albite grains are commonly observed as overgrowth on grains of oligoclase. There remains the possibility that

oligoclase grains were not metamorphosed. Fig. App.-1 shows the variation of the Ab-content of grains against metamorphic grade. The coexisting albite and oligoclase in the same specimen shows the same symbol. The Ab-content of albite phase shows the more albite-rich than the albite phase reported by Maruyama et al. (1982).

Horokanai area

The geological and petrographic characters of constituent rocks and the peristerite gap in Horokanai area were studied by Ishizuka (1985). The samples used in the present study were collected from the locality and their polished thin sections were observed under SEM. Most samples include homogeneous grains of albite (Ab_{1-2}), but the coexisting of albite and oligoclase can not be found in every specimen. Fig. App.-2 shows the variation of the Ab-content against metamorphic grade. TEM observation on grains of homogeneous albite (sample No.12) shows no micro-texture such as exsolution lamella (Fig. App.-3).

East Antarctica area

The micro-texture of oligoclase (An15) at Akebono Rock, East Antarctica was observed under TEM. The exsolution lamellae formed by the spinodal decomposition were found (Fig. App.-4).

Sanbagawa area

The micro-texture of oligoclase (An15) at locality A in the Sanbagawa belt in the Besshi area (Shirahata and Hirajima, 1995) was observed under the TEM. The exsolution lamellae formed by the spinodal decomposition were found (Fig. App.-5). 'e'-reflections were observed around 01½ reflection in an electron diffraction pattern from the area shown in Fig. App.-5 (Fig. App.-6).

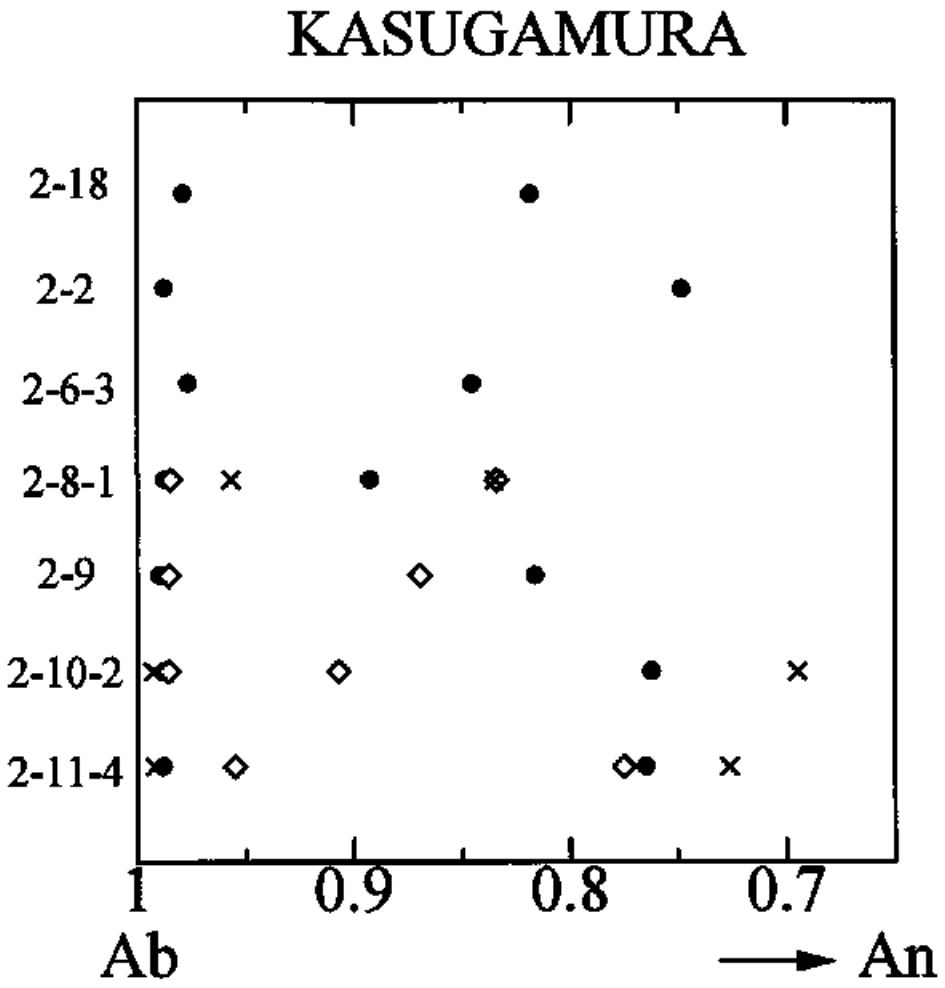

Fig. App.-1. Variation of the Ab-content of plagioclase against metamorphic grade in Kasugamura Area. Vertical axis is arbitrary scale and the upper in the figure is higher grade. The same symbols indicate the coexisting albite and oligoclase in the same specimen.

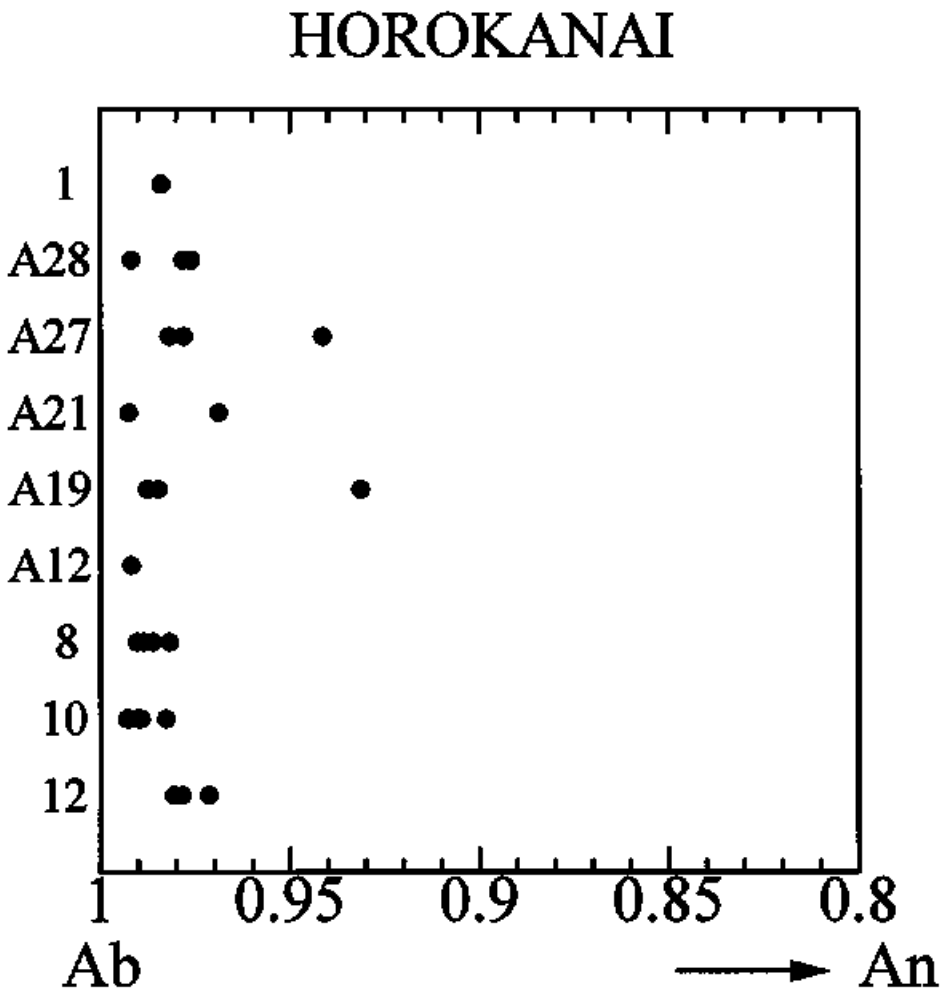

Fig. App.-2. Variation of the Ab-content of plagioclase against metamorphic grade in Horokanai Area. Vertical axis is arbitrary scale and the upper in the figure is higher grade.

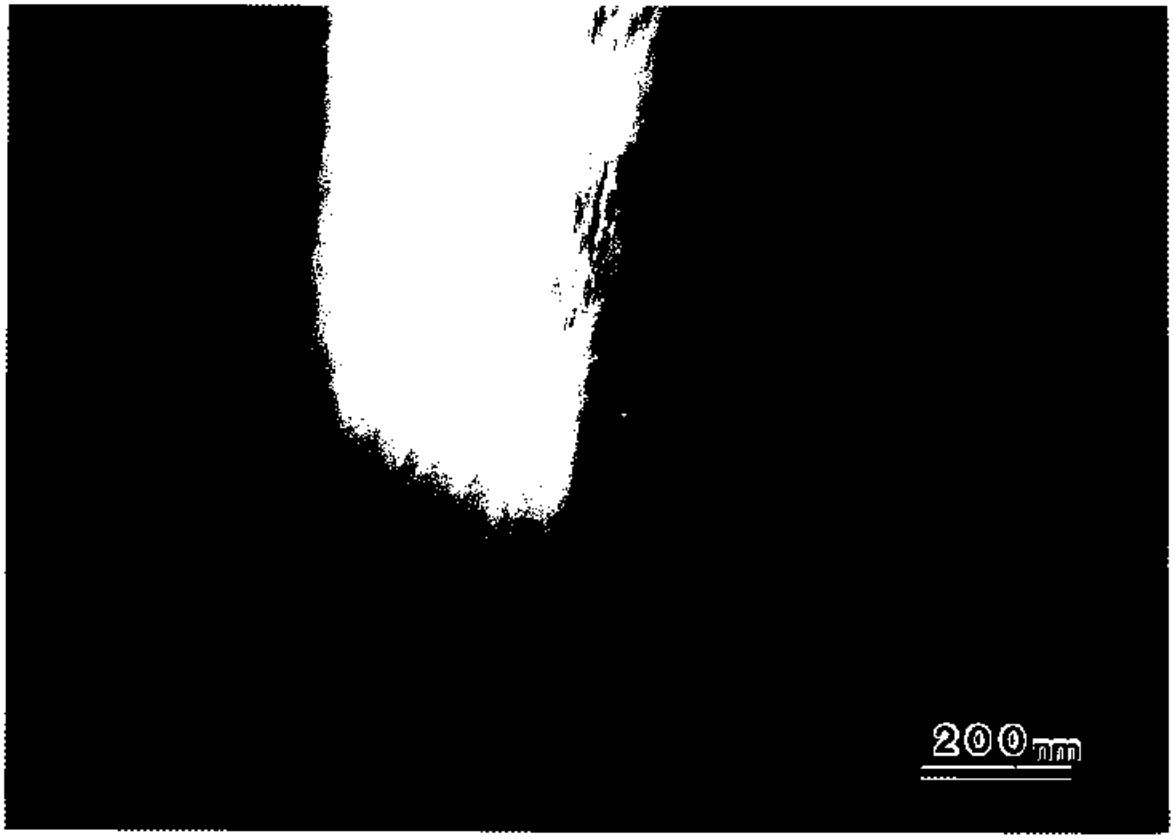

Fig. App.-3. Dark-field electron micrograph of albite (sample No.12) in Horokanai area.

No micro-textures are observed.

Fig. App.-4. Dark-field electron micrograph of oligoclase in Akebono Rock, East Antarctica area. The exsolution lamellae formed by the spinodal decomposition are observed.

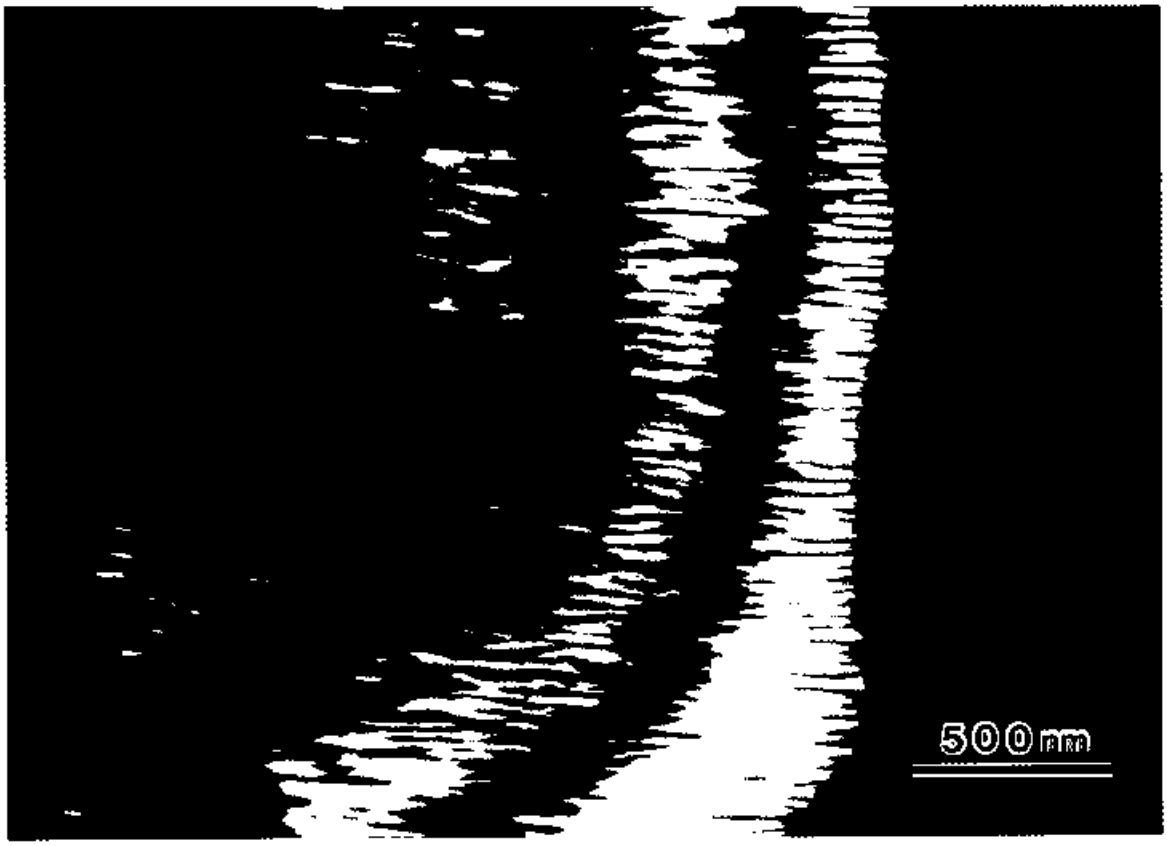

Fig. App.-5. Dark-field electron micrograph of oligoclase (An15) at locality A in the Sanbagawa belt in the Besshi area (Shirahata and Hirajima, 1995). The exsolution lamellae formed by the spinodal decomposition are observed.

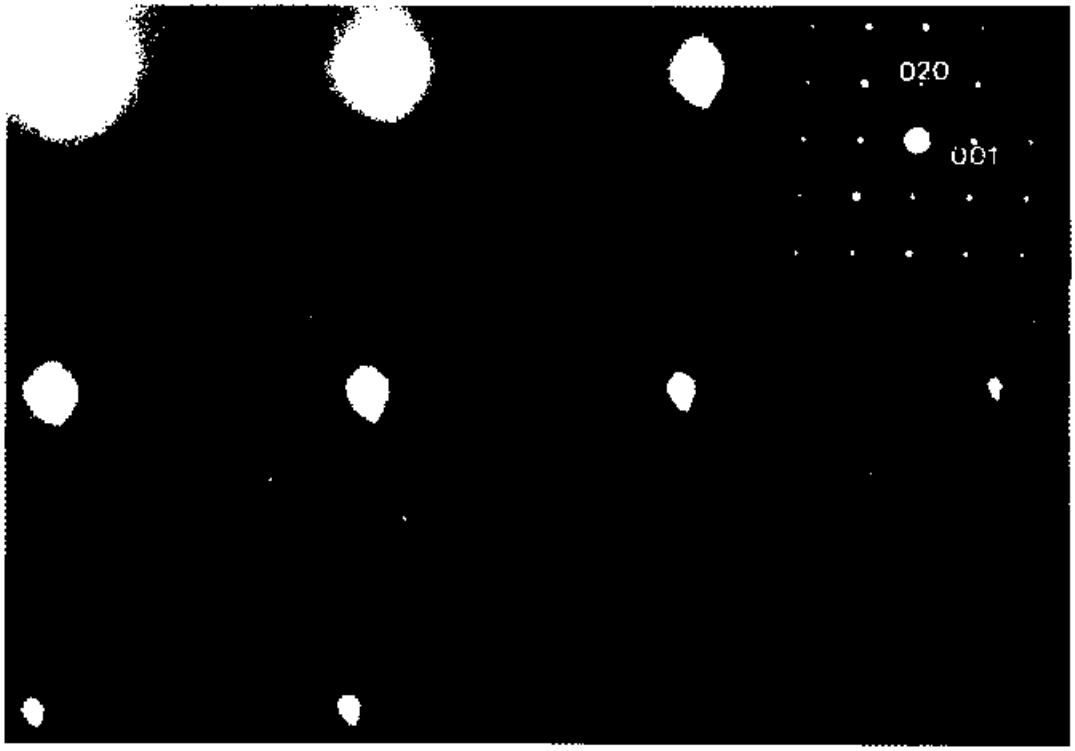

Fig. App.-6. Electron diffraction pattern from the area shown in Fig. Ap-5. 'e' reflections around {01½} is lightly observed.